1-16-2015

Memory T Cells Specific for Murine Cytomegalovirus Re-Emerge after Multiple Challenges and Recapitulate Immunity in Various Adoptive Transfer Scenarios.

Michael Quinn
Department of Microbiology and Immunology, Jefferson Medical College, Thomas Jefferson University, michael.quinn@jefferson.edu

Holly Turula
Thomas Jefferson University, holly.turula@jefferson.edu

Mayank Tandon
Department of Microbiology and Immunology, Jefferson Medical College, Thomas Jefferson University, mayank.tandon@jefferson.edu

Berthony Deslouches
Department of Microbiology and Immunology, Jefferson Medical College, Thomas Jefferson University, berthony.deslouches@jefferson.edu

Toktam Moghbeli
Department of Microbiology and Immunology, Jefferson Medical College, Thomas Jefferson University, Toktam.Moghbeli@jefferson.edu

See next page for additional authors

Authors
Michael Quinn, Holly Turula, Mayank Tandon, Berthony Deslouches, Toktam Moghbeli, and Christopher M. Snyder

Memory T cells specific for murine CMV reemerge after multiple challenges and recapitulate immunity in various adoptive transfer scenarios

Michael Quinn, Holly Turula[1,2], Mayank Tandon[1,3], Berthony Deslouches[4], Toktam Moghbeli, Christopher M. Snyder

Department of Microbiology and Immunology, Kimmel Cancer Center, Thomas Jefferson University, Philadelphia, PA

Corresponding author:

Dr. Christopher M. Snyder; 233 S. 10th St. BLSB Rm 526 , Philadelphia, PA 19107; christopher.snyder@jefferson.edu; Phone: 215-503-2543; Fax: 215-923-9248

Running Title: Memory T cells recapitulate MCMV immunity after transfer

Abstract

Reconstitution of CMV-specific immunity following transplant remains a primary clinical objective to prevent CMV disease, and adoptive immunotherapy of CMV-specific T cells can be an effective therapeutic approach. Due to viral persistence, most CMV-specific $CD8^{pos}$ T cells become terminally differentiated effector cells (T_{EFF}). A minor subset retains a memory-like phenotype (T_M), but it is unknown whether these cells retain memory function or persist over time. Interestingly, recent studies suggest that CMV-specific $CD8^{pos}$ T cells with different phenotypes have different abilities to reconstitute sustained immunity following transfer. The immunology of human CMV (HCMV) infections is reflected in the murine model (MCMV). We found that HCMV- and MCMV-specific T cells displayed shared genetic programs, validating the MCMV model for studies of CMV-specific T cells *in vivo*. The MCMV-specific T_M population was stable over time and retained a proliferative capacity that was vastly superior to T_{EFF} cells. Strikingly, after transfer, T_M cells established sustained and diverse T cell populations even after multiple challenges. Although both T_{EFF} and T_M cells could protect Rag-/- mice, only T_M cells persisted after transfer into immune replete, latently-infected recipients and responded if recipient immunity was lost. Interestingly, transferred T_M cells did not expand until recipient immunity was lost, supporting that competition limits the antigen stimulation of T_M cells. Ultimately, these data show that CMV-specific T_M cells retain memory function during MCMV infection and can reestablish CMV immunity when necessary. Thus, T_M cells may be a critical component for consistent, long-term adoptive immunotherapy success.

Introduction

Latent Cytomegalovirus (CMV) is present within a large percentage of the population but is effectively controlled by the immune system (1-6). However, in transplant patients, immune suppression can allow CMV reactivations to progress to disease and increase mortality. Despite the advancements of anti-viral medications, long-term prevention of CMV disease is dependent on the reconstitution of CMV-specific immunity, which can be achieved through adoptive immunotherapy (5-18).

In adoptive immunotherapy, healthy CMV-seropositive donors provide CMV-specific T cells to an immune suppressed recipient. Due to the persistent nature of CMV infection, CMV-seropositive donors accumulate large numbers of CMV-specific $CD8^{pos}$ T cells (approximately 5-10% of the total $CD8^{pos}$ T cells), a process termed “memory inflation," (19-28). Studies in humans and the well-characterized mouse model (MCMV) have shown that the majority of inflationary populations are composed of terminally differentiated effector phenotype (T_{EFF}) T cells that presumably develop as a result of repeated antigen stimulation and may not possess the proliferative or survival capacity necessary for long-term maintenance of CMV immunity (22, 27, 29-34). Interestingly however, a fraction of these inflationary T cells retain a memory-like (T_M) phenotype, despite sharing epitope specificity and T cell receptor sequences with the T_{EFF} subset (23, 25, 35-37). Studies with other infection models have shown that such a memory phenotype can identify cells that have “stem-cell like” characteristics (38, 39). If this model holds true for CMV immunity, the CMV-specific T_M cells would be ideal to use in an adoptive immunotherapy setting. Recent evidence supports this hypothesis. In a non-human primate model, CMV-specific effector T cells that were expanded in vitro from sorted T_M cell had a superior ability to survive after adoptive transfer (40). Moreover, a human study showed a positive correlation between the presence of CMV-specific T_M cells in a donor transfer and the

long-term maintenance of donor derived cells (41).

The goal of our study was to utilize the mouse model (MCMV) to directly address the capacity of the CMV-specific T_M population to restore long-term CMV-specific immunity after transfer. Importantly, we found that the MCMV-specific T_M cells share a common genetic program with their human CMV-specific counterparts and that these cells could repeatedly restore long-term CMV-specific immunity under a spectrum of transfer scenarios. Our data suggest that adoptive immunotherapy with CMV-specific T_M cells will improve consistency and clinical outcomes in patients at-risk for developing CMV disease.

Materials and Methods

Mice

Unless otherwise indicated, C57BL/6 mice, CD45.1 mice (B6.SJL-Ptprc^{a} Pepc^{b}/BoyJ), Thy1.1 mice (B6.PL-Thy1^{a}/CyJ) and Rag-/- mice (B6.129S7-Rag1<tm1Mom>J) were purchased from Jackson Laboratory. OT-I transgenic mice (C57BL/6-Tg(TcraTcrb)1100Mjb/J) also purchased from Jackson, were bred with CD45.1 mice to produce double positive (CD45.2^{pos}/CD45.1^{pos}) OT-I mice. All protocols were approved by the Thomas Jefferson University Institutional Animal Care and Use Committee.

Infections

Unless otherwise indicated, mice were infected intraperitoneally (i.p.) with 2 x 10^5 pfu of MCMV strain MW97.01 (42). Mice were considered latently-infected at 8 weeks post-infection. Rag-/- mice were infected with 5 x 10^4 pfu of MCMV-TK virus (43). OT-I T cell transfer recipients were challenged with 2 x 10^5 pfu MCMV-SL8, which expresses the SIINFEKL peptide (44, 45).

Tetramer Staining, Antibodies and FACS Analysis

MHC-tetramers were provided by the NIH Tetramer Core Facility (http://tetramer.yerkes.emory.edu/) and have been described previously (27). Staining was performed as described previously (27) with tetramers and the following antibodies: [CD8(53-6.7); CD44(IM7); CD27(LG.3A10); CD127(A7R34); KLRG1(2F1); CD62L(MEL-14); CD45.1(A20); CD45.1(104); Thy1.1(OX-7); Thy1.2(30-H12); IFN-γ(XMG1.2); TNF−α(MP6-XT22); CD107a(1D4B)]. In all cases, samples were collected on an LSR II and analyzed with FlowJo software (Tree Star). The gating strategy for phenotypic characterization of tetramer^{pos} CD8^{pos} T cells involved first gating lymphocytes and then singlets. CD8^{pos} cells were gated as

frequency of singlets. Tetramer^{pos} cells were identified as a frequency of CD8^{pos} cells. A B8R tetramer (specific for the B8R peptide from Vaccinia), was used as a negative tetramer control. Tetramer^{pos} cells were phenotypically defined by they expression of KLRG1, CD27, CD127 or CD62L.

Adoptive Transfers

CD8^{pos} splenocytes from latently-infected donors were enriched using EasySep Biotin selection kit (StemCell Technologies) and biotinylated antibodies against RBCs(Ter^{119}), CD4(GK1.5) and CD19(6D5) according to the recommended protocol. Enriched cells were stained to determine the frequency of tetramer^{pos} cells within the enriched fraction and then sorted on either a MoFlo (Dako Cytomation) or an ARIA II (BD Biosciences) cell sorter. Sorted cells were counted, and 5 x 10^4 cells were transferred via the retro-orbital sinus. Sort purity was analyzed on an LSR II. The number of transferred tetramer-binding CD8^{pos} T cells was estimated using the tetramer frequency within the enriched CD8^{pos} population and the post-sort purity analysis. Fold change was calculated as the number of tetramer-binding T cells in the spleen 7 days post-challenge over the total number of tetramer^{pos} cells transferred (assuming 100% engraftment). The gating strategy for analyzing donor cells in the recipients was identical to that described above with antibodies specific for the relevant congenic marker (CD45.1 or Thy1.2).

For OT-I adoptive transfers, splenocytes from naive mice containing 600 OT-I T cells were transferred. Recipients were challenged with MCMV-SL8. To establish secondary and tertiary populations, OT-I T_M CD8^{pos} T cells were FACS sorted and transferred as described in Supplemental Figure 1 and the legend for Figure 5. Following challenge with MCMV-SL8, the frequencies of donor OT-Is were determined in the blood of recipients using the strategy described above except that singlets were not identified and OT-I donors were identified by

151 expression CD45.1 and Vα2.

152

153 Intracellular Stimulation (ICS)

154 ICS and staining was performed as previously described (27, 45), with minor modifications.

155 Specifically, cells were incubated with 1 μg/mL peptide (Genemed Synthesis), 1 μg/mL

156 brefeldin A (GolgiPlug, BD Biosciences) and CD107a-specific antibody for 3 hours.

157

158 CD70 Blocking Antibody Treatment

159 CD70 antibody blockade was performed as previously described (46), with minor modifications.

160 Briefly, mice received either 150 μg of anti-CD70(FR70) or control rat IgG2b (both from

161 BioXCell) via the i.p. route. Injections were administered at days -1, 0 and 3 post-infection.

162

163 Antibody Depletions

164 Antibody depletions were performed with Thy1.1(19E12), CD4(GK1.5) and NK1.1(PK136)

165 antibodies. 300 μg of each antibody were administered i.p. in PBS. Three subsequent injections

166 of 100 μg of each antibody were given at 7 day intervals.

167

168 Microarray

169 Splenocytes from latently-infected mice were co-stained with tetramers loaded with the antigenic

170 peptides from M38, m139 and IE3 (25) and sorted on a MoFlo (Dako Cytomation) cell sorter.

171 MCMV-specific T cells were identified as $CD8^{pos}$, $CD44^{hi}$ and tetramer binding and then further

172 segregated into T_M and T_{EFF} cells subsets by expression of KLRG1 and CD127. Naïve $CD8^{pos}$

173 cells were $CD44^{lo}$. Total RNA was isolated using the Qiagen RNAeasy Plus Kit (Qiagen),

174 quantified on a NanoDrop 2000c Spectrophotometer (Thermo Scientific) and processed at the

175 Microarray Core Facility at Thomas Jefferson University. Briefly, 2.5 μg fragmented and

biotinylated cDNA was hybridized to Mouse gene 1.0 ST array (Affymetrix). Chips were scanned on an Affymetrix Gene Chip Scanner 3000 and data were analyzed using the R programming language and various packages from Bioconductor (47). The oligo package (48) was used to extract expression data from the Affymterix CEL files and perform background and RMA normalization (49). Annotation information was added using the mogene10sttranscriptcluster.db (50) package. Probes without valid annotations (7,196 of 35,556 probes) were removed before differential expression analysis using the limma package's (51) linear modeling and Bayes methods (52). Genes showing up- or down-regulation of at least two-fold and p-value < 0.05 in each of three contrasts (T_{EFF} vs. Naïve, T_M vs. Naïve, and T_{EFF} vs. T_M) were considered for gene set enrichment analysis (GSEA). Microarray data have been deposited in the Gene Expression Omnibus (GEO) database (53) (accession number: GSE61927)

Gene Set Enrichment Analysis

Human data for series GSE24151 (54) was retrieved from NCBI's GEO database (53), extracted using Partek® Genomics Suite® software, version 6.6 (Partek Inc., St. Louis, MO) and curated for input into GSEA software (55) (http://www.broadinstitute.org/gsea/). Since the data for GSE24151 have been deposited in GEO as $\log_{10}$ ratios of the reference pool to sample, each value was inverted by multiplying by -1. Gene names in the six mouse gene lists (up- or down-regulated in each of the three contrasts described above) were converted to human names using data from NCBI's Homologene database, Release 68 (http://www.ncbi.nlm.nih.gov/homologene). The converted gene lists along with genes specific to the liver and the TCR receptor pathway from the Molecular Signature Database (MSigDB) (55) were analyzed for enrichment in the human data using recommended settings for the GSEA command-line interface.

Results

MCMV-specific inflationary T_M populations are stable and share a common transcriptional program with HCMV-specific $CD8^{pos}$ T cells in humans

In the mouse model, MCMV infection of C57BL/6 (B6) mice results in inflation of select MCMV-specific $CD8^{pos}$ T cells specific for peptides from the viral proteins M38, m139 and IE3 (Fig. 1A and (25, 27, 28)). As in humans infected with human CMV (HCMV), the majority of MCMV-specific inflationary T cells express a T_{EFF} phenotype (often defined as T_{EMRA} in humans), while only a small fraction express a T_M-like phenotype, defined here as $KLRG1^{lo}/CD27^{hi}$ and further sub-divided into central memory (T_{CM} – $CD127^{hi}/CD62L^{hi}$) and effector memory (T_{EM} – $CD127^{hi}/CD62L^{lo}$) subsets (Fig. 1A and (22, 23, 27, 29-33, 56)). In contrast, "non-inflationary" MCMV-specific $CD8^{pos}$ T cell responses, represented by the response against the viral protein M45, contract after acute infection and are thought to be maintained by homeostatic mechanisms thereafter (Fig. 1A and (25, 27, 57)). As expected, non-inflators express a predominately memory (T_M) phenotype, which also includes both T_{CM} and T_{EM} subsets (Fig. 1A and (23, 27)).

It remains unknown whether the constant immune stimulation needed to maintain memory inflation causes a decline of the T_M subset within inflationary populations over time. Using infection-matched cohorts, we found that the numbers of T_M cells that were specific for inflationary antigens were stable over time and remarkably similar to the numbers of non-inflationary T_M cells, despite great differences between the numbers of inflationary and non-inflationary T_{EFF} cells (Fig. 1B, 1C). Thus, although continuous antigen stimulation maintains memory inflation, the inflationary T_M population remains stable.

The MCMV model is well characterized and the T cell responses clearly recapitulate those seen

in HCMV-infected people. To determine whether MCMV-specific T_M and T_{EFF} cells share a common transcriptional program with their human counterparts, we sorted MCMV-specific T_M ($CD44^{hi}/CD127^{hi}/KLRG1^{lo}$) and T_{EFF} ($CD44^{hi}/CD127^{lo}/KLRG1^{hi}$) cells specific for the M38, m139 and IE3 antigens. Microarray analyses were performed on these cells. Genes that were significantly up- or down-regulated in T_M and T_{EFF} subsets relative to each other or to naïve ($CD44^{low}$) T cells, were mapped to the corresponding human genes and compared with the profiles of HCMV-specific T cells, previously defined by the van Lier group as $CD27^{hi}/CD45RA^{lo}$ (T_M) or $CD27^{lo}/CD45RA^{hi}$ (T_{EFF}) (54). The CD27 and CD127 (IL-7Rα) molecules both mark CMV-specific T cells with a memory phenotype in mice and humans (27, 29, 32, 58, 59) and nearly all MCMV-specific $KLRG1^{lo}/CD27^{hi}$ cells (T_M) co-expressed CD127 (either T_{CM} or T_{EM}, Figure 1A). Gene set enrichment analyses (GSEA) were used to measure the overall correlation between the mouse and human gene expression data. As shown in Fig. 2A, genes that distinguished mouse T_{EFF} and T_M cells from each other were highly enriched within the corresponding human data set. That is: genes up-regulated specifically in mouse T_M cells relative to mouse T_{EFF} cells were highly enriched within the genes that distinguish human T_M cells from human T_{EFF} and vice versa. Moreover, relative to naive T cells, mouse genes that were up and down-regulated by T_{EFF} or T_M cells were highly enriched within genes that distinguished their human counterparts from human naive T cells (Fig. 2B). The analyzed mouse genes and the core enrichment profiles of each comparison are listed in Supplemental Table 1. Importantly, several of these genes corresponded to our sorting parameters and the known phenotypes of T_M and T_{EFF} populations. As controls, identical analyses were performed with genes associated with the T cell receptor signaling pathway or liver and the data exhibited expected patterns (Fig. 2B).

Overall, these data show that MCMV-specific and HCMV-specific T cells share a common genetic program, validating the use of the MCMV model to investigate the function of HCMV-

specific T cells. To our knowledge, this is the first direct comparison of MCMV-specific and HCMV-specific T cell gene expression profiles.

The inflationary T_M population retains proliferative capacity

To test the proliferative capacity of the T_M and T_{EFF} cells, both populations were sorted from spleens of latently-infected B6 mice (>3 months post-infection) using their differential expression of KLRG1 and CD27. Sorted cells were transferred into naive congenic recipients and re-challenged. The M45- and M38-specific T_M cells proliferated robustly within 7 days after challenge, each expanding almost 1000-fold in the spleen alone, assuming 100% engraftment of the donor cells (Fig. 3A, 3B). In contrast, the M38-specific T_{EFF} population expanded less than 10-fold in the same time period. Importantly, while the T_{EFF} donor cells remained exclusively $KLRG1^{hi}$, the T_M donor cells produced large numbers of both T_{EFF} and T_M progeny (Fig. 3C). In fact, donor M45- and M38-specific T_M phenotype cells were present in the spleen 7 days after challenge at numbers that were approximately 50 to 100-fold higher than had been transferred (dotted line, Fig. 3D), indicating expansion of this subset without terminal differentiation. These data show that MCMV-specific T_M cells retain robust proliferative capacity and can produce phenotypically diverse progeny including new T_M-phenotype cells.

Recent work has shown that interaction between CD27 and its ligand CD70 plays a functional role in the proliferation of MCMV-specific inflationary T cells (46). To test the contribution of this interaction specifically within the T_M population, we sorted and transferred T_M cells as above and blocked the CD27-CD70 interaction as described in the Methods. Blocking the CD27-CD70 interaction significantly decreased the expansion of the M38- and M45-specific T_M cells 7 days post-challenge by approximately 4- to 6-fold (Fig. 3E), which is in line with the impact of CD70 blockade on unsorted (i.e. combined T_M and T_{EFF} populations) inflationary T cells (46). These

data further suggest that the majority of proliferative potential of inflationary T cells is contained within the minor T_M subset. It should be noted that even in the presence of CD70 blockade, the T_M population retained a proliferative capacity that was greater than the T_{EFF} population, suggesting that additional pathways contribute to the total proliferative potential of these cells (Fig. 3B, 3E and unpublished observations).

The inflationary T_M population persists and can repeatedly recapitulate memory inflation

To determine the ability of the T_M donor cells to persist long-term, we tracked the progeny from T_M donor cells in the blood after re-challenge. M38-specific T cells from T_M-sorted donors persisted at high frequencies in recipients, while the M45-specific donor cells contracted after their initial expansion in the same mice (Fig. 4A, 4B). Despite their initial T_M phenotype, the donor M38-specific T cells largely expressed a T_{EFF} phenotype after challenge (Fig. 4C, 4D), consistent with a typical "inflationary" population. The population as a whole retained its ability produce IFN-γ, TNF-α and expose CD107a (Fig. 4E, 4F). Importantly, a small portion of donor T cells retained their T_M phenotype even after this secondary challenge (Fig. 4C, 4D).

To understand whether these persistent T_M phenotype donors continued to be functional, we turned to the OT-I transgenic system to facilitate sorting and avoid the possible selection of different T cell clones (Fig. 5A). As shown previously, transferred naive OT-Is undergo inflation and produce both T_M and T_{EFF} progeny after primary challenge with SIINFEKL-expressing MCMV-SL8 (45). We sorted the T_M phenotype OT-I cells that formed after primary challenge, transferred these cells and challenged the recipients to establish secondary populations (Supplemental Fig. 1A). As with non-transgenic T cells (Fig. 4), secondary challenge of T_M OT-Is induced inflation and T_{EFF} formation as well as a persistent $KLRG1^{lo}$ population (Supplemental Fig. 1B). These secondary T_M cells were again sorted (Supplemental Fig. 1C),

transferred into a 3rd set of naïve recipients and re-challenged. Incredibly, the donor secondary T_M population inflated and produced both KLRG1^{hi} and KLRG1^{lo} progeny following this tertiary challenge (Fig. 5B-5E).

Repeated acute viral challenges of small numbers of T cells in naive mice drives T_{EFF} differentiation (60-63) and indeed the overall frequency of tertiary inflationary cells that retained a T_M phenotype was reduced (Fig. 5E and Supplemental Fig. 1B). However, these tertiary stimulated OT-Is remained functional, producing both IFN-γ and TNF-α, as well as exposing CD107a (Fig. 5F, 5G). These data show that T_M phenotype T cells specific for inflationary antigens can repeatedly recapitulate memory inflation upon viral challenge and produce functional T_{EFF} and T_M progeny.

Memory and Effector Subsets protect Rag-/- mice

To test the ability of transferred T_M cells to protect against a lethal MCMV challenge, T_M and T_{EFF} populations were sorted from latently-infected B6 mice as above and transferred into Rag-/- recipients. One day later, the Rag-/- recipients were challenged with MCMV-TK, which lacks the m157 gene and is therefore resistant to NK-mediated control (43). Both transferred T_M or T_{EFF} cells expanded following the challenge and were sufficient to protect the recipients (Fig. 6A, 6B). In contrast, Rag-/- mice that received no T cell therapy became moribund in 2-4 weeks and had to be sacrificed (Fig. 6B). Notably, the T_{EFF} population, which proliferated very poorly in immune replete mice (Fig. 3), expanded and persisted in immune deficient hosts for at least 11 weeks post-challenge (Fig. 6A, 6B). However, the T_{EFF} responses lacked M45-specific, non-inflationary T cells (Fig. 6A). These data show that MCMV-specific T_M cells are capable of protecting immune deficient mice and producing immune responses with broad specificities.

The T_M population can persist long-term and respond when necessary

Patients undergoing hematopoietic stem cell transplantation (HSCT) are most susceptible to late-onset (>100 days) reactivating CMV, as opposed to an acute CMV infection ((12, 64-66) and reviewed in (67)). Furthermore, transferred CMV-specific T cells will need to compete with host immunity. Therefore, we developed a model to test whether T_M and T_{EFF} subsets could respond to viral reactivation after a long delay. To this end, T_M and T_{EFF} cells were sorted from latently-infected mice (> 3 months post-infection) and transferred into immune replete, infection matched or naive, congenic recipients differing at the Thy1 locus (Fig. 7A). Following the transfer, the latently-infected recipients were rested as described in the figure legend. Donor T cells did not expand dramatically in any animal following transfer (Supplemental Fig. 2A) supporting our previous conclusion that competition between T cells dictates MCMV-specific T cell expansion (45). Recipient T cells and NK cells were then eliminated in all mice using a cocktail of depletion antibodies that targeted the host cells (Thy1.1^{pos}), but left the donor cells (Thy1.2^{pos}) intact (Fig. 7B and Supplemental Fig. 2B). This depletion protocol did not induce detectible viral transcription in any animal as assessed by nested RT-PCR (unpublished observations), likely due to the presence of anti-viral antibodies (68). Despite the 9-12 week rest period, MCMV-specific donor T_M cells responded robustly in all infected recipients after host depletion (Fig. 7C and 7D). Importantly, donor T_M cells did not expand to detectible levels in depleted naive recipients (Supplemental Fig. 2C). However, viral challenge of naïve mice that received T_M donor cells 12 weeks previously induced a robust donor response in 3 of the 4 animals, indicating that the T_M cells persisted in these mice, even without any antigen (Supplemental Fig. 2C). Thus, antigen rather than homeostatic mechanisms accounts for the donor T_M response in infected recipients.

In marked contrast, after depletion, donor T cells were only detectible in 2 animals that had received T_{EFF} cells and then only at very low frequencies (Fig. 7C, 7D). Control experiments

(Supplemental Fig. 3A-3C) supported previous work (69) suggesting that the KLRG1-specific antibody did not induce depletion of the transferred T_{EFF} subset. Thus, the failure of T_{EFF} cells to expand in this setting is not a sorting artifact, but rather the inability to persist and/or expand in response to low amounts of viral antigen.

After expansion, all infected mice that received T_M cells had a donor population specific for multiple epitopes and the progeny had differentiated to form new T_{EFF} populations (Fig. 7E and unpublished observations). Furthermore, the four tetramers used only stained ~60% of the total donor population in each animal (Fig. 7E), suggesting that the remaining 40% of each donor population contained cells specific for additional MCMV antigens. In contrast, in the two animals in which T_{EFF} donors expanded to detectible levels, each was skewed substantially towards a single inflationary epitope (Fig. 7E). Since these sorted T_{EFF} populations included large numbers of T cells specific for M38, m139 and IE3, this "hit-or-miss" expansion of donor T cells with select specificities implies that a very small number of non-T_{EFF} cells may have contaminated the transfer.

In the mice that received T_M donor cells, their diverse progeny persisted in recipients for more than 11 weeks after termination of the depletion regimen, even though host immunity had returned (Fig. 7F). These data suggest that T_M cells with inflationary specificities are capable of surviving in an environment with very little or no antigen stimulation and then responding as needed during a period in which the host is immune compromised and viral antigen becomes available.

In total, these data show that protective MCMV-specific T_M cells persist throughout infection, retain superior proliferative function, and can respond to viral antigen as needed, in contrast to

the numerically dominant T_{EFF} cells. Since MCMV-specific T_M cells share a transcriptional program with HCMV-specific T_M cells, our data suggest that T_M cells may be ideal candidates to restore functional immune surveillance in patients at risk for CMV reactivation.

Discussion

Adoptive immunotherapy using CMV-specific $CD8^{pos}$ T cells can be a successful therapeutic strategy for combating CMV reactivations (5-18). However, the majority of CMV-specific $CD8^{pos}$ T cells isolated from healthy donors will express an effector-differentiated phenotype ($CD27^{lo}/CD127^{lo}/CD45RA^{hi}/KLRG\text{-}1^{hi}/CD57^{hi}$ - reviewed in (70)), and in vitro expansion of CMV-specific T cells drives their differentiation towards an effector phenotype (40). We used the MCMV model to show that the ability to restore MCMV-immunity is contained almost entirely within the minor T_M subset that retains CD27. Although both T_M and T_{EFF} cells protected Rag-/- mice (Fig. 6), humans are unlikely to remain completely immune depleted like Rag-/- mice, and bolus CMV infections are of lesser concern than reactivation following transplantation. The inability of the T_{EFF} population to consistently expand after immune depletion in latently-infected hosts, suggests that these cells will only be protective under limited conditions. These data support a previous study in humans that correlated the transfer of $CD27^{hi}$ CMV-specific T cells with an increased likelihood of T cell persistence and expansion (41).

To validate the use of the MCMV model, we compared human and mouse MCMV-specific T cells and show for the first time, to our knowledge, that T_M and T_{EFF} populations in mice and humans share a common transcriptional profile. The power of the GSEA analysis used for this comparison is that it identifies significant correlations across the entire transcriptional profile, rather than comparing individual genes. Nevertheless, we expect that future studies examining conserved and divergent genetic pathways will reveal significant and relevant information about CMV-specific immunity in mouse and man. These results highlight the usefulness of the MCMV model to: 1) perform CMV-specific $CD8^{pos}$ T cell functional studies that are difficult or impossible to perform in humans and 2) provide translational insights into novel or improved therapeutic strategies.

Understanding how CMV-specific T cell immunity is maintained is critical for the improvement of CMV adoptive immunotherapy. Persistent antigen stimulation from CMV reactivations results in the majority of inflationary $CD8^{pos}$ T cells developing a T_{EFF} phenotype and function. However, our previous work showed that unsorted inflationary $CD8^{pos}$ T cells, containing primarily T_{EFF} cells, declined after transfer into congenic, latently-infected recipients (27). These data suggest that MCMV-specific T_{EFF} cells are unable to sustain themselves in an immune replete environment, even in the presence of antigen. Thus, we proposed that the accumulation of T_{EFF} cells is the result of continual antigen stimulation of the T_M population. Our data show that a small, stable MCMV-specific T_M population has strong functional similarities to classical memory T cells that develop after acute infections. For example, the ability to proliferate in response to antigen without terminal differentiation is hallmark of functional memory T cells (71). In addition to producing differentiated progeny that accumulated after MCMV challenge (Figure 4D), donor T_M cells also produced T_M phenotype progeny that outnumbered the cells transferred (Fig. 3C and D) and persisted throughout our observation period (Fig. 4C and D). These data suggest that MCMV-specific T_M cells have the ability to replace themselves even while producing differentiated progeny in response to antigen. Importantly, this was true through at least three rounds of stimulation using sorted splenic T_M cells (Figure 5). Thus, MCMV-specific T_M cells have the capacity to respond repeatedly to viral antigen during this persistent infection and can recapitulate memory inflation.

It is interesting that transferred T_M cells failed to expand in immune-replete, latently-infected hosts. Detectible numbers of donor T cells were only evident in one out of six mice prior to immune depletion (Supplemental Fig. 2A). In this case, the donors were not positive for any of the tetramers used in the analyses and made up less than 1% of the total $CD8^{pos}$ population.

However, loss of the host T cell populations led to rapid and robust expansion of donor T cells with diverse specificities and phenotypes in all T_M cell recipients (Figure 7). The failure of transferred T_M cells to expand in the presence of host MCMV-specific immunity may reflect the relative lack of available antigen during the latent phase of MCMV infection. Indeed, viral reactivations occur in only a fraction of latently-infected cells at any given time, and only rarely produce infectious viral particles (72, 73). Moreover, we have found that competition between T cells for access to this limited antigen regulates the expansion of individual T cell clones (45). Thus, the combination of low antigen and large numbers of MCMV-specific T cells in the recipients may have "shielded" the majority of the donor T_M cells from the ongoing infection – an idea we have proposed previously (45, 74). Importantly, MCMV antigen is not required for MCMV-specific T_M cell survival. We have previously shown that MCMV-specific T_M cells divide at a consistent rate with or without antigen (28) and our new data (Supplemental Fig. 2C) show that inflationary T_M cells can survive in naïve mice without any antigen. Thus, homeostatic mechanisms can support the inflationary T_M population when it does not have access to antigen, which may partially explain the preservation of memory function within the T_M subset. Taken together, these data suggest that the highly functional T_M population, which can persist without access to antigen, proliferates robustly and produces new T_M cells as well as more differentiated progeny upon antigen stimulation.

Overall, our data further support the model that the burden of maintaining memory inflation falls on the functional T_M population, which can provide a stable and consistent source of new T_{EFF} progeny whenever needed, over for prolonged periods of time. However, T cell competition for limited antigen appears to prevent the continuous stimulation of most T_M cells. Nonetheless, the T_M population is capable of robustly responding if T cell competition is lost - a conclusion with important clinical implications for adoptive immunotherapy. Variations in transplant protocols,

patients and anti-viral therapy responses make it difficult to predict and standardize CMV prevention therapies. Our data suggest that the plasticity of the T_M population, transferred before any disease develops, may offer a "personalized" therapy, where the treatment adapts to the conditions of the patient and responds if and when antigen becomes available. Future studies will be needed to explore whether the addition of homeostatic cytokines (e.g. IL-15) or pharmacotherapeutics (e.g. rapamycin (75)) preserves the T_M phenotype either *in vivo* or during *in vitro* expansion.

Acknowledgments

We thank the Kimmel Cancer Center Flow Cytometry Facility and Animal Facility at Thomas Jefferson University.

Conflict-of-Interest

The authors declare no conflict-of-interests.

References

1. Staras, S. A., S. C. Dollard, K. W. Radford, W. D. Flanders, R. F. Pass, and M. J. Cannon. 2006. Seroprevalence of cytomegalovirus infection in the United States, 1988-1994. *Clin. Infect. Dis.* 43: 1143-1151.
2. Polić, B., H. Hengel, A. Krmpotić, J. Trgovcich, I. Pavić, P. Lučin, S. Jonjić, and U. H. Koszinowski. 1998. Hierarchical and redundant lymphocyte subset control precludes cytomegalovirus replication during latent infection. *J. Exp. Med.* 188: 1047-1054.
3. Simon, C. O., R. Holtappels, H.-M. Tervo, V. Böhm, T. Däubner, S. A. Oehrlein-Karpi, B. Kühnapfel, A. Renzaho, D. Strand, and J. Podlech. 2006. CD8 T cells control cytomegalovirus latency by epitope-specific sensing of transcriptional reactivation. *J. Virol.* 80: 10436-10456.
4. Holtappels, R., V. Bohm, J. Podlech, and M. J. Reddehase. 2008. CD8 T-cell-based immunotherapy of cytomegalovirus infection: "proof of concept" provided by the murine model. *Med. Microbiol. Immunol.* 197: 125-134.
5. Walter, E. A., P. D. Greenberg, M. J. Gilbert, R. J. Finch, K. S. Watanabe, E. D. Thomas, and S. R. Riddell. 1995. Reconstitution of cellular immunity against cytomegalovirus in recipients of allogeneic bone marrow by transfer of T-cell clones from the donor. *N. Engl. J. Med.* 333: 1038-1044.
6. Riddell, S. R., K. S. Watanabe, J. M. Goodrich, C. R. Li, M. E. Agha, and P. D. Greenberg. 1992. Restoration of viral immunity in immunodeficient humans by the adoptive transfer of T cell clones. *Science* 257: 238-241.
7. Barron, M. A., D. Gao, K. L. Springer, J. A. Patterson, M. W. Brunvand, P. A. McSweeney, Z. Chang, A. E. Barón, and A. Weinberg. 2009. Relationship of reconstituted adaptive and innate cytomegalovirus (CMV)-specific immune responses with CMV

viremia in hematopoietic stem cell transplant recipients. *Clin. Infect. Dis.* 49: 1777-1783.

8. Feuchtinger, T., K. Opherk, W. A. Bethge, M. S. Topp, F. R. Schuster, E. M. Weissinger, M. Mohty, R. Or, M. Maschan, M. Schumm, K. Hamprecht, R. Handgretinger, P. Lang, and H. Einsele. 2010. Adoptive transfer of pp65-specific T cells for the treatment of chemorefractory cytomegalovirus disease or reactivation after haploidentical and matched unrelated stem cell transplantation. *Blood* 116: 4360-4367.

9. Reusser, P., S. R. Riddell, J. D. Meyers, and P. D. Greenberg. 1991. Cytotoxic T-lymphocyte response to cytomegalovirus after human allogeneic bone marrow transplantation: pattern of recovery and correlation with cytomegalovirus infection and disease. *Blood* 78: 1373-1380.

10. Li, C. R., P. D. Greenberg, M. J. Gilbert, J. M. Goodrich, and S. R. Riddell. 1994. Recovery of HLA-restricted cytomegalovirus (CMV)-specific T-cell responses after allogeneic bone marrow transplant: correlation with CMV disease and effect of ganciclovir prophylaxis. *Blood* 83: 1971-1979.

11. Gratama, J. W., M. Boeckh, R. Nakamura, J. J. Cornelissen, R. A. Brooimans, J. A. Zaia, S. J. Forman, K. Gaal, K. R. Bray, G. H. Gasior, C. S. Boyce, L. A. Sullivan, and P. C. Southwick. 2010. Immune monitoring with iTAg MHC Tetramers for prediction of recurrent or persistent cytomegalovirus infection or disease in allogeneic hematopoietic stem cell transplant recipients: a prospective multicenter study. *Blood* 116: 1655-1662.

12. Boeckh, M., W. Leisenring, S. R. Riddell, R. A. Bowden, M. L. Huang, D. Myerson, T. Stevens-Ayers, M. E. Flowers, T. Cunningham, and L. Corey. 2003. Late cytomegalovirus disease and mortality in recipients of allogeneic hematopoietic stem cell transplants: importance of viral load and T-cell immunity. *Blood* 101: 407-414.

13. Peggs, K. S., S. Verfuerth, A. Pizzey, S. L. Chow, K. Thomson, and S. Mackinnon. 2009. Cytomegalovirus-specific T cell immunotherapy promotes restoration of durable functional

551 antiviral immunity following allogeneic stem cell transplantation. *Clin. Infect. Dis.* 49:
552 1851-1860.

553 14. Peggs, K. S., K. Thomson, E. Samuel, G. Dyer, J. Armoogum, R. Chakraverty, K. Pang, S.
554 Mackinnon, and M. W. Lowdell. 2011. Directly selected cytomegalovirus-reactive donor T
555 cells confer rapid and safe systemic reconstitution of virus-specific immunity following
556 stem cell transplantation. *Clin. Infect. Dis.* 52: 49-57.

557 15. Schmitt, A., T. Tonn, D. H. Busch, G. U. Grigoleit, H. Einsele, M. Odendahl, L.
558 Germeroth, M. Ringhoffer, S. Ringhoffer, M. Wiesneth, J. Greiner, D. Michel, T. Mertens,
559 M. Rojewski, M. Marx, S. von Harsdorf, H. Dohner, E. Seifried, D. Bunjes, and M.
560 Schmitt. 2011. Adoptive transfer and selective reconstitution of streptamer-selected
561 cytomegalovirus-specific CD8+ T cells leads to virus clearance in patients after allogeneic
562 peripheral blood stem cell transplantation. *Transfusion* 51: 591-599.

563 16. Blyth, E., L. Clancy, R. Simms, C. K. K. Ma, J. Burgess, S. Deo, K. Byth, M.-C. Dubosq,
564 P. J. Shaw, and K. P. Micklethwaite. 2013. Donor-derived CMV-specific T cells reduce the
565 requirement for CMV-directed pharmacotherapy after allogeneic stem cell transplantation.
566 *Blood* 121: 3745-3758.

567 17. Cobbold, M., N. Khan, B. Pourgheysari, S. Tauro, D. McDonald, H. Osman, M.
568 Assenmacher, L. Billingham, C. Steward, C. Crawley, E. Olavarria, J. Goldman, R.
569 Chakraverty, P. Mahendra, C. Craddock, and P. A. Moss. 2005. Adoptive transfer of
570 cytomegalovirus-specific CTL to stem cell transplant patients after selection by HLA-
571 peptide tetramers. *J. Exp. Med.* 202: 379-386.

572 18. Papadopoulou, A., U. Gerdemann, U. L. Katari, I. Tzannou, H. Liu, C. Martinez, K. Leung,
573 G. Carrum, A. P. Gee, J. F. Vera, R. A. Krance, M. K. Brenner, C. M. Rooney, H. E.
574 Heslop, and A. M. Leen. 2014. Activity of broad-spectrum T cells as treatment for AdV,
575 EBV, CMV, BKV, and HHV6 infections after HSCT. *Sci. Transl. Med.* 6: 242ra283.

19. Holtappels, R., M. F. Pahl-Seibert, D. Thomas, and M. J. Reddehase. 2000. Enrichment of immediate-early 1 (m123/pp89) peptide-specific CD8 T cells in a pulmonary CD62L(lo) memory-effector cell pool during latent murine cytomegalovirus infection of the lungs. *J. Virol.* 74: 11495-11503.

20. Holtappels, R., D. Thomas, J. Podlech, and M. J. Reddehase. 2002. Two antigenic peptides from genes m123 and m164 of murine cytomegalovirus quantitatively dominate CD8 T-cell memory in the H-2d haplotype. *J. Virol.* 76: 151-164.

21. Karrer, U., S. Sierro, M. Wagner, A. Oxenius, H. Hengel, U. H. Koszinowski, R. E. Phillips, and P. Klenerman. 2003. Memory inflation: continuous accumulation of antiviral CD8+ T cells over time. *J. Immunol.* 170: 2022-2029.

22. Ouyang, Q., W. M. Wagner, D. Voehringer, A. Wikby, T. Klatt, S. Walter, C. A. Muller, H. Pircher, and G. Pawelec. 2003. Age-associated accumulation of CMV-specific CD8+ T cells expressing the inhibitory killer cell lectin-like receptor G1 (KLRG1). *Exp. Gerontol.* 38: 911-920.

23. Sierro, S., R. Rothkopf, and P. Klenerman. 2005. Evolution of diverse antiviral CD8+ T cell populations after murine cytomegalovirus infection. *Eur. J. Immunol.* 35: 1113-1123.

24. Sylwester, A. W., B. L. Mitchell, J. B. Edgar, C. Taormina, C. Pelte, F. Ruchti, P. R. Sleath, K. H. Grabstein, N. A. Hosken, F. Kern, J. A. Nelson, and L. J. Picker. 2005. Broadly targeted human cytomegalovirus-specific CD4+ and CD8+ T cells dominate the memory compartments of exposed subjects. *J. Exp. Med.* 202: 673-685.

25. Munks, M. W., K. S. Cho, A. K. Pinto, S. Sierro, P. Klenerman, and A. B. Hill. 2006. Four distinct patterns of memory CD8 T cell responses to chronic murine cytomegalovirus infection. *J. Immunol.* 177: 450-458.

26. Komatsu, H., A. Inui, T. Sogo, T. Fujisawa, H. Nagasaka, S. Nonoyama, S. Sierro, J. Northfield, M. Lucas, A. Vargas, and P. Klenerman. 2006. Large scale analysis of pediatric

601 antiviral CD8+ T cell populations reveals sustained, functional and mature responses.
602 *Immun. Ageing* 3: 11.
603 27. Snyder, C. M., K. S. Cho, E. L. Bonnett, S. van Dommelen, G. R. Shellam, and A. B. Hill.
604 2008. Memory inflation during chronic viral infection is maintained by continuous
605 production of short-lived, functional T cells. *Immunity* 29: 650-659.
606 28. Smith, C. J., H. Turula, and C. M. Snyder. 2014. Systemic Hematogenous Maintenance of
607 Memory Inflation by MCMV Infection. *PLoS Pathog.* 10: e1004233.
608 29. Appay, V., P. R. Dunbar, M. Callan, P. Klenerman, G. M. Gillespie, L. Papagno, G. S.
609 Ogg, A. King, F. Lechner, C. A. Spina, S. Little, D. V. Havlir, D. D. Richman, N. Gruener,
610 G. Pape, A. Waters, P. Easterbrook, M. Salio, V. Cerundolo, A. J. McMichael, and S. L.
611 Rowland-Jones. 2002. Memory CD8+ T cells vary in differentiation phenotype in different
612 persistent virus infections. *Nat. Med.* 8: 379-385.
613 30. van Leeuwen, E. M., L. E. Gamadia, P. A. Baars, E. B. Remmerswaal, I. J. ten Berge, and
614 R. A. van Lier. 2002. Proliferation requirements of cytomegalovirus-specific, effector-type
615 human CD8+ T cells. *J. Immunol.* 169: 5838-5843.
616 31. Gamadia, L. E., E. M. van Leeuwen, E. B. Remmerswaal, S. L. Yong, S. Surachno, P. M.
617 Wertheim-van Dillen, I. J. Ten Berge, and R. A. Van Lier. 2004. The size and phenotype of
618 virus-specific T cell populations is determined by repetitive antigenic stimulation and
619 environmental cytokines. *J. Immunol.* 172: 6107-6114.
620 32. van Leeuwen, E. M., G. J. de Bree, E. B. Remmerswaal, S. L. Yong, K. Tesselaar, I. J. ten
621 Berge, and R. A. van Lier. 2005. IL-7 receptor alpha chain expression distinguishes
622 functional subsets of virus-specific human CD8+ T cells. *Blood* 106: 2091-2098.
623 33. Waller, E. C., N. McKinney, R. Hicks, A. J. Carmichael, J. G. Sissons, and M. R. Wills.
624 2007. Differential costimulation through CD137 (4-1BB) restores proliferation of human
625 virus-specific "effector memory" (CD28 CD45RAHI) CD8+ T cells. *Blood* 110: 4360-

4366.

34. Wallace, D. L., J. E. Masters, C. M. De Lara, S. M. Henson, A. Worth, Y. Zhang, S. R. Kumar, P. C. Beverley, A. N. Akbar, and D. C. Macallan. 2011. Human cytomegalovirus-specific CD8+ T-cell expansions contain long-lived cells that retain functional capacity in both young and elderly subjects. *Immunology* 132: 27-38.

35. Rufer, N., A. Zippelius, P. Batard, M. J. Pittet, I. Kurth, P. Corthesy, J. C. Cerottini, S. Leyvraz, E. Roosnek, M. Nabholz, and P. Romero. 2003. Ex vivo characterization of human CD8+ T subsets with distinct replicative history and partial effector functions. *Blood* 102: 1779-1787.

36. Price, D. A., J. M. Brenchley, L. E. Ruff, M. R. Betts, B. J. Hill, M. Roederer, R. A. Koup, S. A. Migueles, E. Gostick, and L. Wooldridge. 2005. Avidity for antigen shapes clonal dominance in CD8+ T cell populations specific for persistent DNA viruses. *J. Exp. Med.* 202: 1349-1361.

37. Iancu, E. M., P. Corthesy, P. Baumgaertner, E. Devevre, V. Voelter, P. Romero, D. E. Speiser, and N. Rufer. 2009. Clonotype selection and composition of human CD8 T cells specific for persistent herpes viruses varies with differentiation but is stable over time. *J. Immunol.* 183: 319-331.

38. Gattinoni, L., E. Lugli, Y. Ji, Z. Pos, C. M. Paulos, M. F. Quigley, J. R. Almeida, E. Gostick, Z. Yu, and C. Carpenito. 2011. A human memory T cell subset with stem cell-like properties. *Nat. Med.* 17: 1290-1297.

39. Graef, P., V. R. Buchholz, C. Stemberger, M. Flossdorf, L. Henkel, M. Schiemann, I. Drexler, T. Höfer, S. R. Riddell, and D. H. Busch. 2014. Serial Transfer of Single-Cell-Derived Immunocompetence Reveals Stemness of CD8+ Central Memory T Cells. *Immunity* 41: 116-126.

40. Berger, C., M. C. Jensen, P. M. Lansdorp, M. Gough, C. Elliott, and S. R. Riddell. 2008.

651 Adoptive transfer of effector CD8+ T cells derived from central memory cells establishes
652 persistent T cell memory in primates. *J. Clin. Invest.* 118: 294-305.
653 41. Scheinberg, P., J. J. Melenhorst, J. M. Brenchley, B. J. Hill, N. F. Hensel, P. K.
654 Chattopadhyay, M. Roederer, L. J. Picker, D. A. Price, and A. J. Barrett. 2009. The transfer
655 of adaptive immunity to CMV during hematopoietic stem cell transplantation is dependent
656 on the specificity and phenotype of CMV-specific T cells in the donor. *Blood* 114: 5071-
657 5080.
658 42. Wagner, M., S. Jonjic, U. H. Koszinowski, and M. Messerle. 1999. Systematic excision of
659 vector sequences from the BAC-cloned herpesvirus genome during virus reconstitution. *J.*
660 *Virol.* 73: 7056-7060.
661 43. Snyder, C. M., K. S. Cho, E. L. Bonnett, J. E. Allan, and A. B. Hill. 2011. Sustained CD8+
662 T cell memory inflation after infection with a single-cycle cytomegalovirus. *PLoS Pathog.*
663 7: e1002295.
664 44. Farrington, L. A., T. A. Smith, F. Grey, A. B. Hill, and C. M. Snyder. 2013. Competition
665 for antigen at the level of the APC is a major determinant of immunodominance during
666 memory inflation in murine cytomegalovirus infection. *J. Immunol.* 190: 3410-3416.
667 45. Turula, H., C. J. Smith, F. Grey, K. A. Zurbach, and C. M. Snyder. 2013. Competition
668 between T cells maintains clonal dominance during memory inflation induced by MCMV.
669 *Eur. J. Immunol.* 43: 1252-1263.
670 46. Welten, S. P. M., A. Redeker, K. L. Franken, C. A. Benedict, H. Yagita, F. M. Wensveen,
671 J. Borst, C. J. M. Melief, R. A. W. van Lier, and K. P. J. M. van Gisbergen. 2013. CD27-
672 CD70 Costimulation Controls T Cell Immunity during Acute and Persistent
673 Cytomegalovirus Infection. *J. Virol.* 87: 6851-6865.
674 47. Gentleman, R. C., V. J. Carey, D. M. Bates, B. Bolstad, M. Dettling, S. Dudoit, B. Ellis, L.
675 Gautier, Y. Ge, and J. Gentry. 2004. Bioconductor: open software development for

676 computational biology and bioinformatics. *Genome biology* 5: R80.

677 48. Carvalho, B. S., and R. A. Irizarry. 2010. A framework for oligonucleotide microarray
678 preprocessing. *Bioinformatics* 26: 2363-2367.

679 49. Irizarry, R. A., B. Hobbs, F. Collin, Y. D. Beazer-Barclay, K. J. Antonellis, U. Scherf, and
680 T. P. Speed. 2003. Exploration, normalization, and summaries of high density
681 oligonucleotide array probe level data. *Biostatistics* 4: 249-264.

682 50. MacDonald, J. W. *mogene10sttranscriptcluster.db: Affymetrix mogene10 annotation data
683 (chip mogene10sttranscriptcluster)*. R package version 8.1.0.

684 51. Smyth, G. K. 2005. Limma: linear models for microarray data. In *Bioinformatics and
685 computational biology solutions using R and Bioconductor*, ed. Springer, New York, NY:
686 p. 397-420.

687 52. Smyth, G. K. 2004. Linear models and empirical bayes methods for assessing differential
688 expression in microarray experiments. *Stat. Appl. Genet. Molec. Biol.* 3: Article 3.

689 53. Edgar, R., M. Domrachev, and A. E. Lash. 2002. Gene Expression Omnibus: NCBI gene
690 expression and hybridization array data repository. *Nucleic Acids Res.* 30: 207-210.

691 54. Hertoghs, K. M. L., P. D. Moerland, A. van Stijn, E. B. M. Remmerswaal, S. L. Yong, P. J.
692 E. J. van de Berg, S. M. van Ham, F. Baas, I. J. M. ten Berge, and R. A. W. van Lier. 2010.
693 Molecular profiling of cytomegalovirus-induced human CD8+ T cell differentiation. *J.
694 Clin. Invest.* 120: 4077-4090.

695 55. Subramanian, A., P. Tamayo, V. K. Mootha, S. Mukherjee, B. L. Ebert, M. A. Gillette, A.
696 Paulovich, S. L. Pomeroy, T. R. Golub, and E. S. Lander. 2005. Gene set enrichment
697 analysis: a knowledge-based approach for interpreting genome-wide expression profiles.
698 *Proc. Natl. Acad. Sci. USA* 102: 15545-15550.

699 56. Thimme, R., V. Appay, M. Koschella, E. Panther, E. Roth, A. D. Hislop, A. B. Rickinson,
700 S. L. Rowland-Jones, H. E. Blum, and H. Pircher. 2005. Increased expression of the NK

cell receptor KLRG1 by virus-specific CD8 T cells during persistent antigen stimulation. *J. Virol.* 79: 12112-12116.

57. Hutchinson, S., S. Sims, G. O'Hara, J. Silk, U. Gileadi, V. Cerundolo, and P. Klenerman. 2011. A dominant role for the immunoproteasome in CD8 T cell responses to murine cytomegalovirus. *PLoS One* 6: e14646.

58. Kern, F., E. Khatamzas, I. Surel, C. Frommel, P. Reinke, S. L. Waldrop, L. J. Picker, and H. D. Volk. 1999. Distribution of human CMV-specific memory T cells among the CD8pos. subsets defined by CD57, CD27, and CD45 isoforms. *Eur. J. Immunol.* 29: 2908-2915.

59. Tomiyama, H., H. Takata, T. Matsuda, and M. Takiguchi. 2004. Phenotypic classification of human CD8+ T cells reflecting their function: inverse correlation between quantitative expression of CD27 and cytotoxic effector function. *Eur. J. Immunol.* 34: 999-1010.

60. Jabbari, A., and J. T. Harty. 2006. Secondary memory CD8+ T cells are more protective but slower to acquire a central-memory phenotype. *J. Exp. Med.* 203: 919-932.

61. Masopust, D., S. J. Ha, V. Vezys, and R. Ahmed. 2006. Stimulation history dictates memory CD8 T cell phenotype: implications for prime-boost vaccination. *J. Immunol.* 177: 831-839.

62. Wirth, T. C., H. H. Xue, D. Rai, J. T. Sabel, T. Bair, J. T. Harty, and V. P. Badovinac. 2010. Repetitive antigen stimulation induces stepwise transcriptome diversification but preserves a core signature of memory CD8(+) T cell differentiation. *Immunity* 33: 128-140.

63. Fraser, K. A., J. M. Schenkel, S. C. Jameson, V. Vezys, and D. Masopust. 2013. Preexisting High Frequencies of Memory CD8+ T Cells Favor Rapid Memory Differentiation and Preservation of Proliferative Potential upon Boosting. *Immunity* 39: 171-183.

64. Kumar, D., S. Chernenko, G. Moussa, I. Cobos, O. Manuel, J. Preiksaitis, S.

Venkataraman, and A. Humar. 2009. Cell-mediated immunity to predict cytomegalovirus disease in high-risk solid organ transplant recipients. *Am. J. Transplant.* 9: 1214-1222.

65. Harvala, H., C. Stewart, K. Muller, S. Burns, L. Marson, A. MacGilchrist, and I. Johannessen. 2013. High risk of cytomegalovirus infection following solid organ transplantation despite prophylactic therapy. *J. Med. Virol.* 85: 893-898.

66. Manuel, O., S. Husain, D. Kumar, C. Zayas, S. Mawhorter, M. E. Levi, J. Kalpoe, L. Lisboa, L. Ely, and D. R. Kaul. 2013. Assessment of cytomegalovirus-specific cell-mediated immunity for the prediction of cytomegalovirus disease in high-risk solid-organ transplant recipients: a multicenter cohort study. *Clin. Infect. Dis.* 56: 817-824.

67. Ljungman, P., M. Hakki, and M. Boeckh. 2011. Cytomegalovirus in hematopoietic stem cell transplant recipients. *Hematol. Oncol. Clin. North. Am.* 25: 151-169.

68. Jonjic, S., I. Pavic, B. Polic, I. Crnkovic, P. Lucin, and U. H. Koszinowski. 1994. Antibodies are not essential for the resolution of primary cytomegalovirus infection but limit dissemination of recurrent virus. *J. Exp. Med.* 179: 1713-1717.

69. Cush, S. S., and E. Flaño. 2011. KLRG1+ NKG2A+ CD8 T cells mediate protection and participate in memory responses during γ-herpesvirus infection. *J. Immunol.* 186: 4051-4058.

70. Appay, V., R. A. W. Van Lier, F. Sallusto, and M. Roederer. 2008. Phenotype and function of human T lymphocyte subsets: consensus and issues. *Cytometry Part A* 73: 975-983.

71. Ciocca, M. L., B. E. Barnett, J. K. Burkhardt, J. T. Chang, and S. L. Reiner. 2012. Cutting edge: asymmetric memory T cell division in response to rechallenge. *J. Immunol.* 188: 4145-4148.

72. Kurz, S. K., M. Rapp, H. P. Steffens, N. K. Grzimek, S. Schmalz, M. J. Reddehase. 1999. Focal transcriptional activity of murine cytomegalovirus during latency in the lungs. *J. Virol.* **73**: 482–494.

73. Kurz, S. K., M. J. Reddehase. 1999. Patchwork pattern of transcriptional reactivation in the lungs indicates sequential checkpoints in the transition from murine cytomegalovirus latency to recurrence. *J. Virol.* **73**: 8612–8622.

74. Snyder, C. M. 2011. Buffered memory: a hypothesis for the maintenance of functional, virus-specific CD8(+) T cells during cytomegalovirus infection. *Immunol. Res.* 51: 195-204.

75. Araki, K., A. P. Turner, V. O. Shaffer, S. Gangappa, S. A. Keller, M. F. Bachmann, C. P. Larsen, and R. Ahmed. 2009. mTOR regulates memory CD8 T-cell differentiation. *Nature* 460: 108-112.

776 **Footnotes**

777 1. H.T. and M.T. contributed equally to this work

778 2. Current address: University of Michigan, Ann Harbor, MI

779 3. Current address: National Institutes of Health, Bethesda, MD

780 4. Current address: University of Pittsburgh, Pittsburgh, PA

781 5. This work was supported by a faculty start-up package from Thomas Jefferson University
782 and grants from the National Institutes of Health (K22-AI081866 and RO1AI106810
783 grants awarded to CMS).

784 6. Experiments conceived and designed by MQ and CMS. Experiments conducted by MQ,
785 HT, BD and TM. Data analyzed by MQ, HT, MT and CMS. Manuscript written by MQ
786 and CMS.

787 7. Address Correspondence to Dr. Christopher M. Snyder; 233 S. 10th St. BLSB Rm 526 ,
788 Philadelphia, PA 19107; christopher.snyder@jefferson.edu; Phone: 215-503-2543; Fax:
789 215-923-9248

790 8. Abbreviations: CMV, Cytomegalovirus; HCMV, Human Cytomegalovirus; MCMV,
791 Murine Cytomegalovirus; T_M, memory phenotype CD8+ T cells; T_{EFF}, terminal
792 differentiated effector phenotype CD8+ T cells; T_{CM}, central memory CD8+ T cells; T_{EM},
793 effector memory CD8+ T cells; T_{EMRA}, terminal differentiated CD8+ T cell phenotype in
794 humans; i.p., intraperitoneal route; GSEA, gene set enrichment analysis; GEO, gene
795 expression omnibus; SEM, standard error of the mean

796

Figure Legends

Figure 1: The non-inflationary and inflationary $CD8^{pos}$ T cell populations retain similar numbers of T_M phenotype cells.

Cohorts of age-matched B6 female mice were infected with MCMV and sacrificed at the indicated time points ($n = 4$ per time point). Tetramer staining and phenotypic analyses were performed on blood and splenocytes. (A) Frequency of tetramer-binding $CD8^{pos}$ T cells in the blood at indicated time points. The phenotypic analysis shown was performed at d326 post-infection. T_M cells were identified as $CD27^{hi}/KLRG1^{lo}$. T_{CM} and T_{EM} were further identified as $CD127^{hi}$ and either $CD62L^{hi}$ or $CD62L^{lo}$, respectively. (B) Absolute numbers of $KLRG1^{hi}$ tetramer-binding $CD8^{pos}$ T cells in the spleen. (C) Absolute numbers of T_{CM} and T_{EM} tetramer-binding $CD8^{pos}$ T cells. Data are displayed as mean ± SEM and represent two independent experiments.

Figure 2: Gene Set Enrichment Analyses reveal significant overlap between the transcriptional profile of CMV-specific T cells in humans and mice. (A) Gene set enrichment was performed as described in the Methods. Shown are the enrichment plots for mouse genes that differed in a T_{EFF} vs. T_M comparison, plotted relative to human T_{EFF} and T_M cells. Values represent the normalized enrichment score (NES) and Family Wise Error Rate (FWER), which estimates the probability of a false positive NES. (B) Lists of significantly altered mouse genes (2-fold up or down and $P<.05$) were generated for T_{EFF} and T_M cells relative to each other and relative to naive ($CD44^{low}$) T cells. GSEA analyses were performed with these mouse gene sets relative to each of the indicated human data sets, rank ordered by expression (see methods). Stars indicate FWER corrected significance to control for multiple testing (* $P<.05$, ** $P<.01$, *** $P<.001$).

Figure 3: T_M cells dramatically expand 7 days post-challenge and produce both T_M and T_{EFF} progeny.

Age matched B6 mice received either T_M or T_{EFF} cells and were challenged with MCMV as described in the Methods. Spleens were collected 7 days later for analysis. (A) Representative FACS plots of tetramer^{pos} donors in the spleen 7 days post-challenge. Frequencies in the corner are relative to total CD8^{pos} cells. (B) Fold change of donor cells in the spleen, calculated as described in the Methods, 7 days after challenge. As antigen-specific T cells were not sorted, approximately equal numbers of M38- and M45-specific T_M cells were transferred but ~10-fold more M38-specific T_{EFF} cells were transferred compared with the T_M cells. Due to the extremely low number of M45-specific T_{EFF} transferred and the minimal expansion at day 7, it was not possible to calculate a comparable fold change value for the M45-specific T_{EFF} population. Data were collected from two independent experiments (T_M: n = 6 total; T_{EFF}: n = 5 total) are shown. Statistical significance was determined by a Student's t-test (*** P<.001; **** P<.0001). (C) Representative FACS plots of M38-specific CD8^{pos} T cell progeny from either T_M or T_{EFF} donors in the spleen at 7 days post-challenge. Frequencies in the corner are relative to M38-specific CD8^{pos} cells. (D) Absolute number of T_M and T_{EFF} phenotypic progeny that were produced from T_M donors. Data are from the same experiments described in (B). (E) Fold change of donor cells in the spleen following treatment with either isotype control or anti-CD70 antibody. Data were collected 7 days post-challenge and represent two independent experiments (n = 6 total). Statistical significance was determined by a Student's t-test (*** P<.001; **** P<.0001). All graphical data are displayed as mean ± SEM.

Figure 4: T_M cells reinflate following re-challenge and retain function.

Age matched B6 mice received T_M cells and were challenged with MCMV as in the Methods. (A) Representative FACS plots of donor-derived T cells in the blood 126 days post-challenge.

(B) Frequencies of tetramer-binding T cells in the blood over time. Data were collected from three independent experiments (*n* = 17 total). (C) Representative FACS plot of the phenotype of donor-derived M38-specific T cells in the blood 126 days post-challenge. (D) Frequencies of donor-derived, M38-specific T_M and T_{EFF} cells in the blood over time. Data are from the same experiments described in (B). Each line represents an individual mouse. The square datum point represents a mouse that appeared to lose the donor T cells after day 7 post-challenge, but effectors appeared ~20 weeks after challenge. (E-F) Intracellular cytokine staining was performed on splenocytes 221 days post-challenge. Shown are representative FACS plots of stimulated (with M38 peptide) and unstimulated cells (E) and the frequencies of IFN-γ positive cells that also express TNF-α and/or CD107a (F). Data were collected from a single experiment (*n* = 5) described above. All graphical data are displayed as mean ± SEM.

Figure 5: T_M cells can reinflate following multiple re-challenges.

(A) Schematic of experimental design. To establish primary OT-I inflationary populations, 600 naïve OT-I T cells expressing CD45.1 were transferred into naïve B6 (CD45.2) recipients followed by infection with MCMV-SL8 (i.e. primary challenge). Thirteen weeks later, 6,000 T_M phenotype primary OT-Is, isolated by FACS sorting, were transferred into new B6 recipients followed by MCMV-SL8 challenge (i.e. secondary challenge). This process was repeated a third time, transferring 3,500 T_M OT-Is into naive mice and challenging with MCMV-SL8 (i.e. tertiary challenge). (B-C) Representative FACS plot of the donor stain 91 days post tertiary challenge (B) and frequencies of donor OT-Is (relative to total CD8s) in the blood at the indicated time points after tertiary challenge (C). Data were collected from two independent experiments (*n* = 12 total). Each line represents an individual mouse. (D-E) Phenotypic analyses of the mice described in (B-C). Representative FACS plot of the donor stain 30 weeks post-challenge Frequencies are relative to donor CD8s. (F-G) Intracellular cytokine staining was performed on

872 splenocytes approximately 20 weeks after the tertiary challenge. Shown are representative FACS
873 plots of stimulated (with SIINFEKL peptide) and unstimulated cells (F) and the frequencies of
874 IFN-γ positive cells that also express TNF-α and/or CD107a (G). Data were collected from two
875 independent experiments (n = 12). Data are displayed as mean ± SEM.
876
877 **Figure 6: T_M and T_{EFF} cells protect Rag-/- mice following an acute MCMV challenge**
878 Age matched Rag-/- mice received either T_M or T_{EFF} cells and were challenged with MCMV-TK
879 as described in the Methods. Mice were monitored daily for signs of morbidity (lethargy, raised
880 hair and shaking) and sacrificed if they displayed clear signs of morbidity. Data were collected
881 from two independent experiments. One experiment was carried out until 77 days post-challenge.
882 A second experiment was censored at 33 days post-challenge. (A) Representative tetramer
883 staining of T cells in Rag-/- that received either T_M or T_{EFF} transfers. Data were collected 11
884 weeks post-challenge. Frequencies are relative to total CD8s. (B) Survival curve (n = 7 for
885 control group; n = 7 for T_M group; n = 6 for T_{EFF} group). Statistical significance was determined
886 by a log-rank (Mantel-Cox) test (**** P<.0001).
887
888 **Figure 7: T_M cells persist in latently-infected, immune replete mice and expand when host**
889 **immunity is lost.**
890 (A) Schematic of experimental design. Age matched B6 and Thy1.1 mice were infected with
891 $1x10^6$ pfu MCMV-Smith. Following the establishment of viral latency (>8 weeks post-infection),
892 either T_M or T_{EFF} cells from the B6 donors were transferred, as described in the Methods, into the
893 latently-infected Thy1.1 recipients or into naïve Thy1.1 mice. Latently-infected recipients were
894 rested for 9-12 weeks, while the naïve recipients were rested for approximately 1.5 weeks. (B)
895 Antibody depletion schedule. (C-E) The presence of tetramer^{pos} donors was analyzed by flow
896 cytometry immediately following the depletion schedule. Data were collected from two

897 independent experiments (n = 6 total). Three mice from each group were depleted 9 weeks after
898 the transfer; three mice from each group were depleted 12 weeks after transfer. (C) Histograms
899 of donor T cells within each individual recipient. (D) Representative FACS plots of tetramer^{pos}
900 donors immediately following the depletion regimen. (E) Frequency within each individual
901 recipient of each analyzed tetramer as a percent of total donor CD8+ cells. T_{EFF} recipients 3-6 are
902 excluded because they did not have a donor population. (F) Tetramer staining was performed 11
903 weeks after depletion in one experiment described above (n = 3).

FIGURE 1

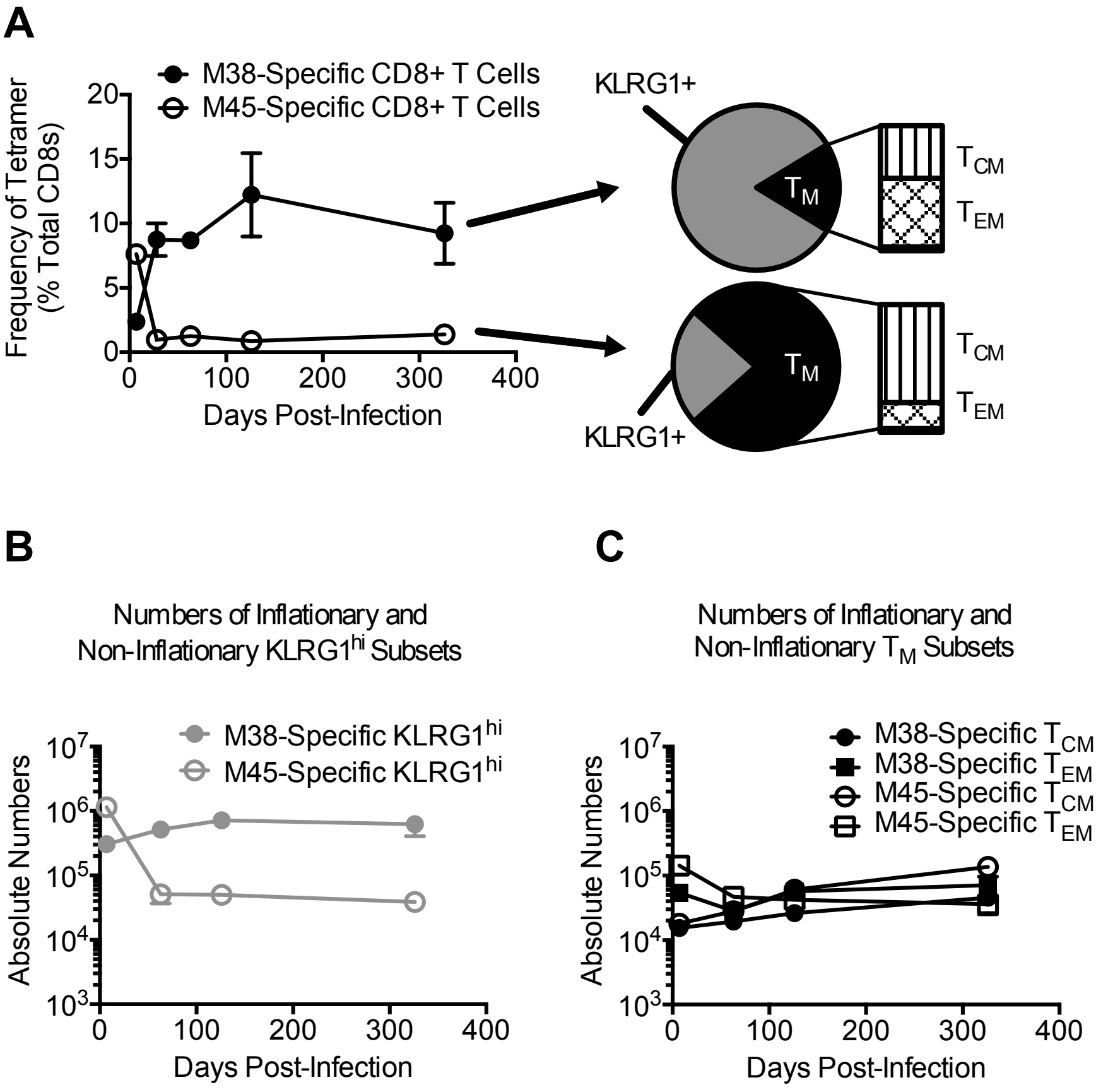
A
M38-Specific CD8+ T Cells
M45-Specific CD8+ T Cells
Frequency of Tetramer (% Total CD8s)
20
15
10
5
0
0
100
200
300
400
Days Post-Infection
KLRG1+
T_M
T_{CM}
T_{EM}
KLRG1+
T_M
T_{CM}
T_{EM}
B
Numbers of Inflationary and Non-Inflationary KLRG1^{hi} Subsets
M38-Specific KLRG1^{hi}
M45-Specific KLRG1^{hi}
Absolute Numbers
10^7
10^6
10^5
10^4
10^3
0
100
200
300
400
Days Post-Infection
C
Numbers of Inflationary and Non-Inflationary T_M Subsets
M38-Specific T_{CM}
M38-Specific T_{EM}
M45-Specific T_{CM}
M45-Specific T_{EM}
Absolute Numbers
10^7
10^6
10^5
10^4
10^3
0
100
200
300
400
Days Post-Infection

FIGURE 2

A

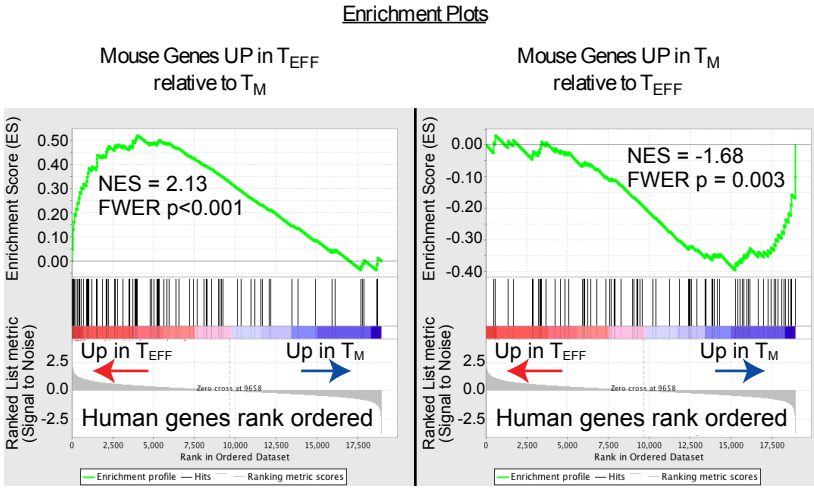
Enrichment Plots
Mouse Genes UP in T_{EFF} relative to T_M
Mouse Genes UP in T_M relative to T_{EFF}
Enrichment Score (ES)
NES = 2.13
FWER p<0.001
NES = -1.68
FWER p = 0.003
Ranked List metric (Signal to Noise)
Up in T_{EFF}
Up in T_M
Human genes rank ordered
Rank in Ordered Dataset
Enrichment profile
Hits
Ranking metric scores

B

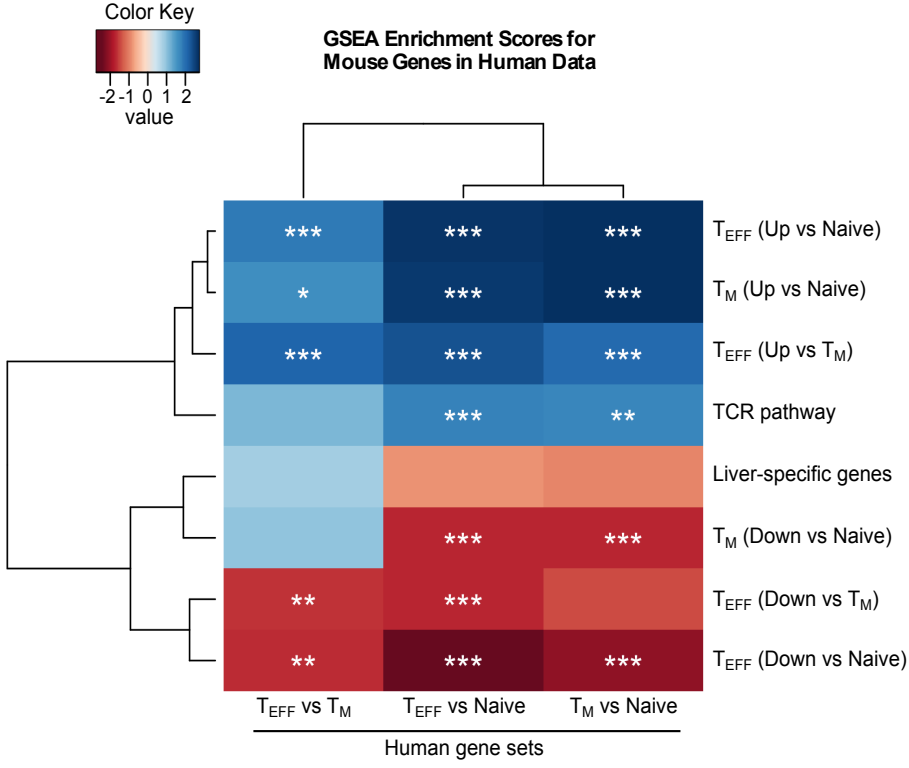
Color Key
-2 -1 0 1 2
value
GSEA Enrichment Scores for Mouse Genes in Human Data
T_{EFF} (Up vs Naive)
T_M (Up vs Naive)
T_{EFF} (Up vs T_M)
TCR pathway
Liver-specific genes
T_M (Down vs Naive)
T_{EFF} (Down vs T_M)
T_{EFF} (Down vs Naive)
Mouse gene sets
T_{EFF} vs T_M
T_{EFF} vs Naive
T_M vs Naive
Human gene sets

FIGURE 3

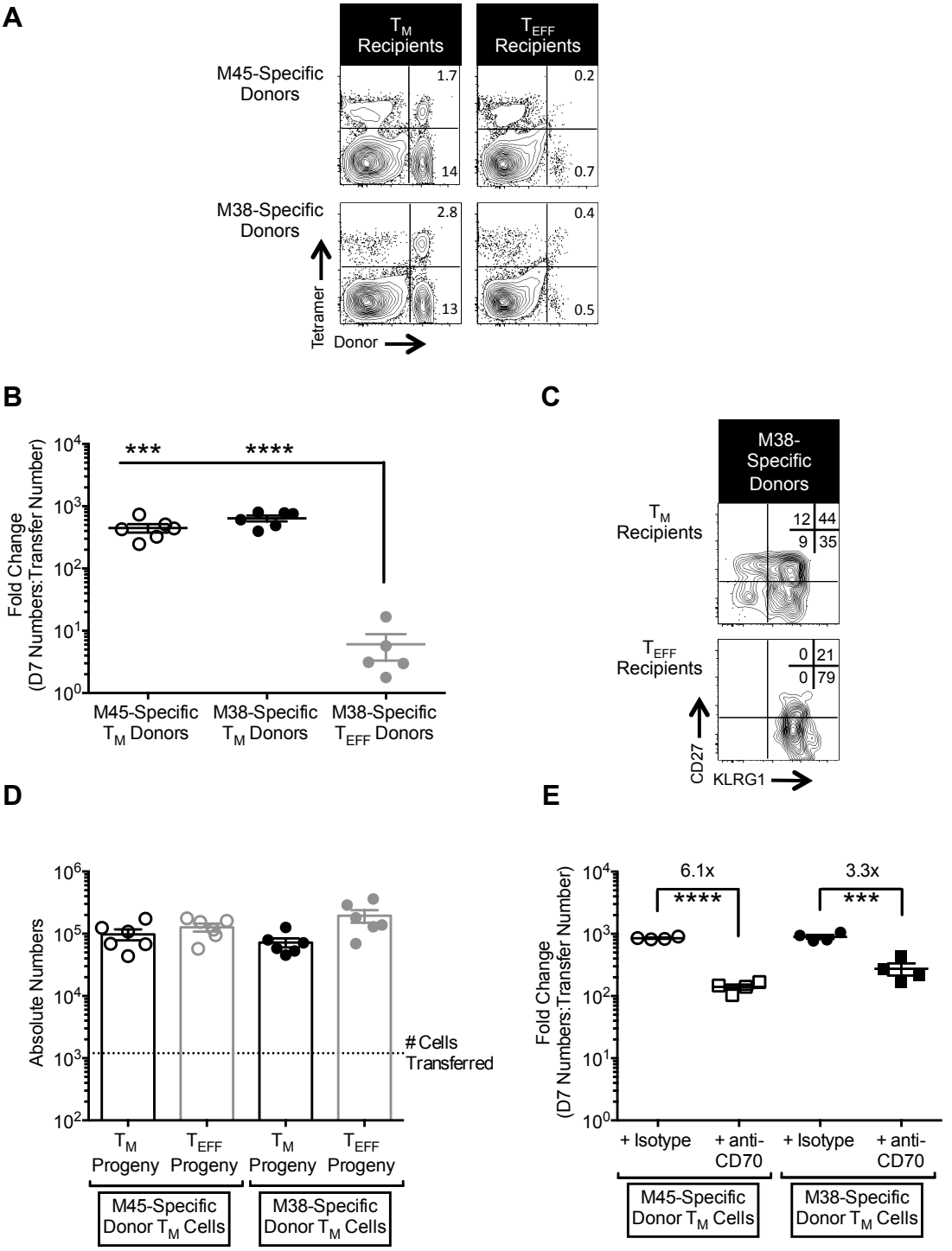
A
T_M Recipients
T_EFF Recipients
M45-Specific Donors
M38-Specific Donors
1.7
14
0.2
0.7
2.8
13
0.4
0.5
Tetramer
Donor
B
Fold Change (D7 Numbers:Transfer Number)
***
****
M45-Specific T_M Donors
M38-Specific T_M Donors
M38-Specific T_EFF Donors
C
M38-Specific Donors
T_M Recipients
T_EFF Recipients
12
44
9
35
0
21
0
79
CD27
KLRG1
D
Absolute Numbers
Cells Transferred
T_M Progeny
T_EFF Progeny
T_M Progeny
T_EFF Progeny
M45-Specific Donor T_M Cells
M38-Specific Donor T_M Cells
E
Fold Change (D7 Numbers:Transfer Number)
6.1x
****
3.3x
***
+ Isotype
+ anti-CD70
+ Isotype
+ anti-CD70
M45-Specific Donor T_M Cells
M38-Specific Donor T_M Cells

FIGURE 4

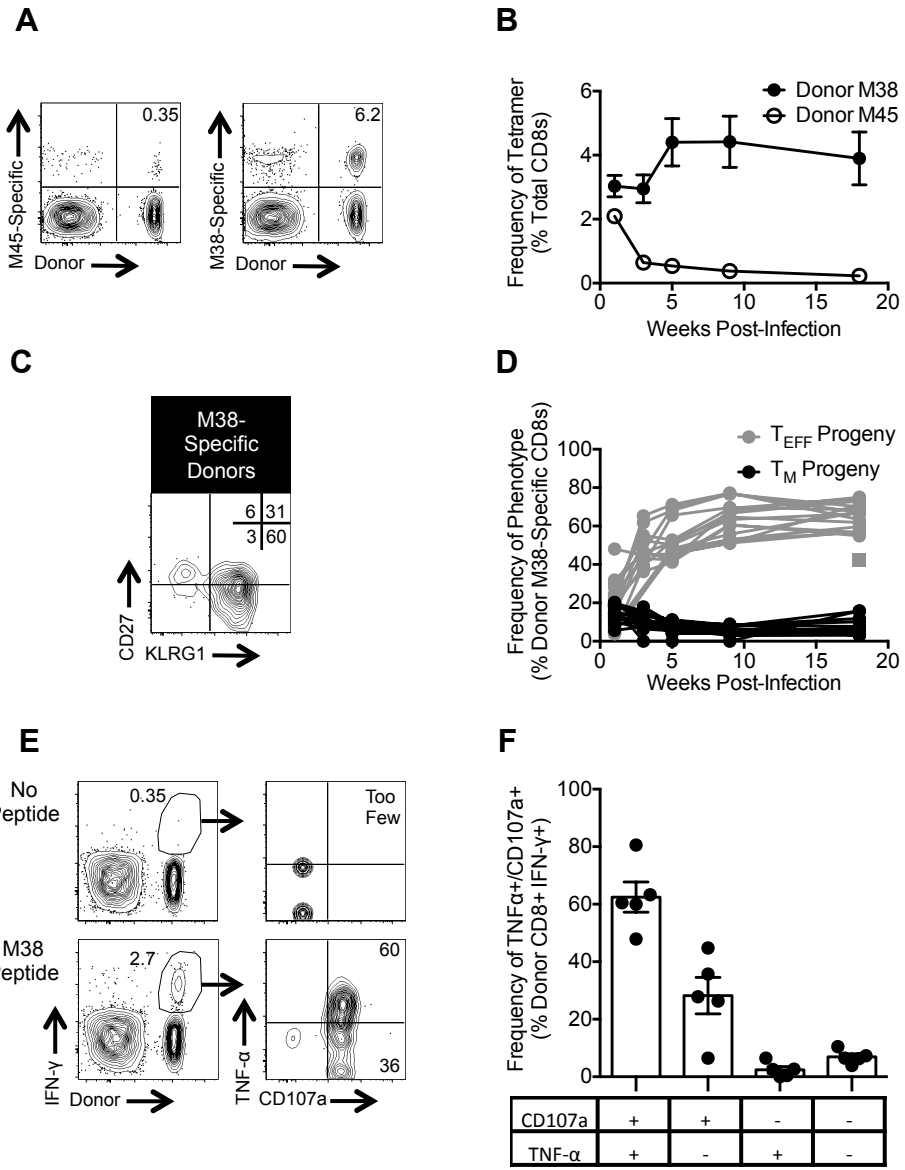
A
0.35
6.2
M45-Specific
M38-Specific
Donor
Donor
B
Donor M38
Donor M45
Frequency of Tetramer (% Total CD8s)
Weeks Post-Infection
C
M38-Specific Donors
6
31
3
60
CD27
KLRG1
D
T_{EFF} Progeny
T_M Progeny
Frequency of Phenotype (% Donor M38-Specific CD8s)
Weeks Post-Infection
E
No Peptide
0.35
Too Few
M38 Peptide
2.7
60
36
IFN-γ
Donor
TNF-α
CD107a
F
Frequency of TNFα+/CD107a+ (% Donor CD8+ IFN-γ+)
CD107a + + - -
TNF-α + - + -

FIGURE 5

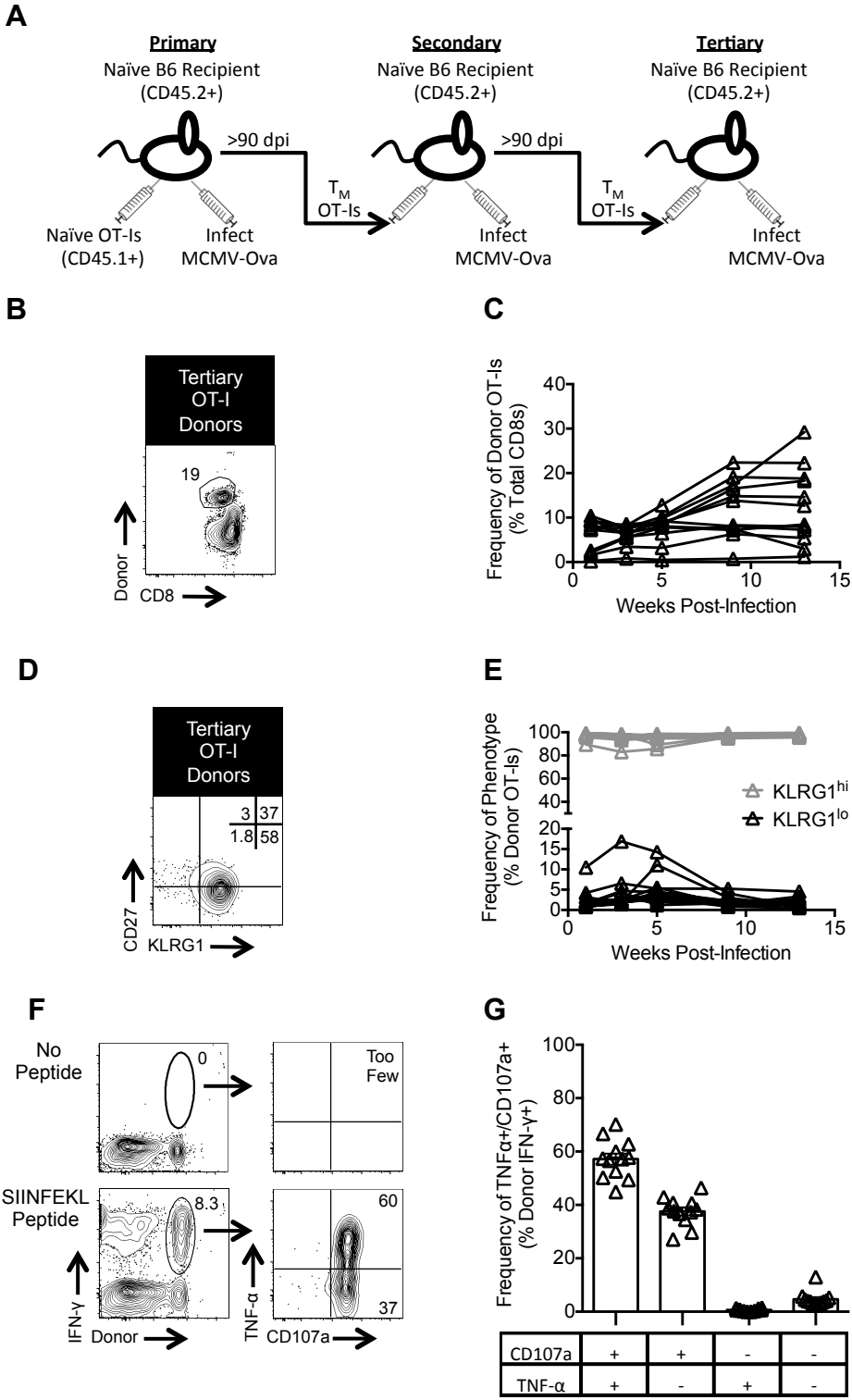
A
Primary
Naïve B6 Recipient
(CD45.2+)
>90 dpi
Naïve OT-Is
(CD45.1+)
Infect
MCMV-Ova
T_M
OT-Is
Secondary
Naïve B6 Recipient
(CD45.2+)
>90 dpi
Infect
MCMV-Ova
T_M
OT-Is
Tertiary
Naïve B6 Recipient
(CD45.2+)
Infect
MCMV-Ova
B
Tertiary
OT-I
Donors
19
Donor
CD8
C
Frequency of Donor OT-Is
(% Total CD8s)
Weeks Post-Infection
D
Tertiary
OT-I
Donors
3
37
1.8
58
CD27
KLRG1
E
Frequency of Phenotype
(% Donor OT-Is)
KLRG1hi
KLRG1lo
Weeks Post-Infection
F
No
Peptide
0
Too
Few
SIINFEKL
Peptide
8.3
60
37
IFN-γ
Donor
TNF-α
CD107a
G
Frequency of TNFα+/CD107a+
(% Donor IFN-γ+)
CD107a + + - -
TNF-α + - + -

FIGURE 6

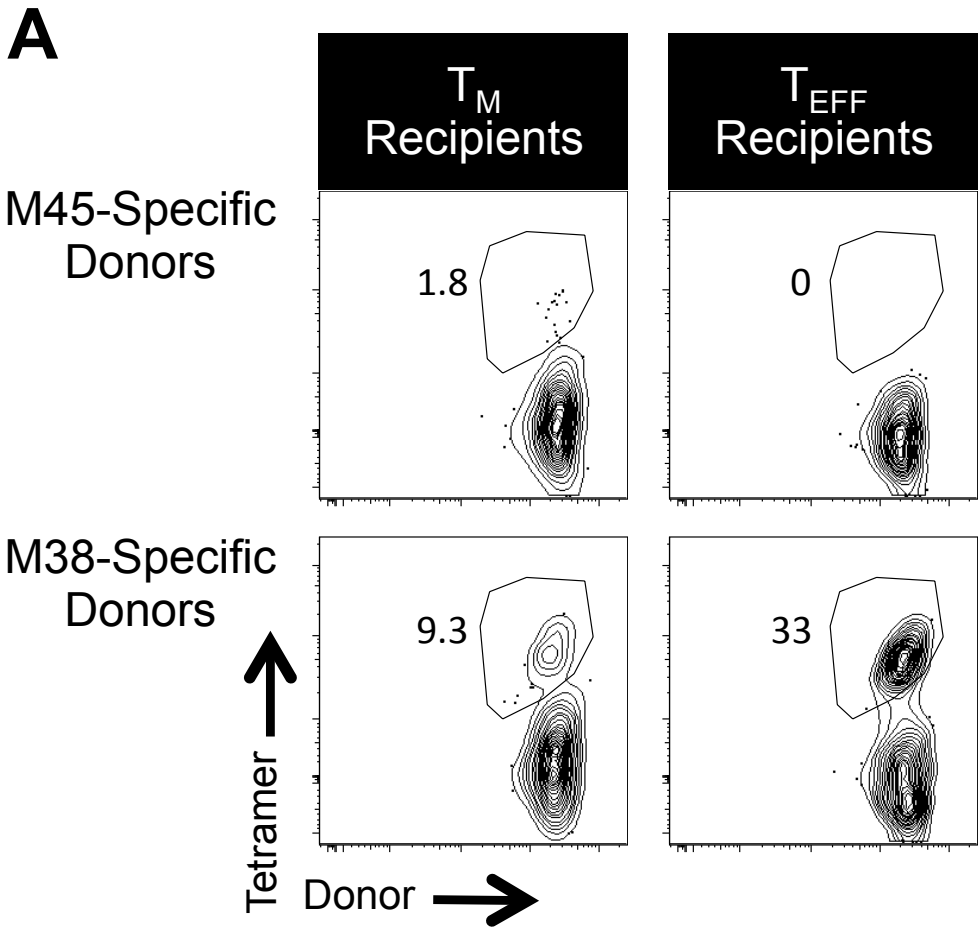
A
T_M Recipients
T_{EFF} Recipients
M45-Specific Donors
M38-Specific Donors
1.8
0
9.3
33
Tetramer
Donor

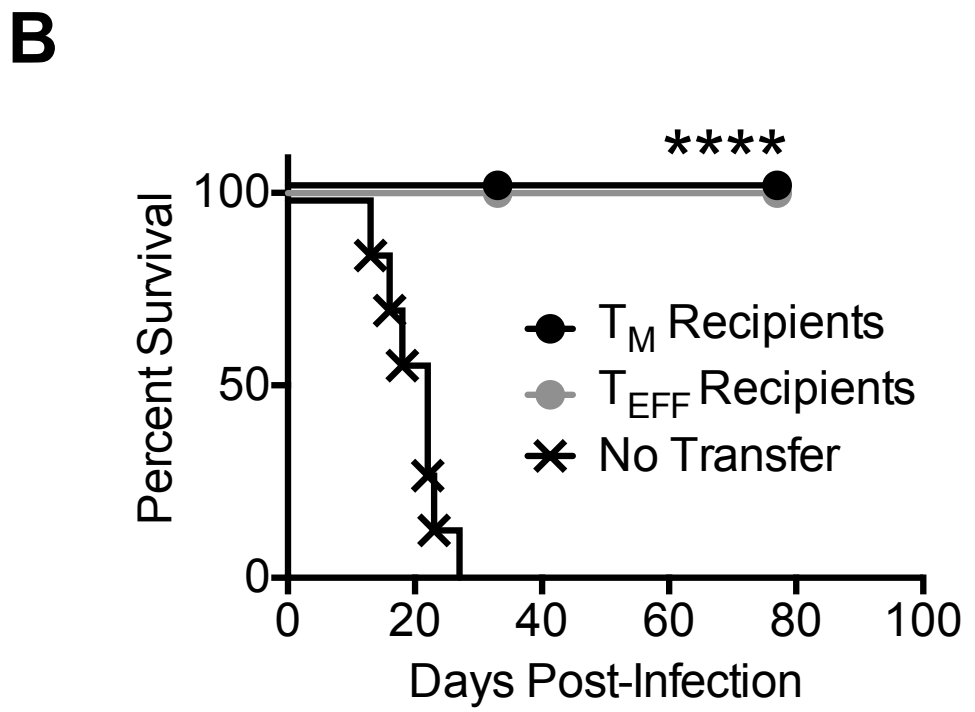
B
****
100
50
0
Percent Survival
T_M Recipients
T_{EFF} Recipients
No Transfer
0
20
40
60
80
100
Days Post-Infection

FIGURE 7

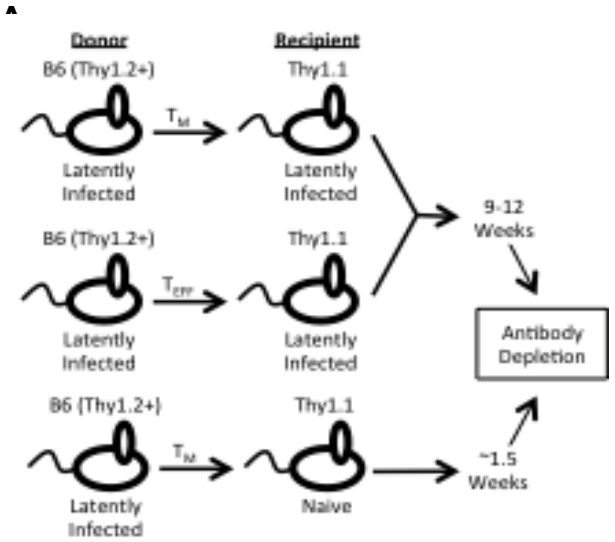
A
Donor
Recipient
B6 (Thy1.2+)
Thy1.1
T_M
Latently Infected
Latently Infected
9-12 Weeks
T_{EFF}
Antibody Depletion
Naive
~1.5 Weeks

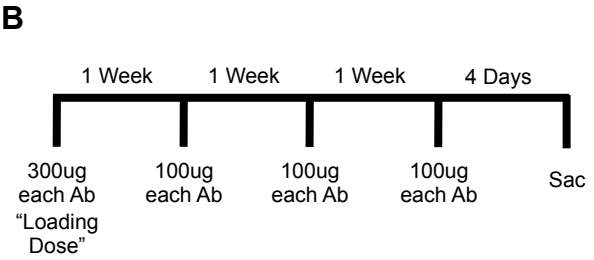
B
1 Week
1 Week
1 Week
4 Days
300ug each Ab "Loading Dose"
100ug each Ab
100ug each Ab
100ug each Ab
Sac
Antibodies = Thy1.1, CD4, NK1.1

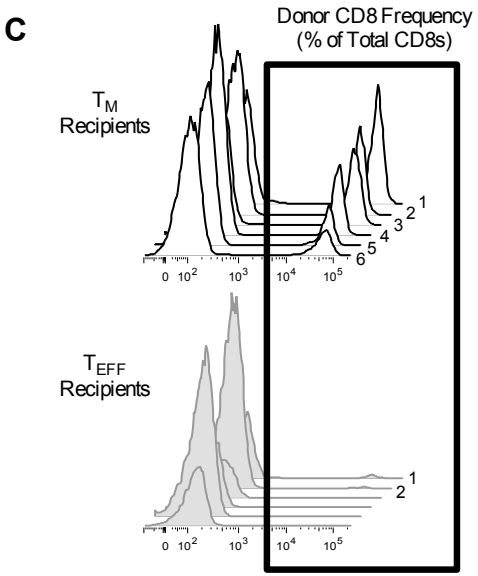
C
Donor CD8 Frequency (% of Total CD8s)
T_M Recipients
T_{EFF} Recipients

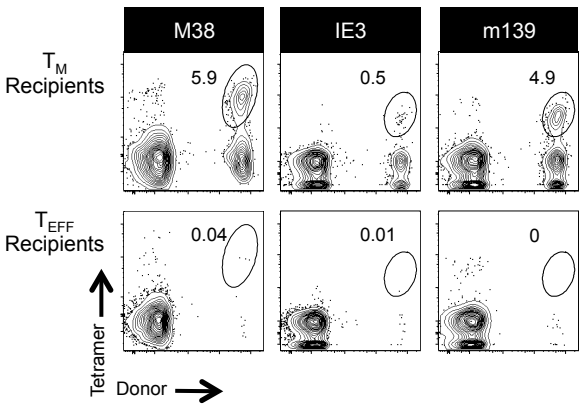
D
M38
IE3
m139
T_M Recipients
T_{EFF} Recipients
5.9
0.5
4.9
0.04
0.01
0
Tetramer
Donor

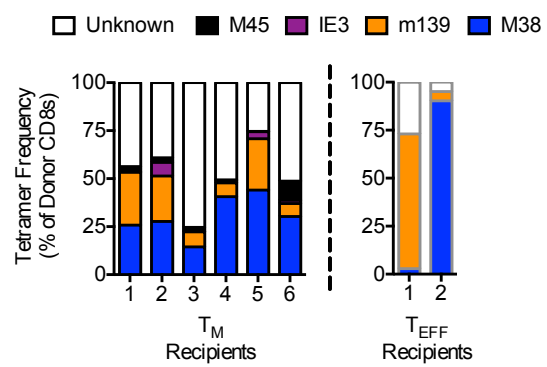
E
Unknown
M45
IE3
m139
M38
Tetramer Frequency (% of Donor CD8s)
T_M Recipients
T_{EFF} Recipients

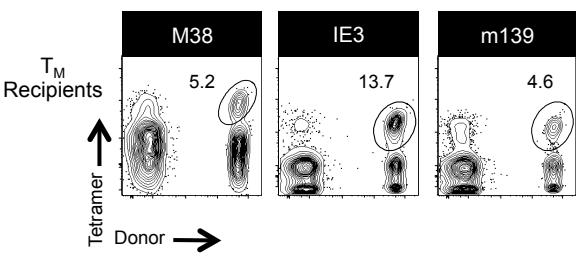
F
M38
IE3
m139
T_M Recipients
5.2
13.7
4.6
Tetramer
Donor

Supplemental Fig. 1

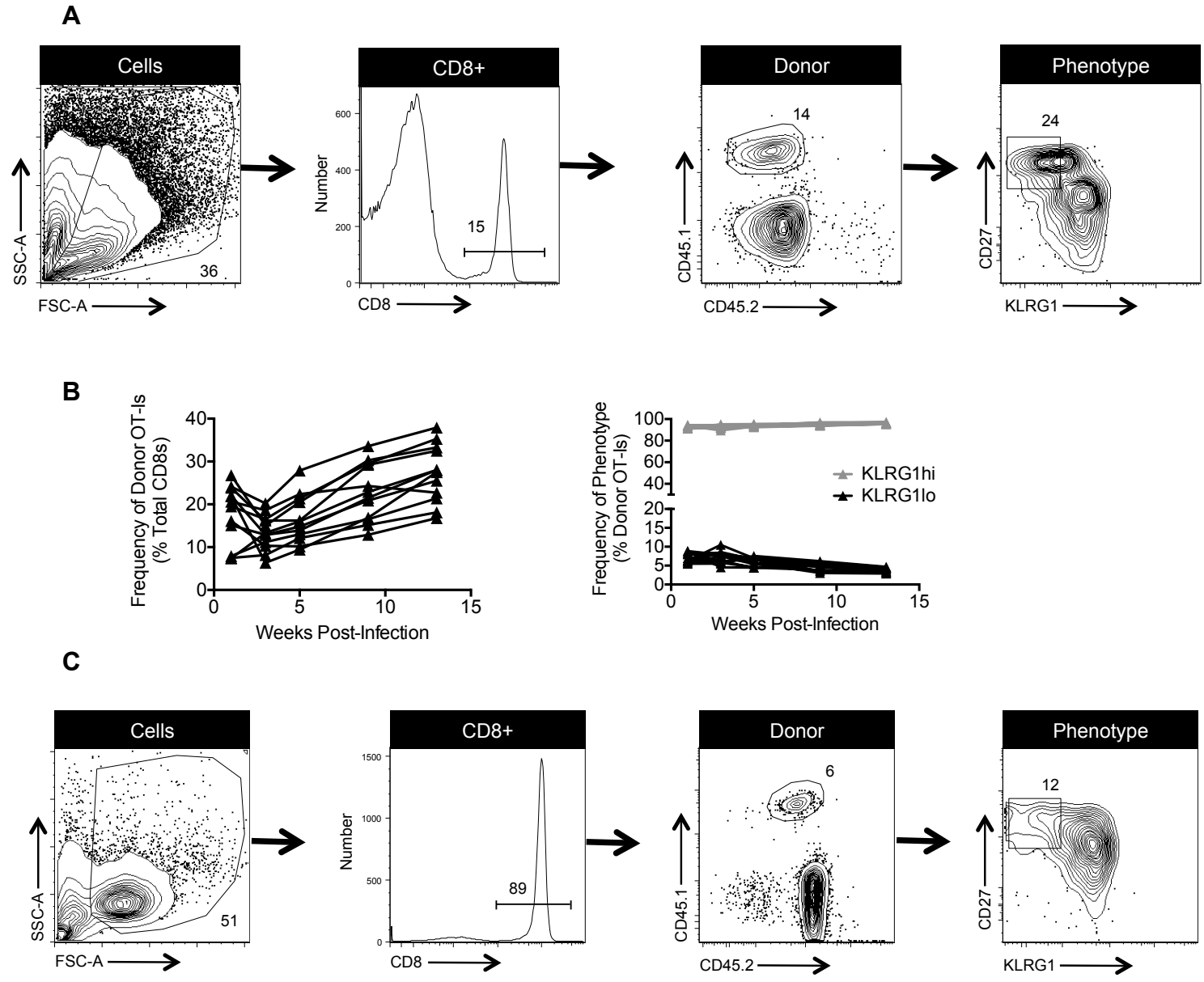

Supplemental Figure 1: Representative plots for repeat transfers and data from secondary stimulated OT-Is

(A) Sorting strategy for isolating OT-I T_M T cells after primary challenge. Briefly, 600 naïve OT-I T cells expressing CD45.1 were transferred into naive B6 (CD45.2) recipients and challenged MCMV-SL8, (i.e. primary challenge). Thirteen weeks after the primary challenge, donor OT-I T cells were sorted using the CD45.1 marker and the T_M subset was identified as $CD27^{hi}$ and $KLRG1^{lo}$. (B) 6,000 sorted T_M OT-I T cells were transferred into naïve B6 recipients and challenged with MCMV-SL8 (i.e. secondary challenge). Shown is the frequency and phenotype of blood-localized OT-Is over time, relative to total $CD8^{pos}$ T cells. Data was collected from two independent experiments (n=7 total). (C) Sorting strategy for isolating OT-I T_M T cells after secondary challenge. Briefly, thirteen weeks after the secondary challenge, donor OT-I T cells were sorted as described in (A).

Supplemental Fig. 2

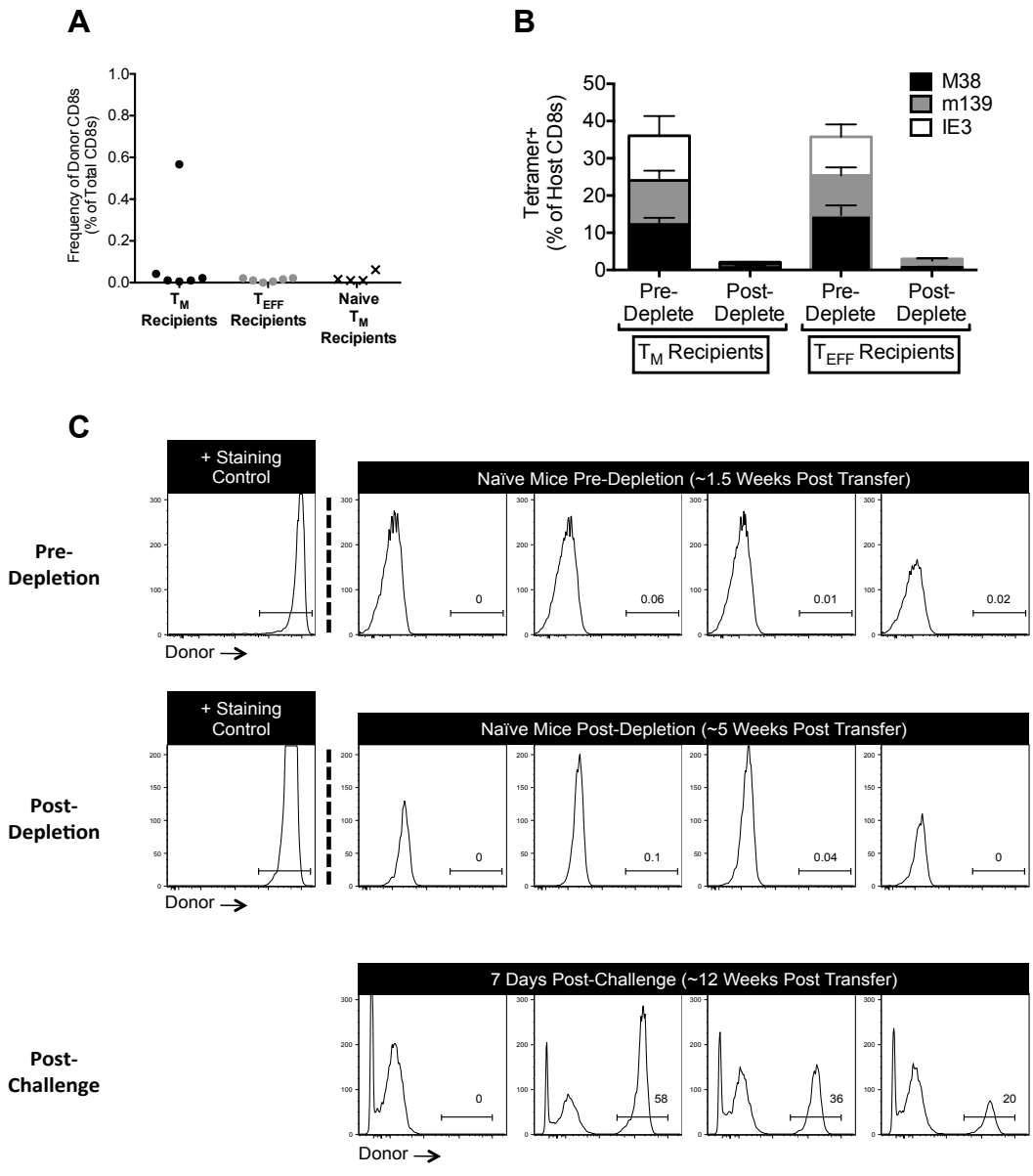

Supplemental Figure 2: Antibody depletion does not induce T_M proliferation in naïve recipients.

(A) Immediately prior to antibody depletion, the presence of donors in the blood was determined by flow cytometry. For T_M and T_{EFF} recipients, data was collected from two independent experiments (*n*=6 total). For naïve recipients, data was collected from one experiment (*n*=4 total) (B) Frequencies of total tetramer-binding $CD8^{pos}$ cells were determined in the blood of the chronically-infected Thy1.1 recipient mice prior to and immediately following the depletion scheduled in Figure 7B. Data was collected from two independent experiments (*n*=6 total) and is displayed as mean ± SEM. (C) Age matched naïve Thy1.1 recipients received T_M cells from a MCMV chronically-infected donor. Recipients were bled "pre-depletion" at 1.5 weeks post-transfer. Mice were started on the antibody depletion regimen immediately following the "pre-depletion" bleed and were bled again "post-depletion" at approximately 5 weeks post-transfer. A B6 mouse ($Thy1.2^{pos}$) was used as the positive staining control. Naïve mice were challenged with MCMV approximately 12 weeks after the adoptive transfer. Data was collected from one experiment (*n*=4 total).

Supplemental Fig. 3

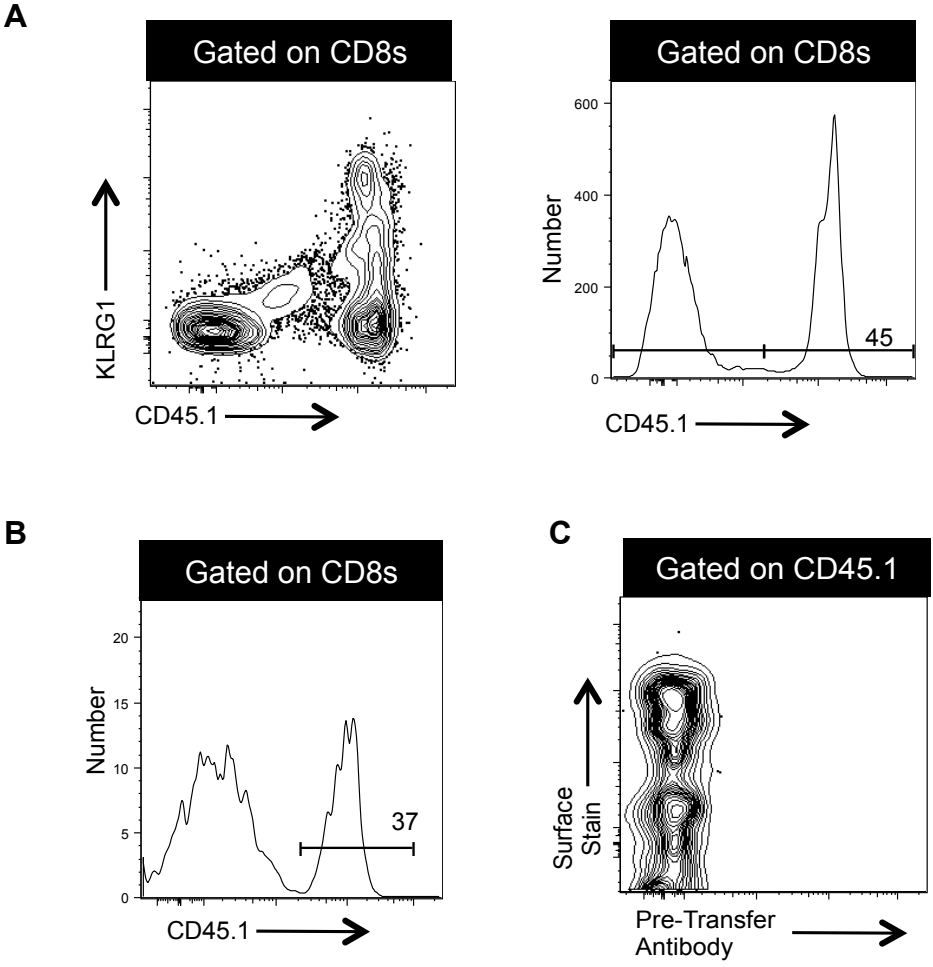

Supplemental Figure 3: The KLRG1-specific antibody used for sorting does not deplete transferred cells.
(A) CD45.1 splenocytes were stained with the anti-KLRG1 antibody (clone 2F1), mixed with unstained CD45.2 splenocytes in a 1:1 ratio and transferred into B6.CB17-*Prkdc*^{scid} (SCID) mice from Jackson. The representative FACS plots show the KLRG1 stain of CD45.1^{pos}, but not CD45.2^{pos} cells (left) and the proportion of transferred cells that were CD45.1^{pos} (right). (B) Six days after transfer, SCID recipients were bled and analyzed by flow cytometry. CD45.1^{pos} cells were still a similar proportion of the transferred T cells (compare to A), suggesting that the large CD45.1^{pos} KLRG1-stained population was not depleted. (C) Anti-KLRG1 staining six days after the transfer showed that there were still KLRG1^{hi} CD45.1^{pos} cells. As KLRG1 expression has been shown to be dependent on antigen stimulation, it is unlikely that the KLRG1^{hi} cells were newly formed. Importantly, the CD45.1^{pos} cells detected 6 days after transfer were no longer positive for the KLRG1 antibody used prior to the transfer (not shown), suggesting that the cells have not been depleted and have cleared the antibody off their surface. Data was collected from a single experiment (n=3 total).

Supplemental Table 1A: Transcripts UP in T_{EFF} relative to T_M

NAME	PROBE	GENE SYMBOL	GENE TITLE	RANK IN GENE LIST	RANK METRIC SCORE	RUNNING ES	CORE ENRICHMENT
row_0	ANXA6	ANXA6	annexin A6	29	2.201579809	0.045963388	Yes
row_1	HMGB2	HMGB2	high-mobility group box 2	48	2.035401106	0.088924415	Yes
row_2	ANXA4	ANXA4	annexin A4	59	1.94921422	0.13044995	Yes
row_3	GZMB	GZMB	granzyme B (granzyme 2, cytotoxic T-lymphocyte-associated serine esterase 1)	123	1.62263608	0.16212006	Yes
row_4	CD244	CD244	CD244 molecule, natural killer cell receptor 2B4	153	1.540912032	0.19382909	Yes
row_5	CAPN2	CAPN2	calpain 2, (m/II) large subunit	271	1.351189613	0.21678028	Yes
row_6	AP1S2	AP1S2	adaptor-related protein complex 1, sigma 2 subunit	332	1.288847923	0.24140769	Yes
row_7	LGALS1	LGALS1	lectin, galactoside-binding, soluble, 1 (galectin 1)	430	1.199626088	0.26214892	Yes
row_8	EBP	EBP	emopamil binding protein (sterol isomerase)	465	1.172553301	0.28564534	Yes
row_9	IKZF3	IKZF3	IKAROS family zinc finger 3 (Aiolos)	582	1.106175661	0.30336317	Yes
row_10	CA5B	CA5B	carbonic anhydrase VB, mitochondrial	710	1.037609816	0.3190186	Yes
row_11	SPN	SPN	sialophorin (leukosialin, CD43)	881	0.962003529	0.33076355	Yes
row_12	CX3CR1	CX3CR1	chemokine (C-X3-C motif) receptor 1	939	0.938199341	0.34798452	Yes
row_13	SEP11	SEP11	septin 11	970	0.926925778	0.3663934	Yes
row_14	STMN1	STMN1	stathmin 1/oncoprotein 18	1020	0.913609505	0.38350785	Yes
row_15	PYCARD	PYCARD	PYD and CARD domain containing	1208	0.852552652	0.39199024	Yes
row_16	NKG7	NKG7	natural killer cell group 7 sequence	1518	0.775441468	0.39234224	Yes
row_17	NSMAF	NSMAF	neutral sphingomyelinase (N-SMase) activation associated factor	1534	0.772185385	0.40820757	Yes
row_18	SYTL2	SYTL2	synaptotagmin-like 2	1560	0.765723646	0.4234034	Yes
row_19	ZEB2	null	null	1566	0.764536202	0.43963376	Yes
row_20	KLRG1	KLRG1	killer cell lectin-like receptor subfamily G, member 1	1857	0.708328545	0.43954486	Yes
row_21	CASP1	CASP1	caspase 1, apoptosis-related cysteine peptidase (interleukin 1, beta, convertase)	2087	0.667113006	0.44180003	Yes
row_22	CRIPT	CRIPT	cysteine-rich PDZ-binding protein	2120	0.659288228	0.45432845	Yes
row_23	S1PR5	null	null	2173	0.652283788	0.4656456	Yes
row_24	RAP2A	RAP2A	RAP2A, member of RAS oncogene family	2263	0.638532639	0.4747049	Yes
row_25	SUOX	SUOX	sulfite oxidase	2596	0.594230175	0.469928	Yes
row_26	NUF2	null	null	2677	0.583921313	0.47828606	Yes
row_27	HIST1H2BN	HIST1H2BN	histone cluster 1, H2bn	2817	0.562394679	0.48305234	Yes
row_28	RAB27A	RAB27A	RAB27A, member RAS oncogene family	3105	0.530466557	0.47928497	Yes
row_29	GZMA	GZMA	granzyme A (granzyme 1, cytotoxic T-lymphocyte-associated serine esterase 3)	3488	0.489474744	0.46959764	Yes
row_30	REEP5	REEP5	receptor accessory protein 5	3539	0.485018671	0.477412	Yes
row_31	SYT11	SYT11	synaptotagmin XI	3719	0.466942877	0.4779986	Yes
row_32	GABARAPL2	GABARAPL2	GABA(A) receptor-associated protein-like 2	3737	0.46474728	0.48712474	Yes
row_33	S100A4	S100A4	S100 calcium binding protein A4	3739	0.464631855	0.49709648	Yes
row_34	SLAMF7	SLAMF7	SLAM family member 7	3882	0.447826445	0.49923187	Yes
row_35	KLRC1	KLRC1	killer cell lectin-like receptor subfamily C, member 1	3929	0.443369746	0.50635964	Yes
row_36	DOCK5	DOCK5	dedicator of cytokinesis 5	3976	0.438772231	0.51338816	Yes
row_37	CD48	CD48	CD48 molecule	4013	0.435482979	0.5208758	Yes
row_38	GIMAP7	GIMAP7	GTPase, IMAP family member 7	4790	0.363893896	0.48759487	No
row_39	FUT11	FUT11	fucosyltransferase 11 (alpha (1,3) fucosyltransferase)	4895	0.355715871	0.48975712	No
row_40	CENPE	CENPE	centromere protein E, 312kDa	5014	0.345196247	0.49095032	No
row_41	KLRD1	KLRD1	killer cell lectin-like receptor subfamily D, member 1	5222	0.32846266	0.487065	No
row_42	RAP1GAP2	null	null	5275	0.322605729	0.49126914	No
row_43	CYSLTR2	CYSLTR2	cysteinyl leukotriene receptor 2	5287	0.321255773	0.4976174	No
row_44	ESM1	ESM1	endothelial cell-specific molecule 1	5351	0.316171378	0.50109965	No
row_45	FGL2	FGL2	fibrinogen-like 2	5635	0.294212759	0.49244696	No
row_46	PLEK	PLEK	pleckstrin	5828	0.278107136	0.48827025	No
row_47	KCNJ8	KCNJ8	potassium inwardly-rectifying channel, subfamily J, member 8	5934	0.270331919	0.48853728	No
row_48	NCAPG	NCAPG	non-SMC condensin I complex, subunit G	6372	0.237775877	0.4705041	No
row_49	ST3GAL4	ST3GAL4	ST3 beta-galactoside alpha-2,3-sialyltransferase 4	6538	0.227307007	0.4666625	No
row_50	INSL6	INSL6	insulin-like 6	7220	0.179024309	0.4344284	No
row_51	MYADM	MYADM	myeloid-associated differentiation marker	7421	0.162519217	0.42733377	No
row_52	KIAA0101	KIAA0101	KIAA0101	7670	0.143709034	0.41728905	No
row_53	KLRK1	KLRK1	killer cell lectin-like receptor subfamily K, member 1	8076	0.112943329	0.3982587	No
row_54	RUNX1	RUNX1	runt-related transcription factor 1 (acute myeloid leukemia 1; aml1 oncogene)	8205	0.104097836	0.39371997	No
row_55	CSPP1	CSPP1	centrosome and spindle pole associated protein 1	8271	0.099030837	0.3924113	No

T-EFF biased	
Normalized Enrichment Score (NES)	2.1315544
Nominal p-value	0
FDR q-value	0
FWER p-Value	0

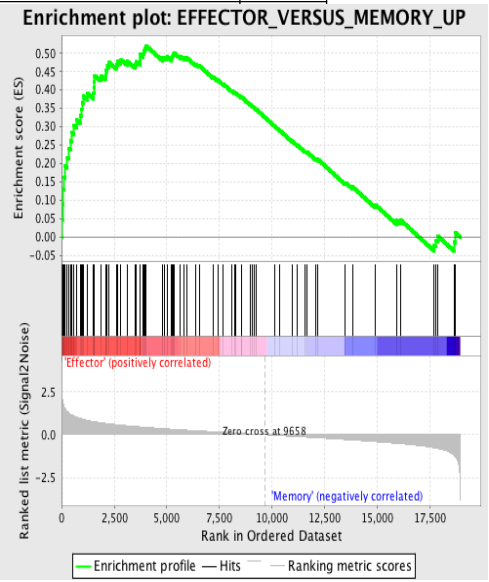

Supplemental Table 1A: Comparing transcripts UP in CMV-specific T_{EFF} relative to CMV-specific T_M cells from mice and humans.
List shows significantly altered mouse genes (2-fold up or down and $p<.05$). The table also includes a GSEA analysis of these mouse gene sets relative to each of the indicated human data sets, rank ordered by expression (see methods) and FWER significance to control for multiple testing.

row_56	TAF9B	TAF9B	TAF9B RNA polymerase II, TATA box binding protein (TBP)-associated factor, 31kDa	8535	0.080059439	0.38019818	No	
row_57	NUSAP1	NUSAP1	nucleolar and spindle associated protein 1	8559	0.078409061	0.3806708	No	
row_58	ANXA1	ANXA1	annexin A1	8977	0.046614461	0.35957327	No	
row_59	GPX8	null	null	9050	0.042167794	0.35666668	No	
row_60	ANXA2	ANXA2	annexin A2	9161	0.033796653	0.35156527	No	
row_61	KIF11	KIF11	kinesin family member 11	9239	0.028000101	0.348088	No	
row_62	CASC5	CASC5	cancer susceptibility candidate 5	10134	-0.028975241	0.3013263	No	**T-MEM biased**
row_63	HIST1H2BI	HIST1H2BI	histone cluster 1, H2bi	10379	-0.047193091	0.28941122	No	
row_64	PRDM1	PRDM1	PR domain containing 1, with ZNF domain	10943	-0.087488279	0.2614568	No	
row_65	RAB5B	RAB5B	RAB5B, member RAS oncogene family	11206	-0.106175564	0.24986018	No	
row_66	SPC25	null	null	11582	-0.130460307	0.23279792	No	
row_67	S100A10	S100A10	S100 calcium binding protein A10	11678	-0.136860937	0.23071527	No	
row_68	SYTL3	SYTL3	synaptotagmin-like 3	12076	-0.165555894	0.21324411	No	
row_69	AS3MT	AS3MT	arsenic (+3 oxidation state) methyltransferase	12183	-0.173790261	0.21137518	No	
row_70	APOBEC2	APOBEC2	apolipoprotein B mRNA editing enzyme, catalytic polypeptide-like 2	13491	-0.275097936	0.14803253	No	
row_71	RPA3	RPA3	replication protein A3, 14kDa	13828	-0.302330554	0.13674569	No	
row_72	OSBPL3	OSBPL3	oxysterol binding protein-like 3	14911	-0.398935348	0.08800114	No	
row_73	MKI67	MKI67	antigen identified by monoclonal antibody Ki-67	15923	-0.497105926	0.04513806	No	
row_74	MXI1	MXI1	MAX interactor 1	16098	-0.51361376	0.04699668	No	
row_75	IL18RAP	IL18RAP	interleukin 18 receptor accessory protein	17706	-0.753345549	-0.02192908	No	
row_76	PRC1	PRC1	protein regulator of cytokinesis 1	17790	-0.772486866	-0.009661613	No	
row_77	CCNA2	CCNA2	cyclin A2	17875	-0.79208225	0.002975634	No	
row_78	GZMK	GZMK	granzyme K (granzyme 3; tryptase II)	18643	-1.195715308	-0.011881162	No	
row_79	TOP2A	TOP2A	topoisomerase (DNA) II alpha 170kDa	18720	-1.290148854	0.011926243	No	

Supplemental Table 1A: Comparing transcripts UP in CMV-specific T_{EFF} relative to CMV-specific T_M cells from mice and humans.
List shows significantly altered mouse genes (2-fold up or down and $p<.05$). The table also includes a GSEA analysis of these mouse gene sets relative to each of the indicated human data sets, rank ordered by expression (see methods) and FWER significance to control for multiple testing.

Supplemental Table 1B: Transcripts UP in T_M relative to T_{EFF}

NAME	PROBE	GENE SYMBOL	GENE TITLE	RANK IN GENE LIST	RANK METRIC SCORE	RUNNING ES	CORE ENRICHMENT
row_0	PHPT1	PHPT1	phosphohistidine phosphatase 1	37	2.124774694	0.026149271	No
row_1	HSPB11	null	null	290	1.328898907	0.030335644	No
row_2	LSM7	LSM7	LSM7 homolog, U6 small nuclear RNA associated (S. cerevisiae)	329	1.291045427	0.045399252	No
row_3	IFI27L2	null	null	592	1.101828933	0.04604919	No
row_4	RTP4	RTP4	receptor transporter protein 4	600	1.096092939	0.060181282	No
row_5	MED4	MED4	mediator of RNA polymerase II transcription, subunit 4 homolog (S. cerevisiae)	842	0.978564978	0.06031665	No
row_6	RPS29	RPS29	ribosomal protein S29	901	0.955645084	0.06987862	No
row_7	RAPGEF4	RAPGEF4	Rap guanine nucleotide exchange factor (GEF) 4	1484	0.782799721	0.049292903	No
row_8	CYB5A	CYB5A	cytochrome b5 type A (microsomal)	1502	0.778091848	0.05868529	No
row_9	MRPS5	MRPS5	mitochondrial ribosomal protein S5	2032	0.676983833	0.03951729	No
row_10	PIP4K2A	null	null	2133	0.656981051	0.04289404	No
row_11	APEX1	APEX1	APEX nuclease (multifunctional DNA repair enzyme) 1	2262	0.638559878	0.0445383	No
row_12	QSER1	QSER1	glutamine and serine rich 1	2270	0.637303054	0.052599363	No
row_13	SH3BP5	SH3BP5	SH3-domain binding protein 5 (BTK-associated)	2576	0.596591115	0.044277374	No
row_14	PDK1	PDK1	pyruvate dehydrogenase kinase, isozyme 1	2753	0.571303666	0.042479545	No
row_15	SEPP1	SEPP1	selenoprotein P, plasma, 1	2844	0.559307992	0.045095507	No
row_16	STAMBPL1	STAMBPL1	STAM binding protein-like 1	3096	0.531519473	0.03878356	No
row_17	ITGAE	ITGAE	integrin, alpha E (antigen CD103, human mucosal lymphocyte antigen 1; alpha polypeptide)	3106	0.530423522	0.04532398	No
row_18	TLR1	TLR1	toll-like receptor 1	3210	0.518464327	0.046708275	No
row_19	ZNF761	ZNF761	zinc finger protein 761	3302	0.50811398	0.04859363	No
row_20	F2RL1	F2RL1	coagulation factor II (thrombin) receptor-like 1	3342	0.504218102	0.053192213	No
row_21	NAT1	NAT1	N-acetyltransferase 1 (arylamine N-acetyltransferase)	3507	0.488090605	0.05093128	No
row_22	DAPL1	DAPL1	death associated protein-like 1	3673	0.47194767	0.04840356	No
row_23	HINT3	HINT3	histidine triad nucleotide binding protein 3	3834	0.453408092	0.04589636	No
row_24	LTV1	LTV1	LTV1 homolog (S. cerevisiae)	4081	0.428189248	0.03848292	No
row_25	IMPDH2	IMPDH2	IMP (inosine monophosphate) dehydrogenase 2	4847	0.359094143	0.002560527	No
row_26	DUSP10	DUSP10	dual specificity phosphatase 10	4855	0.35811159	0.00692713	No
row_27	RRP15	null	null	4880	0.356415987	0.010367425	No
row_28	XCL1	XCL1	chemokine (C motif) ligand 1	5056	0.342206746	0.005591196	No
row_29	BCL9	BCL9	B-cell CLL/lymphoma 9	5238	0.326921731	2.94E-04	No
row_30	PRDX6	PRDX6	peroxiredoxin 6	5248	0.325534701	0.004122876	No
row_31	CD3D	CD3D	CD3d molecule, delta (CD3-TCR complex)	5438	0.309563071	-0.001829683	No
row_32	TOX	TOX	-	5553	0.300573617	-0.003913531	No
row_33	DKC1	DKC1	dyskeratosis congenita 1, dyskerin	5581	0.298592925	-0.001397898	No
row_34	RPS19	RPS19	ribosomal protein S19	5641	0.293431848	-6.52E-04	No
row_35	RPLP1	RPLP1	ribosomal protein, large, P1	5781	0.281639785	-0.004315579	No
row_36	CCDC91	CCDC91	coiled-coil domain containing 91	5822	0.278348088	-0.002759035	No
row_37	SLFN5	SLFN5	schlafen family member 5	5899	0.273217082	-0.003184468	No
row_38	FBL	FBL	fibrillarin	5910	0.27217257	-1.15E-04	No
row_39	TMLHE	TMLHE	trimethyllysine hydroxylase, epsilon	6244	0.246418536	-0.014559025	No
row_40	IFT80	IFT80	intraflagellar transport 80 homolog (Chlamydomonas)	6313	0.242544681	-0.014964985	No
row_41	LY6E	LY6E	lymphocyte antigen 6 complex, locus E	6424	0.234440193	-0.017711282	No
row_42	ATP1B1	ATP1B1	ATPase, Na+/K+ transporting, beta 1 polypeptide	6548	0.226953819	-0.02124784	No
row_43	TTC27	TTC27	tetratricopeptide repeat domain 27	7498	0.156670496	-0.06963192	No
row_44	USP28	USP28	ubiquitin specific peptidase 28	7576	0.150735766	-0.07173128	No
row_45	ACTN1	ACTN1	actinin, alpha 1	7597	0.148684606	-0.07082716	No
row_46	SSBP2	SSBP2	single-stranded DNA binding protein 2	7678	0.14299418	-0.07318846	No
row_47	HRSP12	HRSP12	heat-responsive protein 12	7680	0.142702043	-0.0713533	No
row_48	SLAMF6	SLAMF6	SLAM family member 6	7685	0.142558053	-0.06967954	No
row_49	RPL29	RPL29	ribosomal protein L29	7738	0.138756722	-0.0706082	No
row_50	RPL14	RPL14	ribosomal protein L14	7785	0.135675624	-0.07125861	No
row_51	RRAS2	RRAS2	related RAS viral (r-ras) oncogene homolog 2	7850	0.130808711	-0.07293046	No
row_52	KBTBD11	KBTBD11	kelch repeat and BTB (POZ) domain containing 11	7905	0.126582831	-0.07412655	No
row_53	RPL10A	RPL10A	ribosomal protein L10a	7936	0.123617478	-0.074085824	No
row_54	LZTFL1	LZTFL1	leucine zipper transcription factor-like 1	8371	0.092378221	-0.0959387	No
row_55	TTC3	TTC3	tetratricopeptide repeat domain 3	8384	0.091630973	-0.0953642	No

T-EFF biased	
Normalized Enrichment Score (NES)	-1.6801751
Nominal p-value	0.00777202
FDR q-value	8.90E-04
FWER p-Value	0.003

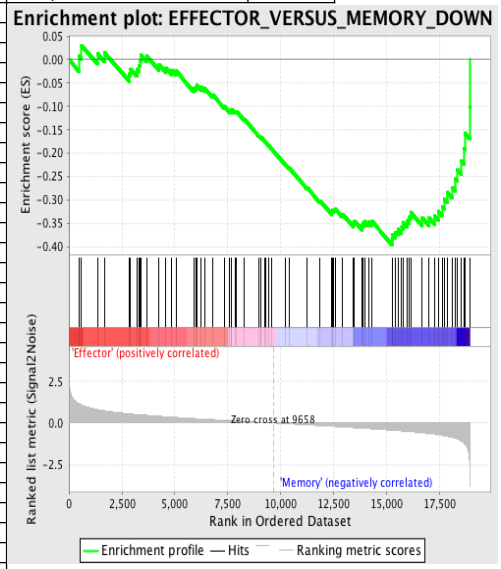

Supplemental Table 1B: Comparing transcripts UP in CMV-specific T_M relative to CMV-specific T_{EFF} cells from mice and humans.
List shows significantly altered mouse genes (2-fold up or down and $p<.05$). The table also includes a GSEA analysis of these mouse gene sets relative to each of the indicated human data sets, rank ordered by expression (see methods) and FWER significance to control for multiple testing.

row_56	RPS26	RPS26	ribosomal protein S26	8636	0.072893247	-0.10774501	No
row_57	KLHDC1	KLHDC1	kelch domain containing 1	8877	0.055129666	-0.11977602	No
row_58	HMP19	HMP19	-	9065	0.040402696	-0.12918396	No
row_59	BZW2	BZW2	basic leucine zipper and W2 domains 2	9068	0.040138628	-0.12875916	No
row_60	GID4	null	null	9096	0.038265821	-0.12968835	No
row_61	CHURC1	CHURC1	churchill domain containing 1	9274	0.025683668	-0.13875937	No
row_62	KIAA1033	KIAA1033	KIAA1033	9314	0.022567095	-0.14053434	No
row_63	MRPL23	MRPL23	mitochondrial ribosomal protein L23	9397	0.016983615	-0.14466944	No
row_64	EGR2	EGR2	early growth response 2 (Krox-20 homolog, Drosophila)	10037	-0.020757651	-0.17836967	No
row_65	LPHN2	LPHN2	latrophilin 2	10097	-0.025689999	-0.1811667	No
row_66	XKRX	XKRX	XK, Kell blood group complex subunit-related, X-linked	10256	-0.038267016	-0.18906099	No
row_67	LCLAT1	null	null	10373	-0.04668713	-0.19461079	No
row_68	INSR	INSR	insulin receptor	10396	-0.048602778	-0.19513735	No
row_69	RPL8	RPL8	ribosomal protein L8	10560	-0.059909303	-0.20301111	No
row_70	GPATCH4	null	null	10752	-0.074455388	-0.21218112	No
row_71	TRIB2	TRIB2	tribbles homolog 2 (Drosophila)	11027	-0.093001895	-0.22551872	No
row_72	RPL18	RPL18	ribosomal protein L18	11234	-0.108678244	-0.23503341	No
row_73	TRIM13	TRIM13	tripartite motif-containing 13	11801	-0.14649047	-0.2631885	No
row_74	LYPD6B	null	null	11911	-0.15424104	-0.2669429	No
row_75	MGST2	MGST2	microsomal glutathione S-transferase 2	11950	-0.156489357	-0.26689252	No
row_76	ACSL3	ACSL3	acyl-CoA synthetase long-chain family member 3	12373	-0.187292844	-0.2868514	No
row_77	DPP4	DPP4	dipeptidyl-peptidase 4 (CD26, adenosine deaminase complexing protein 2)	12434	-0.19199796	-0.2875009	No
row_78	ZBTB10	ZBTB10	zinc finger and BTB domain containing 10	12514	-0.198208988	-0.28907838	No
row_79	NEDD4L	NEDD4L	neural precursor cell expressed, developmentally down-regulated 4-like	12830	-0.22265242	-0.3028803	No
row_80	EPHX1	EPHX1	epoxide hydrolase 1, microsomal (xenobiotic)	12871	-0.225831643	-0.30201867	No
row_81	MYC	MYC	v-myc myelocytomatosis viral oncogene homolog (avian)	12915	-0.229761392	-0.30126455	No
row_82	TSPAN13	TSPAN13	tetraspanin 13	12940	-0.232248098	-0.29946736	No
row_83	EEF1B2	EEF1B2	eukaryotic translation elongation factor 1 beta 2	13130	-0.247839764	-0.30623668	No
row_84	TFRC	TFRC	transferrin receptor (p90, CD71)	13593	-0.283705652	-0.32704648	No
row_85	P2RY10	P2RY10	purinergic receptor P2Y, G-protein coupled, 10	13647	-0.288299233	-0.32604948	No
row_86	LEF1	LEF1	lymphoid enhancer-binding factor 1	13701	-0.291425049	-0.32501107	No
row_87	IFNGR2	IFNGR2	interferon gamma receptor 2 (interferon gamma transducer 1)	13751	-0.295711279	-0.3237033	No
row_88	SPRED2	SPRED2	sprouty-related, EVH1 domain containing 2	13872	-0.30734697	-0.32601652	No
row_89	TNFSF8	TNFSF8	tumor necrosis factor (ligand) superfamily, member 8	13970	-0.315796912	-0.32699504	No
row_90	CMSS1	null	null	13996	-0.318091691	-0.32411507	No
row_91	PECAM1	PECAM1	platelet/endothelial cell adhesion molecule (CD31 antigen)	14002	-0.318354994	-0.3201682	No
row_92	MYB	MYB	v-myb myeloblastosis viral oncogene homolog (avian)	14205	-0.335532546	-0.32646832	No
row_93	JUN	JUN	jun oncogene	14239	-0.338070452	-0.3237493	No
row_94	RPL13	RPL13	ribosomal protein L13	14346	-0.346955091	-0.32479405	No
row_95	RPS2	RPS2	ribosomal protein S2	14452	-0.356475323	-0.32565963	No
row_96	PCGF5	PCGF5	polycomb group ring finger 5	14522	-0.362784624	-0.32452768	No
row_97	CNGA1	CNGA1	cyclic nucleotide gated channel alpha 1	14723	-0.381109834	-0.33011833	No
row_98	GRIA3	GRIA3	glutamate receptor, ionotrophic, AMPA 3	14748	-0.382496178	-0.32633293	No
row_99	DPH5	DPH5	DPH5 homolog (S. cerevisiae)	14846	-0.391592532	-0.32630846	No
row_100	RGS10	RGS10	regulator of G-protein signalling 10	15259	-0.433039695	-0.34248376	No
row_101	EMB	EMB	embigin homolog (mouse)	15436	-0.449893624	-0.34588817	No
row_102	SELL	SELL	selectin L (lymphocyte adhesion molecule 1)	15556	-0.460011512	-0.34612808	No
row_103	RPS5	RPS5	ribosomal protein S5	15705	-0.475598007	-0.3477036	No
row_104	RPL15	RPL15	ribosomal protein L15	15770	-0.480787158	-0.3447443	No
row_105	INPP4B	INPP4B	inositol polyphosphate-4-phosphatase, type II, 105kDa	15848	-0.489236385	-0.34236437	No
row_106	BTF3L4	BTF3L4	basic transcription factor 3-like 4	15895	-0.494006366	-0.3382731	No
row_107	IL6ST	IL6ST	interleukin 6 signal transducer (gp130, oncostatin M receptor)	16084	-0.512494206	-0.34148717	No
row_108	WDR12	WDR12	WD repeat domain 12	16295	-0.535118759	-0.34557158	No
row_109	RPL28	RPL28	ribosomal protein L28	16305	-0.537068784	-0.3389432	No
row_110	ST6GAL1	ST6GAL1	ST6 beta-galactosamide alpha-2,6-sialyltranferase 1	16420	-0.552493393	-0.33769348	No
row_111	ITGA6	ITGA6	integrin, alpha 6	16596	-0.574453831	-0.33939645	No
row_112	RPLP0	RPLP0	ribosomal protein, large, P0	16715	-0.589519203	-0.33786944	No
row_113	PELI1	PELI1	pellino homolog 1 (Drosophila)	17138	-0.650897205	-0.35169357	No
row_114	SATB1	SATB1	special AT-rich sequence binding protein 1 (binds to nuclear matrix/scaffold-associating DNA's)	17264	-0.669767857	-0.34947684	No
row_115	RPSA	RPSA	ribosomal protein SA	17448	-0.702700913	-0.3499081	No
row_116	PPIC	PPIC	peptidylprolyl isomerase C (cyclophilin C)	17721	-0.756398022	-0.35436085	Yes
row_117	DGKA	DGKA	diacylglycerol kinase, alpha 80kDa	17727	-0.758206606	-0.34459355	Yes

T-MEM biased

Supplemental Table 1B: Comparing transcripts UP in CMV-specific T_M relative to CMV-specific T_{EFF} cells from mice and humans.
List shows significantly altered mouse genes (2-fold up or down and $p<.05$). The table also includes a GSEA analysis of these mouse gene sets relative to each of the indicated human data sets, rank ordered by expression (see methods) and FWER significance to control for multiple testing.

row_118	CD69	CD69	CD69 molecule	17870	-0.790673494	-0.3416808	Yes
row_119	ST8SIA1	ST8SIA1	ST8 alpha-N-acetyl-neuraminide alpha-2,8-sialyltransferase 1	17913	-0.802390575	-0.3332961	Yes
row_120	CCR9	CCR9	chemokine (C-C motif) receptor 9	18031	-0.836443365	-0.32844844	Yes
row_121	HOOK1	HOOK1	hook homolog 1 (Drosophila)	18237	-0.906686187	-0.32735014	Yes
row_122	RAB3IP	RAB3IP	RAB3A interacting protein (rabin3)	18248	-0.911961794	-0.3158141	Yes
row_123	TCP11L2	TCP11L2	t-complex 11 (mouse) like 2	18438	-1.008909702	-0.31251243	Yes
row_124	PDE3B	PDE3B	phosphodiesterase 3B, cGMP-inhibited	18484	-1.036287308	-0.30119213	Yes
row_125	CD2AP	CD2AP	CD2-associated protein	18520	-1.068836212	-0.28890944	Yes
row_126	ICOS	ICOS	inducible T-cell co-stimulator	18674	-1.228775859	-0.28078425	Yes
row_127	CD27	null	null	18716	-1.286845565	-0.26593572	Yes
row_128	ZEB1	null	null	18771	-1.377133369	-0.25058365	Yes
row_129	TCF7	TCF7	transcription factor 7 (T-cell specific, HMG-box)	18790	-1.420588374	-0.23274246	Yes
row_130	SH3PXD2A	SH3PXD2A	SH3 and PX domains 2A	18808	-1.47138989	-0.21417587	Yes
row_131	RPS9	RPS9	ribosomal protein S9	18857	-1.63666749	-0.19507043	Yes
row_132	LTB	LTB	lymphotoxin beta (TNF superfamily, member 3)	18891	-1.829720855	-0.17261285	Yes
row_133	SESN3	SESN3	sestrin 3	18900	-1.950626612	-0.14722613	Yes
row_134	CCR7	CCR7	chemokine (C-C motif) receptor 7	18917	-2.157334805	-0.11952945	Yes
row_135	IL7R	IL7R	interleukin 7 receptor	18927	-2.443236351	-0.087677345	Yes
row_136	TRAT1	TRAT1	T cell receptor associated transmembrane adaptor 1	18943	-2.915472031	-0.04989529	Yes
row_137	GPR183	null	null	18945	-3.77461338	-1.15E-07	Yes

Supplemental Table 1B: Comparing transcripts UP in CMV-specific T_M relative to CMV-specific T_{EFF} cells from mice and humans.
List shows significantly altered mouse genes (2-fold up or down and $p<.05$). The table also includes a GSEA analysis of these mouse gene sets relative to each of the indicated human data sets, rank ordered by expression (see methods) and FWER significance to control for multiple testing.

Supplemental Table 1C: Transcripts UP in T_{EFF} relative to Naïve

NAME	PROBE	GENE SYMBOL	GENE TITLE	RANK IN GENE LIST	RANK METRIC SCORE	RUNNING ES	CORE ENRICHMENT
row_0	ITGB1	ITGB1	integrin, beta 1 (fibronectin receptor, beta polypeptide, antigen CD29 includes MDF2, MSK12)	5	4.547115803	0.019984426	Yes
row_1	TBX21	TBX21	T-box 21	12	4.094614983	0.037900336	Yes
row_2	S1PR5	null	null	22	3.814461708	0.054408733	Yes
row_3	GZMB	GZMB	granzyme B (granzyme 2, cytotoxic T-lymphocyte-associated serine esterase 1)	23	3.791385651	0.07129387	Yes
row_4	SAMD3	SAMD3	sterile alpha motif domain containing 3	25	3.75134635	0.08794741	Yes
row_5	GNPTAB	GNPTAB	N-acetylglucosamine-1-phosphate transferase, alpha and beta subunits	45	3.55580759	0.10277109	Yes
row_6	GOLIM4	null	null	57	3.421685934	0.117423676	Yes
row_7	FASLG	FASLG	Fas ligand (TNF superfamily, member 6)	63	3.370791435	0.13216928	Yes
row_8	CHSY1	CHSY1	carbohydrate (chondroitin) synthase 1	64	3.352074385	0.14709792	Yes
row_9	GZMA	GZMA	granzyme A (granzyme 1, cytotoxic T-lymphocyte-associated serine esterase 3)	67	3.331688643	0.16182922	Yes
row_10	CAMK2N1	CAMK2N1	calcium/calmodulin-dependent protein kinase II inhibitor 1	84	3.213935375	0.17529018	Yes
row_11	MYO1F	MYO1F	myosin IF	88	3.202200413	0.18939151	Yes
row_12	RAB8B	RAB8B	RAB8B, member RAS oncogene family	105	3.118102789	0.20242569	Yes
row_13	LGALS1	LGALS1	lectin, galactoside-binding, soluble, 1 (galectin 1)	134	2.969976187	0.2141608	Yes
row_14	CCL5	CCL5	chemokine (C-C motif) ligand 5	152	2.908002853	0.226206	Yes
row_15	BHLHE40	null	null	161	2.877945662	0.23859686	Yes
row_16	ITGAL	ITGAL	integrin, alpha L (antigen CD11A (p180), lymphocyte function-associated antigen 1; alpha polypeptide)	162	2.873387337	0.25139365	Yes
row_17	FAM49A	FAM49A	family with sequence similarity 49, member A	164	2.851606131	0.26404014	Yes
row_18	ITGB2	ITGB2	integrin, beta 2 (complement component 3 receptor 3 and 4 subunit)	169	2.844150066	0.2764936	Yes
row_19	CHST11	CHST11	carbohydrate (chondroitin 4) sulfotransferase 11	186	2.792424679	0.28807735	Yes
row_20	CD244	CD244	CD244 molecule, natural killer cell receptor 2B4	187	2.791054487	0.30050746	Yes
row_21	ZEB2	null	null	188	2.790454865	0.3129349	Yes
row_22	CASP4	CASP4	caspase 4, apoptosis-related cysteine peptidase	197	2.750204802	0.32475683	Yes
row_23	CCL4	CCL4	chemokine (C-C motif) ligand 4	203	2.743010283	0.33670658	Yes
row_24	F2R	F2R	coagulation factor II (thrombin) receptor	209	2.721811771	0.3485619	Yes
row_25	IQGAP2	IQGAP2	IQ motif containing GTPase activating protein 2	213	2.718414068	0.36050868	Yes
row_26	CX3CR1	CX3CR1	chemokine (C-X3-C motif) receptor 1	227	2.690318346	0.37179753	Yes
row_27	FYN	FYN	FYN oncogene related to SRC, FGR, YES	232	2.68144393	0.38352638	Yes
row_28	PRDM1	PRDM1	PR domain containing 1, with ZNF domain	246	2.635905027	0.39457288	Yes
row_29	KLRG1	KLRG1	killer cell lectin-like receptor subfamily G, member 1	284	2.517981768	0.4038155	Yes
row_30	NKG7	NKG7	natural killer cell group 7 sequence	315	2.45875144	0.41316733	Yes
row_31	ANXA2	ANXA2	annexin A2	326	2.432535887	0.42346796	Yes
row_32	HOPX	null	null	344	2.38733077	0.4331943	Yes
row_33	GOLM1	null	null	357	2.348069429	0.4430122	Yes
row_34	IFNG	IFNG	interferon, gamma	394	2.25906682	0.45115504	Yes
row_35	CXCR3	CXCR3	chemokine (C-X-C motif) receptor 3	404	2.241060257	0.4606562	Yes
row_36	IL18RAP	IL18RAP	interleukin 18 receptor accessory protein	430	2.17173934	0.46899617	Yes
row_37	GGH	GGH	gamma-glutamyl hydrolase (conjugase, folylpolygammaglutamyl hydrolase)	453	2.1221416	0.4772751	Yes
row_38	IL10RA	IL10RA	interleukin 10 receptor, alpha	484	2.0806427	0.48494297	Yes
row_39	S100A4	S100A4	S100 calcium binding protein A4	493	2.068409681	0.49372852	Yes
row_40	ATP2B4	ATP2B4	ATPase, Ca++ transporting, plasma membrane 4	599	1.917457938	0.49667367	Yes
row_41	ANXA4	ANXA4	annexin A4	605	1.91564846	0.5049387	Yes
row_42	CMKLR1	CMKLR1	chemokine-like receptor 1	621	1.891701698	0.51256436	Yes
row_43	SYT11	SYT11	synaptotagmin XI	665	1.837343931	0.51845604	Yes
row_44	HMGB2	HMGB2	high-mobility group box 2	679	1.822000504	0.5258778	Yes
row_45	DSTN	DSTN	destrin (actin depolymerizing factor)	697	1.800909758	0.5329925	Yes
row_46	CDC42EP3	CDC42EP3	CDC42 effector protein (Rho GTPase binding) 3	707	1.787336588	0.540473	Yes
row_47	SLAMF7	SLAMF7	SLAM family member 7	736	1.758211851	0.5468114	Yes
row_48	SLC20A1	SLC20A1	solute carrier family 20 (phosphate transporter), member 1	747	1.752829194	0.55408496	Yes
row_49	CAPN2	CAPN2	calpain 2, (m/II) large subunit	760	1.739896894	0.5611943	Yes
row_50	KLRC1	KLRC1	killer cell lectin-like receptor subfamily C, member 1	829	1.675436616	0.56503296	Yes
row_51	SNX10	SNX10	sorting nexin 10	831	1.672691703	0.5724291	Yes
row_52	CASP1	CASP1	caspase 1, apoptosis-related cysteine peptidase (interleukin 1, beta, convertase)	870	1.62736547	0.57765204	Yes
row_53	SYTL2	SYTL2	synaptotagmin-like 2	912	1.590363145	0.5825504	Yes
row_54	IL18R1	IL18R1	interleukin 18 receptor 1	914	1.5899297	0.5895779	Yes
row_55	TNF	TNF	tumor necrosis factor (TNF superfamily, member 2)	1030	1.50204432	0.5901402	Yes

T-EFF biased	
Normalized Enrichment Score (NES)	2.6822367
Nominal p-value	0
FDR q-value	0
FWER p-Value	0

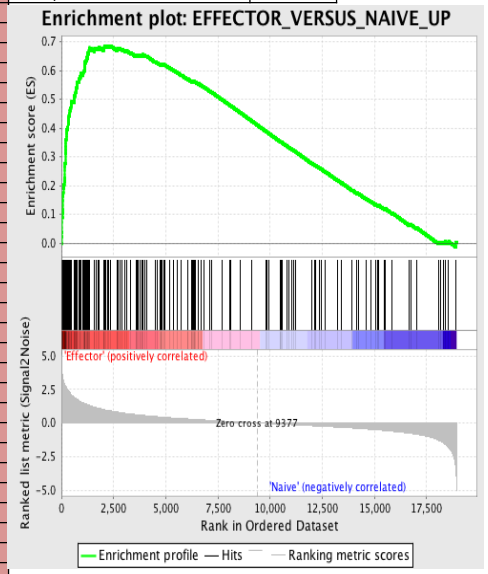

Supplemental Table 1C: Comparing transcripts UP in CMV-specific T_{EFF} relative to Naive T cells from mice and humans.
List shows significantly altered mouse genes (2-fold up or down and $p<.05$). The table also includes a GSEA analysis of these mouse gene sets relative to each of the indicated human data sets, rank ordered by expression (see methods) and FWER significance to control for multiple testing.

row_56	REEP5	REEP5	receptor accessory protein 5	1047	1.485551	0.59590375	Yes
row_57	AHNAK	AHNAK	AHNAK nucleoprotein (desmoyokin)	1089	1.449422479	0.60017437	Yes
row_58	PLEK	PLEK	pleckstrin	1103	1.443816662	0.60591185	Yes
row_59	KLRD1	KLRD1	killer cell lectin-like receptor subfamily D, member 1	1105	1.442571759	0.6122832	Yes
row_60	S100A6	S100A6	S100 calcium binding protein A6	1113	1.434784532	0.6183001	Yes
row_61	SYTL3	SYTL3	synaptotagmin-like 3	1125	1.42879796	0.62407726	Yes
row_62	IKZF3	IKZF3	IKAROS family zinc finger 3 (Aiolos)	1128	1.427701592	0.630329	Yes
row_63	SLC4A7	SLC4A7	solute carrier family 4, sodium bicarbonate cotransporter, member 7	1178	1.401299	0.6339591	Yes
row_64	PTPRJ	PTPRJ	protein tyrosine phosphatase, receptor type, J	1214	1.369297743	0.6381926	Yes
row_65	ITGA4	ITGA4	integrin, alpha 4 (antigen CD49D, alpha 4 subunit of VLA-4 receptor)	1215	1.368969679	0.6442894	Yes
row_66	NSMAF	NSMAF	neutral sphingomyelinase (N-SMase) activation associated factor	1243	1.353946567	0.64888066	Yes
row_67	PTMS	PTMS	parathymosin	1245	1.353373647	0.6548547	Yes
row_68	LMNB1	LMNB1	lamin B1	1263	1.344273448	0.6599358	Yes
row_69	SLC25A24	SLC25A24	solute carrier family 25 (mitochondrial carrier; phosphate carrier), member 24	1309	1.323735595	0.66343355	Yes
row_70	FAM3B	FAM3B	family with sequence similarity 3, member B	1320	1.320166111	0.66878015	Yes
row_71	ATP2B1	ATP2B1	ATPase, Ca++ transporting, plasma membrane 1	1338	1.308222771	0.67370063	Yes
row_72	RAP2A	RAP2A	RAP2A, member of RAS oncogene family	1345	1.304151654	0.6791891	Yes
row_73	CENPE	CENPE	centromere protein E, 312kDa	1574	1.186092257	0.6723237	Yes
row_74	FCHO2	FCHO2	FCH domain only 2	1591	1.179958582	0.6767263	Yes
row_75	ANXA1	ANXA1	annexin A1	1668	1.140519023	0.67775637	Yes
row_76	PPP1R12A	PPP1R12A	protein phosphatase 1, regulatory (inhibitor) subunit 12A	1761	1.099994302	0.67775357	Yes
row_77	SPN	SPN	sialophorin (leukosialin, CD43)	1801	1.082511306	0.6804967	Yes
row_78	AIM1	AIM1	absent in melanoma 1	2012	1.000916958	0.67376566	Yes
row_79	CTSD	CTSD	cathepsin D (lysosomal aspartyl peptidase)	2037	0.994105399	0.6769143	Yes
row_80	ID2	ID2	inhibitor of DNA binding 2, dominant negative helix-loop-helix protein	2052	0.98960793	0.68057567	Yes
row_81	DOCK5	DOCK5	dedicator of cytokinesis 5	2061	0.986442983	0.6845426	Yes
row_82	RORA	RORA	RAR-related orphan receptor A	2125	0.963672876	0.68547773	Yes
row_83	ARSB	ARSB	arylsulfatase B	2225	0.930148363	0.68434554	Yes
row_84	RAP1GAP2	null	null	2273	0.917509854	0.6859276	Yes
row_85	OSBPL3	OSBPL3	oxysterol binding protein-like 3	2337	0.898226559	0.6865713	Yes
row_86	SEP11	SEP11	septin 11	2657	0.81385839	0.6731998	No
row_87	SLC9A7	SLC9A7	solute carrier family 9 (sodium/hydrogen exchanger), member 7	2683	0.806290448	0.67545867	No
row_88	S100A10	S100A10	S100 calcium binding protein A10	2710	0.799574256	0.6776343	No
row_89	PRR13	PRR13	proline rich 13	2811	0.772674739	0.6757475	No
row_90	ITGAX	ITGAX	integrin, alpha X (complement component 3 receptor 4 subunit)	2898	0.752966523	0.6745189	No
row_91	IER3	IER3	immediate early response 3	3054	0.718982935	0.6694626	No
row_92	PRC1	PRC1	protein regulator of cytokinesis 1	3147	0.702128828	0.6676879	No
row_93	ZDHHC2	ZDHHC2	zinc finger, DHHC-type containing 2	3316	0.668632925	0.66171473	No
row_94	KCNJ8	KCNJ8	potassium inwardly-rectifying channel, subfamily J, member 8	3565	0.622722626	0.6512748	No
row_95	PRR11	PRR11	proline rich 11	3576	0.62104547	0.6535079	No
row_96	GZMK	GZMK	granzyme K (granzyme 3; tryptase II)	3622	0.614801168	0.65384835	No
row_97	NABP1	null	null	3696	0.603634	0.65264726	No
row_98	ARHGAP26	ARHGAP26	Rho GTPase activating protein 26	3752	0.59414047	0.65236294	No
row_99	NOD1	null	null	3788	0.589279234	0.65312254	No
row_100	CCR5	CCR5	chemokine (C-C motif) receptor 5	3858	0.57842803	0.65202236	No
row_101	MAPRE2	MAPRE2	microtubule-associated protein, RP/EB family, member 2	3870	0.577029943	0.6540061	No
row_102	FAM204A	null	null	3886	0.574480057	0.6557654	No
row_103	ELL2	ELL2	elongation factor, RNA polymerase II, 2	3978	0.556759	0.65339655	No
row_104	DAPK2	DAPK2	death-associated protein kinase 2	4080	0.540438652	0.6504222	No
row_105	CD38	CD38	CD38 molecule	4498	0.478245825	0.6303346	No
row_106	FGL2	FGL2	fibrinogen-like 2	4605	0.466220081	0.62676334	No
row_107	SERPINB9	SERPINB9	serpin peptidase inhibitor, clade B (ovalbumin), member 9	4733	0.447111845	0.62198806	No
row_108	RUNX1	RUNX1	runt-related transcription factor 1 (acute myeloid leukemia 1; aml1 oncogene)	4775	0.441229612	0.62176865	No
row_109	PDE8A	PDE8A	phosphodiesterase 8A	4779	0.440728962	0.62357163	No
row_110	CPEB2	CPEB2	cytoplasmic polyadenylation element binding protein 2	4840	0.432008088	0.62229884	No
row_111	CCNB2	CCNB2	cyclin B2	4902	0.424213678	0.62093806	No
row_112	RNF216	null	null	4949	0.418337315	0.6203503	No
row_113	KLRK1	KLRK1	killer cell lectin-like receptor subfamily K, member 1	5195	0.387992203	0.6090248	No
row_114	PRUNE	PRUNE	prune homolog (Drosophila)	5385	0.366202533	0.60058594	No
row_115	CYSLTR2	CYSLTR2	cysteinyl leukotriene receptor 2	5555	0.350188047	0.5931413	No
row_116	METTL7A	METTL7A	methyltransferase like 7A	5745	0.330821484	0.58454484	No
row_117	LAMC1	LAMC1	laminin, gamma 1 (formerly LAMB2)	6032	0.300099283	0.5706434	No

Supplemental Table 1C: Comparing transcripts UP in CMV-specific T_{EFF} relative to Naive T cells from mice and humans.
List shows significantly altered mouse genes (2-fold up or down and $p<.05$). The table also includes a GSEA analysis of these mouse gene sets relative to each of the indicated human data sets, rank ordered by expression (see methods) and FWER significance to control for multiple testing.

row_118	IL12RB2	IL12RB2	interleukin 12 receptor, beta 2	6066	0.29641816	0.57020533	No	
row_119	NRP1	NRP1	neuropilin 1	6243	0.279611409	0.56207347	No	
row_120	CHPT1	CHPT1	choline phosphotransferase 1	6252	0.279017806	0.5628898	No	
row_121	RPA2	RPA2	replication protein A2, 32kDa	6281	0.275597423	0.5626254	No	
row_122	NUDT4	NUDT4	nudix (nucleoside diphosphate linked moiety X)-type motif 4	6342	0.268916696	0.56062627	No	
row_123	TM6SF1	TM6SF1	transmembrane 6 superfamily member 1	6361	0.266775548	0.5608553	No	
row_124	F2RL2	F2RL2	coagulation factor II (thrombin) receptor-like 2	6367	0.266414434	0.56177545	No	
row_125	NCAPG	NCAPG	non-SMC condensin I complex, subunit G	6414	0.2617791	0.5604904	No	
row_126	CASC5	CASC5	cancer susceptibility candidate 5	6573	0.245987505	0.5531678	No	
row_127	PLOD2	PLOD2	procollagen-lysine, 2-oxoglutarate 5-dioxygenase 2	6580	0.24478434	0.5539383	No	
row_128	GBP4	GBP4	guanylate binding protein 4	6681	0.235348612	0.5496585	No	
row_129	ESM1	ESM1	endothelial cell-specific molecule 1	6827	0.220466107	0.54291487	No	
row_130	STMN1	STMN1	stathmin 1/oncoprotein 18	7111	0.19096157	0.52868724	No	
row_131	ATF6	ATF6	activating transcription factor 6	7209	0.181822732	0.52432895	No	
row_132	CLIC4	CLIC4	chloride intracellular channel 4	7692	0.13941212	0.49926916	No	
row_133	CXCR6	CXCR6	chemokine (C-X-C motif) receptor 6	8054	0.106374994	0.48050907	No	
row_134	CD44	CD44	CD44 molecule (Indian blood group)	8103	0.102266327	0.4784071	No	
row_135	EEA1	EEA1	early endosome antigen 1, 162kD	8584	0.063421227	0.45311546	No	
row_136	VIM	VIM	vimentin	9105	0.021833856	0.42550746	No	
row_137	MYADM	MYADM	myeloid-associated differentiation marker	9817	-0.020807154	0.3877185	No	**T-Naive biased**
row_138	MKI67	MKI67	antigen identified by monoclonal antibody Ki-67	9850	-0.023376763	0.38611767	No	
row_139	KIAA0101	KIAA0101	KIAA0101	9923	-0.029381931	0.3824124	No	
row_140	ITGA1	ITGA1	integrin, alpha 1	10477	-0.07660681	0.3532901	No	
row_141	ST3GAL6	ST3GAL6	ST3 beta-galactoside alpha-2,3-sialyltransferase 6	10483	-0.076973282	0.35336652	No	
row_142	CROT	CROT	carnitine O-octanoyltransferase	10549	-0.082258396	0.3502697	No	
row_143	NUSAP1	NUSAP1	nucleolar and spindle associated protein 1	10569	-0.083916672	0.34963113	No	
row_144	NDNF	null	null	10795	-0.101919957	0.33809718	No	
row_145	AS3MT	AS3MT	arsenic (+3 oxidation state) methyltransferase	10916	-0.110689312	0.33219662	No	
row_146	USP48	USP48	ubiquitin specific peptidase 48	11039	-0.121618956	0.3262382	No	
row_147	TTC39B	null	null	11153	-0.130319729	0.32079798	No	
row_148	INSL6	INSL6	insulin-like 6	11231	-0.136164784	0.3173019	No	
row_149	LAIR1	LAIR1	leukocyte-associated immunoglobulin-like receptor 1	11995	-0.199535102	0.27753842	No	
row_150	APOBEC2	APOBEC2	apolipoprotein B mRNA editing enzyme, catalytic polypeptide-like 2	12148	-0.213587001	0.27039117	No	
row_151	CA5B	CA5B	carbonic anhydrase VB, mitochondrial	12176	-0.216359437	0.2699162	No	
row_152	GPX8	null	null	12358	-0.229924336	0.2612966	No	
row_153	TTC39C	null	null	12451	-0.236867934	0.2574498	No	
row_154	S100A9	S100A9	S100 calcium binding protein A9	12649	-0.252709955	0.24807924	No	
row_155	PLSCR1	PLSCR1	phospholipid scramblase 1	13247	-0.305294454	0.21763112	No	
row_156	LGALSL	null	null	13438	-0.32125023	0.20893875	No	
row_157	GIMAP7	GIMAP7	GTPase, IMAP family member 7	13941	-0.372332722	0.18385072	No	
row_158	KIF11	KIF11	kinesin family member 11	14172	-0.395769566	0.17335905	No	
row_159	PFKP	PFKP	phosphofructokinase, platelet	14258	-0.406878978	0.17064238	No	
row_160	TOP2A	TOP2A	topoisomerase (DNA) II alpha 170kDa	14614	-0.448333681	0.15372488	No	
row_161	ABCB1	ABCB1	ATP-binding cassette, sub-family B (MDR/TAP), member 1	14816	-0.4721964	0.14511868	No	
row_162	ENTPD1	ENTPD1	ectonucleoside triphosphate diphosphohydrolase 1	15062	-0.5	0.13429202	No	
row_163	DDX28	DDX28	DEAD (Asp-Glu-Ala-Asp) box polypeptide 28	15159	-0.51004833	0.13144873	No	
row_164	SPC25	null	null	15182	-0.512632906	0.13255963	No	
row_165	EMP1	EMP1	epithelial membrane protein 1	15494	-0.558685958	0.11847789	No	
row_166	PTGER4	PTGER4	prostaglandin E receptor 4 (subtype EP4)	15502	-0.559961319	0.120598756	No	
row_167	TRPS1	TRPS1	trichorhinophalangeal syndrome I	15864	-0.615894198	0.10410783	No	
row_168	PRKAR2B	PRKAR2B	protein kinase, cAMP-dependent, regulatory, type II, beta	16668	-0.758772969	0.064703755	No	
row_169	GSTM3	GSTM3	glutathione S-transferase M3 (brain)	16749	-0.77436173	0.06389007	No	
row_170	BCL2A1	BCL2A1	BCL2-related protein A1	17032	-0.847740293	0.052640747	No	
row_171	DENND4A	DENND4A	DENN/MADD domain containing 4A	18063	-1.284453034	0.003483407	No	
row_172	EID3	EID3	-	18196	-1.37605083	0.00257885	No	
row_173	SYPL1	SYPL1	synaptophysin-like 1	18299	-1.472677708	0.003703007	No	
row_174	CD48	CD48	CD48 molecule	18401	-1.591840267	0.005411139	No	
row_175	CCNA2	CCNA2	cyclin A2	18565	-1.803973913	0.0047607	No	
row_176	DENND5A	null	null	18912	-3.465185165	0.001758436	No	

Supplemental Table 1C: Comparing transcripts UP in CMV-specific T_{EFF} relative to Naive T cells from mice and humans.
List shows significantly altered mouse genes (2-fold up or down and $p<.05$). The table also includes a GSEA analysis of these mouse gene sets relative to each of the indicated human data sets, rank ordered by expression (see methods) and FWER significance to control for multiple testing.

Supplemental Table 1D: Transcripts DOWN in T_{EFF} relative to Naïve

NAME	PROBE	GENE SYMBOL	GENE TITLE	RANK IN GENE LIST	RANK METRIC SCORE	RUNNING ES	CORE ENRICHMENT
row_0	DUSP10	DUSP10	dual specificity phosphatase 10	141	2.939956188	0.011949813	No
row_1	PIP4K2A	null	null	199	2.746984005	0.027089376	No
row_2	XCL1	XCL1	chemokine (C motif) ligand 1	329	2.424889326	0.036270257	No
row_3	SH3BP5	SH3BP5	SH3-domain binding protein 5 (BTK-associated)	434	2.161664009	0.04503923	No
row_4	HSPB11	null	null	794	1.710548043	0.03726619	No
row_5	TOX	TOX	-	1049	1.482677102	0.03356861	No
row_6	MRPS5	MRPS5	mitochondrial ribosomal protein S5	1126	1.428400517	0.038976066	No
row_7	SLAMF6	SLAMF6	SLAM family member 6	1145	1.419834614	0.04741066	No
row_8	IFI27L2	null	null	1403	1.269733906	0.042145036	No
row_9	LZTFL1	LZTFL1	leucine zipper transcription factor-like 1	1557	1.191928625	0.041894328	No
row_10	LY6E	LY6E	lymphocyte antigen 6 complex, locus E	1603	1.174182415	0.04726847	No
row_11	EMB	EMB	embigin homolog (mouse)	1737	1.11072886	0.047544036	No
row_12	ST8SIA1	ST8SIA1	ST8 alpha-N-acetyl-neuraminide alpha-2,8-sialyltransferase 1	1791	1.085347176	0.05190522	No
row_13	STAMBPL1	STAMBPL1	STAM binding protein-like 1	1935	1.02846241	0.051104933	No
row_14	MED4	MED4	mediator of RNA polymerase II transcription, subunit 4 homolog (S. cerevisiae)	2034	0.994327545	0.05247146	No
row_15	RTP4	RTP4	receptor transporter protein 4	2082	0.977881908	0.056440815	No
row_16	PHPT1	PHPT1	phosphohistidine phosphatase 1	2204	0.936563373	0.05620237	No
row_17	EGR2	EGR2	early growth response 2 (Krox-20 homolog, Drosophila)	2325	0.900809228	0.055780597	No
row_18	SPRED2	SPRED2	sprouty-related, EVH1 domain containing 2	2460	0.864051044	0.05437132	No
row_19	RPLP1	RPLP1	ribosomal protein, large, P1	2933	0.746564031	0.034213834	No
row_20	ATP1B1	ATP1B1	ATPase, Na+/K+ transporting, beta 1 polypeptide	3246	0.683011651	0.022142995	No
row_21	NAT1	NAT1	N-acetyltransferase 1 (arylamine N-acetyltransferase)	3671	0.606945157	0.003614093	No
row_22	HINT3	HINT3	histidine triad nucleotide binding protein 3	4043	0.546061218	-0.012499581	No
row_23	ITGAE	ITGAE	integrin, alpha E (antigen CD103, human mucosal lymphocyte antigen 1; alpha polypeptide)	4278	0.5118379	-0.021555495	No
row_24	USP28	USP28	ubiquitin specific peptidase 28	4424	0.48942703	-0.026027618	No
row_25	GID4	null	null	4838	0.432452857	-0.045125857	No
row_26	HMP19	HMP19	-	4885	0.425784498	-0.04475523	No
row_27	JUN	JUN	jun oncogene	5091	0.399972111	-0.053009197	No
row_28	ACSL3	ACSL3	acyl-CoA synthetase long-chain family member 3	5165	0.391422004	-0.054301426	No
row_29	SLFN5	SLFN5	schlafen family member 5	5772	0.32738024	-0.08435627	No
row_30	BCL9	BCL9	B-cell CLL/lymphoma 9	6430	0.260354906	-0.11756607	No
row_31	CCR9	CCR9	chemokine (C-C motif) receptor 9	6700	0.233178288	-0.1303261	No
row_32	TTC27	TTC27	tetratricopeptide repeat domain 27	6854	0.218153343	-0.13701795	No
row_33	CD3D	CD3D	CD3d molecule, delta (CD3-TCR complex)	6890	0.215069339	-0.13745627	No
row_34	LPHN2	LPHN2	latrophilin 2	6942	0.210390016	-0.13877623	No
row_35	SEPP1	SEPP1	selenoprotein P, plasma, 1	7007	0.202965602	-0.1408365	No
row_36	HRSP12	HRSP12	heat-responsive protein 12	7324	0.171926096	-0.15650065	No
row_37	PPIC	PPIC	peptidylprolyl isomerase C (cyclophilin C)	7382	0.1669918	-0.15842669	No
row_38	EPHX1	EPHX1	epoxide hydrolase 1, microsomal (xenobiotic)	7497	0.156613216	-0.163452	No
row_39	IFT80	IFT80	intraflagellar transport 80 homolog (Chlamydomonas)	7613	0.146471366	-0.16859758	No
row_40	PRDX6	PRDX6	peroxiredoxin 6	7705	0.138377637	-0.17252062	No
row_41	RPS26	RPS26	ribosomal protein S26	7821	0.12824057	-0.17778678	No
row_42	TLR1	TLR1	toll-like receptor 1	8020	0.109741025	-0.18758833	No
row_43	TMLHE	TMLHE	trimethyllysine hydroxylase, epsilon	8072	0.104750194	-0.18960707	No
row_44	TRIM13	TRIM13	tripartite motif-containing 13	8261	0.088052206	-0.19902039	No
row_45	NEDD4L	NEDD4L	neural precursor cell expressed, developmentally down-regulated 4-like	8274	0.0869992	-0.19908294	No
row_46	DAPL1	DAPL1	death associated protein-like 1	8730	0.05147025	-0.22293432	No
row_47	QSER1	QSER1	glutamine and serine rich 1	9237	0.011975013	-0.24975856	No
row_48	GRIA3	GRIA3	glutamate receptor, ionotrophic, AMPA 3	10043	-0.039689511	-0.29229698	No
row_49	DKC1	DKC1	dyskeratosis congenita 1, dyskerin	10139	-0.049450032	-0.2970209	No
row_50	RRAS2	RRAS2	related RAS viral (r-ras) oncogene homolog 2	10748	-0.098168731	-0.32869825	No
row_51	LYPD6B	null	null	10756	-0.098722182	-0.32841742	No
row_52	F2RL1	F2RL1	coagulation factor II (thrombin) receptor-like 1	11236	-0.136392936	-0.35298312	No
row_53	DPP4	DPP4	dipeptidyl-peptidase 4 (CD26, adenosine deaminase complexing protein 2)	11283	-0.140664518	-0.35449845	No
row_54	RAPGEF4	RAPGEF4	Rap guanine nucleotide exchange factor (GEF) 4	11391	-0.149277762	-0.3592001	No
row_55	TFRC	TFRC	transferrin receptor (p90, CD71)	11483	-0.15601249	-0.3630065	No

T-EFF biased	
Normalized Enrichment Score (NES)	-2.4599857
Nominal p-value	0
FDR q-value	0
FWER p-Value	0

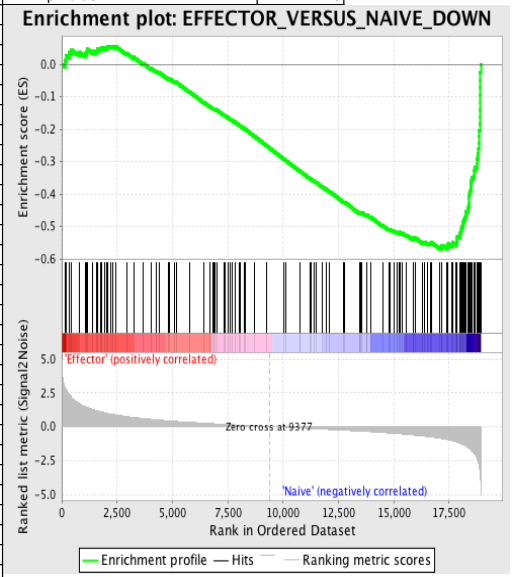

T-Naive biased

Supplemental Table 1D: Comparing transcripts DOWN in CMV-specific T_{EFF} relative to Naïve T cells from mice and humans.
List shows significantly altered mouse genes (2-fold up or down and $p<.05$). The table also includes a GSEA analysis of these mouse gene sets relative to each of the indicated human data sets, rank ordered by expression (see methods) and FWER significance to control for multiple testing.

row_56	KIAA1033	KIAA1033	KIAA1033	11781	-0.183877766	-0.3775814	No
row_57	ICOS	ICOS	inducible T-cell co-stimulator	11945	-0.196053505	-0.38495108	No
row_58	RRP15	null	null	12080	-0.207625285	-0.39070237	No
row_59	INSR	INSR	insulin receptor	12743	-0.260480523	-0.42417717	No
row_60	CD2AP	CD2AP	CD2-associated protein	12789	-0.264684618	-0.424819	No
row_61	TSPAN13	TSPAN13	tetraspanin 13	13458	-0.323553056	-0.45819563	No
row_62	MGST2	MGST2	microsomal glutathione S-transferase 2	13478	-0.325819671	-0.45705065	No
row_63	XKRX	XKRX	XK, Kell blood group complex subunit-related, X-linked	13496	-0.328198284	-0.45578364	No
row_64	ZNF761	ZNF761	zinc finger protein 761	13578	-0.335966825	-0.45786804	No
row_65	RPS29	RPS29	ribosomal protein S29	13767	-0.35352698	-0.46552533	No
row_66	CHURC1	CHURC1	churchill domain containing 1	13799	-0.356838018	-0.46481323	No
row_67	RPL8	RPL8	ribosomal protein L8	13990	-0.376885176	-0.47242236	No
row_68	LCLAT1	null	null	14502	-0.434282362	-0.49671906	No
row_69	CNGA1	CNGA1	cyclic nucleotide gated channel alpha 1	14777	-0.467894018	-0.5081924	No
row_70	RPSA	RPSA	ribosomal protein SA	14858	-0.476895005	-0.5092914	No
row_71	WDR12	WDR12	WD repeat domain 12	15015	-0.496033192	-0.5143047	No
row_72	KLHDC1	KLHDC1	kelch domain containing 1	15155	-0.509133816	-0.5183275	No
row_73	ZBTB10	ZBTB10	zinc finger and BTB domain containing 10	15248	-0.523607731	-0.51975554	No
row_74	TTC3	TTC3	tetratricopeptide repeat domain 3	15281	-0.528237998	-0.5179629	No
row_75	PCGF5	PCGF5	polycomb group ring finger 5	15374	-0.540068984	-0.5192821	No
row_76	MYC	MYC	v-myc myelocytomatosis viral oncogene homolog (avian)	15574	-0.571345031	-0.52608347	No
row_77	RPL14	RPL14	ribosomal protein L14	15877	-0.618567109	-0.5380489	No
row_78	TRAT1	TRAT1	T cell receptor associated transmembrane adaptor 1	15885	-0.619778156	-0.5343215	No
row_79	RPLP0	RPLP0	ribosomal protein, large, P0	15971	-0.63402319	-0.53464705	No
row_80	CCDC91	CCDC91	coiled-coil domain containing 91	16303	-0.687809348	-0.54769635	No
row_81	MRPL23	MRPL23	mitochondrial ribosomal protein L23	16385	-0.704515219	-0.54734296	No
row_82	KBTBD11	KBTBD11	kelch repeat and BTB (POZ) domain containing 11	16543	-0.733644545	-0.5508377	No
row_83	RPS2	RPS2	ribosomal protein S2	16655	-0.757363677	-0.5517298	No
row_84	RPS19	RPS19	ribosomal protein S19	16716	-0.768323898	-0.54983777	No
row_85	RPL10A	RPL10A	ribosomal protein L10a	17070	-0.856434166	-0.56294143	No
row_86	CYB5A	CYB5A	cytochrome b5 type A (microsomal)	17166	-0.881539941	-0.56216145	No
row_87	BTF3L4	BTF3L4	basic transcription factor 3-like 4	17188	-0.886925817	-0.5574113	No
row_88	IMPDH2	IMPDH2	IMP (inosine monophosphate) dehydrogenase 2	17415	-0.955320895	-0.56310844	Yes
row_89	CMSS1	null	null	17453	-0.969784021	-0.5586609	Yes
row_90	P2RY10	P2RY10	purinergic receptor P2Y, G-protein coupled, 10	17467	-0.974344432	-0.5529072	Yes
row_91	LTV1	LTV1	LTV1 homolog (S. cerevisiae)	17636	-1.036688805	-0.5549823	Yes
row_92	TNFSF8	TNFSF8	tumor necrosis factor (ligand) superfamily, member 8	17663	-1.047024012	-0.5494391	Yes
row_93	ST6GAL1	ST6GAL1	ST6 beta-galactosamide alpha-2,6-sialyltranferase 1	17827	-1.123234868	-0.55067587	Yes
row_94	CD69	CD69	CD69 molecule	17857	-1.142017961	-0.5446638	Yes
row_95	LSM7	LSM7	LSM7 homolog, U6 small nuclear RNA associated (S. cerevisiae)	17871	-1.145340919	-0.537779	Yes
row_96	RAB3IP	RAB3IP	RAB3A interacting protein (rabin3)	17878	-1.147305012	-0.53050905	Yes
row_97	HOOK1	HOOK1	hook homolog 1 (Drosophila)	17979	-1.21851027	-0.527766	Yes
row_98	SATB1	SATB1	special AT-rich sequence binding protein 1 (binds to nuclear matrix/scaffold-associating DNA's)	17993	-1.225864649	-0.52034855	Yes
row_99	FBL	FBL	fibrillarin	18055	-1.275766611	-0.51515317	Yes
row_100	SESN3	SESN3	sestrin 3	18061	-1.280887604	-0.5069465	Yes
row_101	PDE3B	PDE3B	phosphodiesterase 3B, cGMP-inhibited	18103	-1.315524936	-0.50042474	Yes
row_102	PELI1	PELI1	pellino homolog 1 (Drosophila)	18124	-1.324875116	-0.4927246	Yes
row_103	SSBP2	SSBP2	single-stranded DNA binding protein 2	18126	-1.326386809	-0.48400426	Yes
row_104	RPL13	RPL13	ribosomal protein L13	18189	-1.370167017	-0.47823763	Yes
row_105	APEX1	APEX1	APEX nuclease (multifunctional DNA repair enzyme) 1	18231	-1.406233907	-0.4711159	Yes
row_106	INPP4B	INPP4B	inositol polyphosphate-4-phosphatase, type II, 105kDa	18255	-1.430721879	-0.46287513	Yes
row_107	RPL29	RPL29	ribosomal protein L29	18282	-1.452724934	-0.45464832	Yes
row_108	RPL18	RPL18	ribosomal protein L18	18347	-1.518245578	-0.44800857	Yes
row_109	BZW2	BZW2	basic leucine zipper and W2 domains 2	18379	-1.561169744	-0.43933028	Yes
row_110	CD27	null	null	18403	-1.594195485	-0.4300082	Yes
row_111	GPATCH4	null	null	18411	-1.60322082	-0.41977572	Yes
row_112	GPR183	null	null	18412	-1.608658433	-0.4091351	Yes
row_113	EEF1B2	EEF1B2	eukaryotic translation elongation factor 1 beta 2	18428	-1.626211882	-0.3991759	Yes
row_114	RPL28	RPL28	ribosomal protein L28	18463	-1.667272091	-0.3899553	Yes
row_115	TRIB2	TRIB2	tribbles homolog 2 (Drosophila)	18496	-1.701058149	-0.38040492	Yes
row_116	PDK1	PDK1	pyruvate dehydrogenase kinase, isozyme 1	18502	-1.709740758	-0.36936152	Yes
row_117	DGKA	DGKA	diacylglycerol kinase, alpha 80kDa	18512	-1.720613718	-0.35845888	Yes

Supplemental Table 1D: Comparing transcripts DOWN in CMV-specific T_{EFF} relative to Naïve T cells from mice and humans.
List shows significantly altered mouse genes (2-fold up or down and $p<.05$). The table also includes a GSEA analysis of these mouse gene sets relative to each of the indicated human data sets, rank ordered by expression (see methods) and FWER significance to control for multiple testing.

row_118	TCP11L2	TCP11L2	t-complex 11 (mouse) like 2	18552	-1.774849534	-0.34879252	Yes
row_119	RPS9	RPS9	ribosomal protein S9	18631	-1.944758415	-0.3400759	Yes
row_120	RPL15	RPL15	ribosomal protein L15	18634	-1.947595	-0.3272997	Yes
row_121	MYB	MYB	v-myb myeloblastosis viral oncogene homolog (avian)	18678	-2.026391506	-0.3161822	Yes
row_122	ITGA6	ITGA6	integrin, alpha 6	18768	-2.315096617	-0.3056008	Yes
row_123	SELL	SELL	selectin L (lymphocyte adhesion molecule 1)	18773	-2.32630682	-0.2904259	Yes
row_124	IL7R	IL7R	interleukin 7 receptor	18808	-2.507570744	-0.27564707	Yes
row_125	ZEB1	null	null	18839	-2.68319726	-0.2594939	Yes
row_126	SH3PXD2A	SH3PXD2A	SH3 and PX domains 2A	18846	-2.73724103	-0.24170715	Yes
row_127	TCF7	TCF7	transcription factor 7 (T-cell specific, HMG-box)	18862	-2.879874945	-0.22345547	Yes
row_128	LTB	LTB	lymphotoxin beta (TNF superfamily, member 3)	18866	-2.933085918	-0.2042138	Yes
row_129	IL6ST	IL6ST	interleukin 6 signal transducer (gp130, oncostatin M receptor)	18893	-3.206775904	-0.18438466	Yes
row_130	IFNGR2	IFNGR2	interferon gamma receptor 2 (interferon gamma transducer 1)	18901	-3.34031558	-0.162662	Yes
row_131	PECAM1	PECAM1	platelet/endothelial cell adhesion molecule (CD31 antigen)	18903	-3.406530619	-0.14018235	Yes
row_132	CCR7	CCR7	chemokine (C-C motif) receptor 7	18906	-3.42228055	-0.117651686	Yes
row_133	DPH5	DPH5	DPH5 homolog (S. cerevisiae)	18907	-3.440943003	-0.094891235	Yes
row_134	RGS10	RGS10	regulator of G-protein signalling 10	18910	-3.448899031	-0.0721845	Yes
row_135	RPS5	RPS5	ribosomal protein S5	18913	-3.483943701	-0.049245965	Yes
row_136	ACTN1	ACTN1	actinin, alpha 1	18917	-3.560284615	-0.025855627	Yes
row_137	LEF1	LEF1	lymphoid enhancer-binding factor 1	18933	-4.125883102	6.38E-04	Yes

Supplemental Table 1D: Comparing transcripts DOWN in CMV-specific T_{EFF} relative to Naïve T cells from mice and humans.
List shows significantly altered mouse genes (2-fold up or down and $p<.05$). The table also includes a GSEA analysis of these mouse gene sets relative to each of the indicated human data sets, rank ordered by expression (see methods) and FWER significance to control for multiple testing.

Supplemental Table 1E: Transcripts UP in T_M relative to Naïve

NAME	PROBE	GENE SYMBOL	GENE TITLE	RANK IN GENE LIST	RANK METRIC SCORE	RUNNING ES	CORE ENRICHMENT
row_0	ITGB1	ITGB1	integrin, beta 1 (fibronectin receptor, beta polypeptide, antigen CD29 includes MDF2, MSK12)	3	4.403458118	0.033498626	Yes
row_1	TBX21	TBX21	T-box 21	9	3.787709236	0.06218451	Yes
row_2	IER3	IER3	immediate early response 3	27	3.474953413	0.087842345	Yes
row_3	ANXA2	ANXA2	annexin A2	29	3.467990398	0.114296935	Yes
row_4	IL18R1	IL18R1	interleukin 18 receptor 1	30	3.436789513	0.14056617	Yes
row_5	PRDM1	PRDM1	PR domain containing 1, with ZNF domain	32	3.428418159	0.16671829	Yes
row_6	TNF	TNF	tumor necrosis factor (TNF superfamily, member 2)	39	3.323193789	0.1918005	Yes
row_7	GZMA	GZMA	granzyme A (granzyme 1, cytotoxic T-lymphocyte-associated serine esterase 3)	63	3.111444473	0.2143611	Yes
row_8	BHLHE40	null	null	83	2.946973085	0.23587705	Yes
row_9	CXCR3	CXCR3	chemokine (C-X-C motif) receptor 3	84	2.945517063	0.25839123	Yes
row_10	MYO1F	MYO1F	myosin IF	96	2.830258846	0.27944005	Yes
row_11	GZMK	GZMK	granzyme K (granzyme 3; tryptase II)	101	2.814285755	0.30073866	Yes
row_12	CCL5	CCL5	chemokine (C-C motif) ligand 5	103	2.810801268	0.32217	Yes
row_13	SLAMF7	SLAMF7	SLAM family member 7	112	2.729997635	0.34261185	Yes
row_14	IFNG	IFNG	interferon, gamma	168	2.514009953	0.35890597	Yes
row_15	ZEB2	null	null	203	2.384581566	0.37532642	Yes
row_16	IL18RAP	IL18RAP	interleukin 18 receptor accessory protein	205	2.380190134	0.39346638	Yes
row_17	CAMK2N1	CAMK2N1	calcium/calmodulin-dependent protein kinase II inhibitor 1	206	2.379069328	0.41165087	Yes
row_18	PTPRJ	PTPRJ	protein tyrosine phosphatase, receptor type, J	210	2.366587877	0.4295806	Yes
row_19	S1PR5	null	null	213	2.358679295	0.44750303	Yes
row_20	XCL1	XCL1	chemokine (C motif) ligand 1	246	2.268402576	0.46314168	Yes
row_21	LGALS1	LGALS1	lectin, galactoside-binding, soluble, 1 (galectin 1)	262	2.228570938	0.479379	Yes
row_22	FCHO2	FCHO2	FCH domain only 2	299	2.135591984	0.49379003	Yes
row_23	RGS1	RGS1	regulator of G-protein signalling 1	305	2.109815836	0.5096509	Yes
row_24	CCL4	CCL4	chemokine (C-C motif) ligand 4	368	1.997584224	0.5216258	Yes
row_25	CD44	CD44	CD44 molecule (Indian blood group)	508	1.743003964	0.52756435	Yes
row_26	HOPX	null	null	511	1.739763975	0.54075605	Yes
row_27	IL2RB	IL2RB	interleukin 2 receptor, beta	605	1.639035821	0.54834354	Yes
row_28	CCR5	CCR5	chemokine (C-C motif) receptor 5	627	1.613669157	0.5595621	Yes
row_29	S100A4	S100A4	S100 calcium binding protein A4	637	1.605283499	0.57135403	Yes
row_30	CHSY1	CHSY1	carbohydrate (chondroitin) synthase 1	656	1.586069226	0.582521	Yes
row_31	ITGA4	ITGA4	integrin, alpha 4 (antigen CD49D, alpha 4 subunit of VLA-4 receptor)	783	1.489005804	0.5872087	Yes
row_32	AHNAK	AHNAK	AHNAK nucleoprotein (desmoyokin)	925	1.377583385	0.59024787	Yes
row_33	TYROBP	TYROBP	TYRO protein tyrosine kinase binding protein	1012	1.307673335	0.59567446	Yes
row_34	FASLG	FASLG	Fas ligand (TNF superfamily, member 6)	1108	1.245491982	0.60014766	Yes
row_35	PTPN3	PTPN3	protein tyrosine phosphatase, non-receptor type 3	1121	1.241511583	0.6089997	Yes
row_36	ATP2B1	ATP2B1	ATPase, Ca++ transporting, plasma membrane 1	1266	1.171560645	0.61030483	Yes
row_37	CTSD	CTSD	cathepsin D (lysosomal aspartyl peptidase)	1342	1.137916207	0.61501825	Yes
row_38	ID2	ID2	inhibitor of DNA binding 2, dominant negative helix-loop-helix protein	1353	1.132620811	0.6231442	Yes
row_39	CASP4	CASP4	caspase 4, apoptosis-related cysteine peptidase	1364	1.127617121	0.63123196	Yes
row_40	ANXA1	ANXA1	annexin A1	1367	1.12607944	0.63973296	Yes
row_41	GZMB	GZMB	granzyme B (granzyme 2, cytotoxic T-lymphocyte-associated serine esterase 1)	1387	1.118411899	0.6472722	Yes
row_42	PLEK	PLEK	pleckstrin	1396	1.115830541	0.65537614	Yes
row_43	KLRG1	KLRG1	killer cell lectin-like receptor subfamily G, member 1	1485	1.075441837	0.6589214	Yes
row_44	SAMD3	SAMD3	sterile alpha motif domain containing 3	1649	1.020359516	0.65806144	Yes
row_45	P2RY13	P2RY13	purinergic receptor P2Y, G-protein coupled, 13	1768	0.977391183	0.65926355	Yes
row_46	HMOX1	HMOX1	heme oxygenase (decycling) 1	1836	0.954161108	0.6629974	Yes
row_47	VCAM1	VCAM1	vascular cell adhesion molecule 1	2118	0.876853645	0.654772	No
row_48	CDC42EP3	CDC42EP3	CDC42 effector protein (Rho GTPase binding) 3	2405	0.811948538	0.64578474	No
row_49	RORA	RORA	RAR-related orphan receptor A	2483	0.79405731	0.6477636	No
row_50	SLC25A24	SLC25A24	solute carrier family 25 (mitochondrial carrier; phosphate carrier), member 24	2523	0.785699964	0.65169734	No
row_51	CAPN2	CAPN2	calpain 2, (m/II) large subunit	2575	0.775719941	0.6549173	No
row_52	DSTN	DSTN	destrin (actin depolymerizing factor)	2742	0.739924014	0.6517544	No
row_53	CD38	CD38	CD38 molecule	2824	0.724371314	0.65298814	No
row_54	S100A6	S100A6	S100 calcium binding protein A6	2842	0.721523046	0.6576	No
row_55	MITF	MITF	microphthalmia-associated transcription factor	3146	0.671954572	0.64663965	No

T-MEM biased	
Normalized Enrichment Score (NES)	2.735306
Nominal p-value	0
FDR q-value	0
FWER p-Value	0

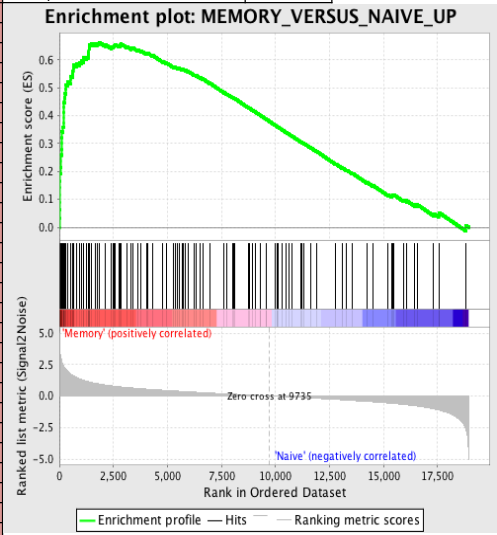

Supplemental Table 1E: Comparing transcripts UP in CMV-specific T_M relative to Naïve T cells from mice and humans.
List shows significantly altered mouse genes (2-fold up or down and *p*<.05). The table also includes a GSEA analysis of these mouse gene sets relative to each of the indicated human data sets, rank ordered by expression (see methods) and FWER significance to control for multiple testing.

row_56	UBD	UBD	ubiquitin D	3333	0.644224048	0.6416828	No	
row_57	SLC9A7	SLC9A7	solute carrier family 9 (sodium/hydrogen exchanger), member 7	3405	0.633073628	0.64274997	No	
row_58	IGF1	IGF1	insulin-like growth factor 1 (somatomedin C)	3628	0.601582348	0.6355547	No	
row_59	CTSB	CTSB	cathepsin B	3760	0.581756353	0.63304216	No	
row_60	KLRC1	KLRC1	killer cell lectin-like receptor subfamily C, member 1	4033	0.549523294	0.62279284	No	
row_61	SYTL2	SYTL2	synaptotagmin-like 2	4107	0.540566444	0.62304664	No	
row_62	ARHGAP26	ARHGAP26	Rho GTPase activating protein 26	4308	0.515345871	0.61636096	No	
row_63	PILRA	PILRA	paired immunoglobin-like type 2 receptor alpha	4785	0.458973765	0.5945823	No	
row_64	GOLIM4	null	null	4971	0.43950215	0.5881138	No	
row_65	GNPTAB	GNPTAB	N-acetylglucosamine-1-phosphate transferase, alpha and beta subunits	5275	0.404915243	0.5751123	No	
row_66	ZDHHC2	ZDHHC2	zinc finger, DHHC-type containing 2	5375	0.395494431	0.57287604	No	
row_67	ITGA1	ITGA1	integrin, alpha 1	5481	0.38406226	0.57023364	No	
row_68	CASP1	CASP1	caspase 1, apoptosis-related cysteine peptidase (interleukin 1, beta, convertase)	5553	0.378048152	0.5693515	No	
row_69	DOCK5	DOCK5	dedicator of cytokinesis 5	5680	0.365191877	0.56544924	No	
row_70	C1QB	C1QB	complement component 1, q subcomponent, B chain	5736	0.359394342	0.5652745	No	
row_71	CX3CR1	CX3CR1	chemokine (C-X3-C motif) receptor 1	5825	0.350362927	0.5632776	No	
row_72	SIRPA	SIRPA	signal-regulatory protein alpha	5967	0.337242603	0.5583649	No	
row_73	CEP290	CEP290	centrosomal protein 290kDa	6252	0.308049321	0.54563236	No	
row_74	ABCB1	ABCB1	ATP-binding cassette, sub-family B (MDR/TAP), member 1	6346	0.298542351	0.54297376	No	
row_75	KCNJ8	KCNJ8	potassium inwardly-rectifying channel, subfamily J, member 8	6525	0.280597478	0.53566253	No	
row_76	SIGLEC8	SIGLEC8	sialic acid binding Ig-like lectin 8	6635	0.270513564	0.53193974	No	
row_77	ENTPD1	ENTPD1	ectonucleoside triphosphate diphosphohydrolase 1	6960	0.239131674	0.5165555	No	
row_78	CHD7	CHD7	chromodomain helicase DNA binding protein 7	7633	0.179831967	0.4822309	No	
row_79	MRC1	MRC1	mannose receptor, C type 1	7750	0.169954807	0.4773676	No	
row_80	NOD1	null	null	8023	0.147540331	0.4640457	No	
row_81	SLC20A1	SLC20A1	solute carrier family 20 (phosphate transporter), member 1	8085	0.141955048	0.46189022	No	
row_82	CLEC12A	CLEC12A	C-type lectin domain family 12, member A	8121	0.139091328	0.46109402	No	
row_83	KLRK1	KLRK1	killer cell lectin-like receptor subfamily K, member 1	8756	0.083828688	0.42805436	No	
row_84	MARCO	MARCO	macrophage receptor with collagenous structure	8799	0.079154007	0.4264282	No	
row_85	BCL2A1	BCL2A1	BCL2-related protein A1	8955	0.066597454	0.41870305	No	
row_86	C1QC	C1QC	complement component 1, q subcomponent, C chain	9054	0.057710547	0.41393805	No	
row_87	FGL2	FGL2	fibrinogen-like 2	9285	0.039783955	0.4020237	No	
row_88	CYSLTR2	CYSLTR2	cysteinyl leukotriene receptor 2	9309	0.03815094	0.40109345	No	
row_89	CD68	CD68	CD68 molecule	9565	0.014540591	0.38765806	No	**T-Naive biased**
row_90	CD5L	CD5L	CD5 molecule-like	9589	0.012351896	0.38653064	No	
row_91	SPIC	SPIC	Spi-C transcription factor (Spi-1/PU.1 related)	9974	-0.013060934	0.36623096	No	
row_92	KCNJ16	KCNJ16	potassium inwardly-rectifying channel, subfamily J, member 16	10081	-0.021453133	0.36076385	No	
row_93	MARCKS	MARCKS	myristoylated alanine-rich protein kinase C substrate	10100	-0.023070196	0.35998395	No	
row_94	TF	TF	transferrin	10110	-0.023738414	0.3596873	No	
row_95	C1QA	C1QA	complement component 1, q subcomponent, A chain	10307	-0.038720008	0.34957102	No	
row_96	DMRTA1	DMRTA1	DMRT-like family A1	10492	-0.053806484	0.34020752	No	
row_97	CD302	CD302	CD302 molecule	10626	-0.066097707	0.3336473	No	
row_98	PLBD1	null	null	10770	-0.080001555	0.3266621	No	
row_99	TM6SF1	TM6SF1	transmembrane 6 superfamily member 1	11164	-0.115543537	0.30666766	No	
row_100	CXCL3	CXCL3	chemokine (C-X-C motif) ligand 3	11234	-0.12114767	0.30392814	No	
row_101	MYADM	MYADM	myeloid-associated differentiation marker	11320	-0.129930556	0.30040574	No	
row_102	EEA1	EEA1	early endosome antigen 1, 162kD	11628	-0.158786342	0.28531048	No	
row_103	LGMN	LGMN	legumain	11900	-0.183479294	0.2723164	No	
row_104	SERPINB6	SERPINB6	serpin peptidase inhibitor, clade B (ovalbumin), member 6	12789	-0.268000066	0.22719103	No	
row_105	ADAMDEC1	ADAMDEC1	ADAM-like, decysin 1	13104	-0.301389694	0.21281388	No	
row_106	ATP6V0D2	ATP6V0D2	ATPase, H+ transporting, lysosomal 38kDa, V0 subunit d2	13305	-0.322526693	0.2046544	No	
row_107	APOE	APOE	apolipoprotein E	13579	-0.353963107	0.19285716	No	
row_108	RAB23	RAB23	RAB23, member RAS oncogene family	14232	-0.426638871	0.16148156	No	
row_109	CCR3	CCR3	chemokine (C-C motif) receptor 3	14513	-0.457534194	0.1501041	No	
row_110	SLC40A1	SLC40A1	solute carrier family 40 (iron-regulated transporter), member 1	15204	-0.549991131	0.11765265	No	
row_111	IL18	IL18	interleukin 18 (interferon-gamma-inducing factor)	15396	-0.576450884	0.11191215	No	
row_112	EMR1	EMR1	egf-like module containing, mucin-like, hormone receptor-like 1	15417	-0.58118856	0.11529201	No	
row_113	TTC39B	null	null	15473	-0.589318216	0.11687469	No	
row_114	TRPS1	TRPS1	trichorhinophalangeal syndrome I	15933	-0.662678242	0.09755613	No	
row_115	MPEG1	MPEG1	-	16069	-0.689519227	0.0956548	No	
row_116	MERTK	MERTK	c-mer proto-oncogene tyrosine kinase	16455	-0.769379318	0.08108297	No	
row_117	CD163	CD163	CD163 molecule	16576	-0.799468338	0.08081889	No	

Supplemental Table 1E: Comparing transcripts UP in CMV-specific T_M relative to Naïve T cells from mice and humans.
List shows significantly altered mouse genes (2-fold up or down and $p<.05$). The table also includes a GSEA analysis of these mouse gene sets relative to each of the indicated human data sets, rank ordered by expression (see methods) and FWER significance to control for multiple testing.

row_118	CSF1R	CSF1R	colony stimulating factor 1 receptor, formerly McDonough feline sarcoma viral (v-fms) oncogene homol	17321	-1.016953349	0.049068	No
row_119	DENND4A	DENND4A	DENN/MADD domain containing 4A	17562	-1.106143713	0.044773173	No
row_120	HPGD	HPGD	hydroxyprostaglandin dehydrogenase 15-(NAD)	17591	-1.119443536	0.05184222	No
row_121	AIF1	AIF1	allograft inflammatory factor 1	18811	-2.621035337	0.007118445	No

Supplemental Table 1E: Comparing transcripts UP in CMV-specific T_M relative to Naïve T cells from mice and humans.
List shows significantly altered mouse genes (2-fold up or down and $p<.05$). The table also includes a GSEA analysis of these mouse gene sets relative to each of the indicated human data sets, rank ordered by expression (see methods) and FWER significance to control for multiple testing.

Supplemental Table 1F: Transcripts DOWN in T_M relative to Naïve

NAME	PROBE	GENE SYMBOL	GENE TITLE	RANK IN GENE LIST	RANK METRIC SCORE	RUNNING ES	CORE ENRICHMENT
row_0	TRAT1	TRAT1	T cell receptor associated transmembrane adaptor 1	252	2.253664494	0.015806396	No
row_1	IFT52	IFT52	intraflagellar transport 52 homolog (Chlamydomonas)	448	1.839338064	0.029272709	No
row_2	MAP1LC3B	MAP1LC3B	microtubule-associated protein 1 light chain 3 beta	478	1.792060494	0.050929733	No
row_3	KIAA1109	KIAA1109	KIAA1109	544	1.710649014	0.06962404	No
row_4	ST8SIA1	ST8SIA1	ST8 alpha-N-acetyl-neuraminide alpha-2,8-sialyltransferase 1	611	1.629442453	0.08721425	No
row_5	SMIM7	null	null	722	1.538029432	0.10128806	No
row_6	SMC4	SMC4	structural maintenance of chromosomes 4	885	1.410843372	0.11095824	No
row_7	PPIC	PPIC	peptidylprolyl isomerase C (cyclophilin C)	1210	1.200220346	0.10931178	No
row_8	CCR9	CCR9	chemokine (C-C motif) receptor 9	1284	1.165769219	0.12052943	No
row_9	H3F3B	H3F3B	H3 histone, family 3B (H3.3B)	1519	1.064026237	0.121892706	No
row_10	EGR2	EGR2	early growth response 2 (Krox-20 homolog, Drosophila)	1588	1.039483428	0.13174096	No
row_11	SDHAF1	null	null	1745	0.984709442	0.13621381	No
row_12	USP31	USP31	ubiquitin specific peptidase 31	1970	0.915602505	0.1361863	No
row_13	CRIPT	CRIPT	cysteine-rich PDZ-binding protein	2043	0.8937971	0.14393681	No
row_14	SESN3	SESN3	sestrin 3	2562	0.777974069	0.12653776	No
row_15	CSPP1	CSPP1	centrosome and spindle pole associated protein 1	2878	0.716659307	0.11910977	No
row_16	SLAMF6	SLAMF6	SLAM family member 6	3602	0.604985237	0.088601	No
row_17	ATP1B1	ATP1B1	ATPase, Na+/K+ transporting, beta 1 polypeptide	4260	0.521278799	0.060508642	No
row_18	IFI27L2	null	null	4472	0.495869935	0.055737853	No
row_19	WDR12	WDR12	WD repeat domain 12	4548	0.486908525	0.058062874	No
row_20	GID4	null	null	5386	0.394062251	0.018778916	No
row_21	GRIA3	GRIA3	glutamate receptor, ionotrophic, AMPA 3	6236	0.309973687	-0.02222974	No
row_22	SMURF2	SMURF2	SMAD specific E3 ubiquitin protein ligase 2	6467	0.286243409	-0.030721275	No
row_23	TRIM13	TRIM13	tripartite motif-containing 13	6601	0.272644997	-0.03424511	No
row_24	CYB5D1	CYB5D1	cytochrome b5 domain containing 1	6628	0.271089345	-0.032115098	No
row_25	EIF4E2	EIF4E2	eukaryotic translation initiation factor 4E member 2	7077	0.228623614	-0.052912492	No
row_26	DIRC2	DIRC2	disrupted in renal carcinoma 2	7948	0.153479651	-0.097060256	No
row_27	DUSP19	DUSP19	dual specificity phosphatase 19	8244	0.129077777	-0.111032814	No
row_28	TMEM50B	TMEM50B	transmembrane protein 50B	8250	0.128792241	-0.10963099	No
row_29	LYPD6B	null	null	8499	0.108135678	-0.12138229	No
row_30	TFRC	TFRC	transferrin receptor (p90, CD71)	8659	0.092881635	-0.12861155	No
row_31	HSPB11	null	null	8816	0.077869982	-0.13587601	No
row_32	DPP4	DPP4	dipeptidyl-peptidase 4 (CD26, adenosine deaminase complexing protein 2)	9355	0.034692306	-0.163956	No
row_33	HIGD2A	HIGD2A	HIG1 domain family, member 2A	9507	0.019503452	-0.17171077	No
row_34	UFM1	UFM1	ubiquitin-fold modifier 1	9836	-2.79E-04	-0.18910031	No
row_35	HRSP12	HRSP12	heat-responsive protein 12	9985	-0.014027056	-0.19676688	No
row_36	PSMA5	PSMA5	proteasome (prosome, macropain) subunit, alpha type, 5	10051	-0.019558406	-0.19996054	No
row_37	APOOL	null	null	10453	-0.050357979	-0.22057295	No
row_38	CD69	CD69	CD69 molecule	10576	-0.061757311	-0.22624302	No
row_39	SF3B14	SF3B14	-	10679	-0.070999824	-0.2307329	No
row_40	IFT80	IFT80	intraflagellar transport 80 homolog (Chlamydomonas)	10922	-0.094206497	-0.24234633	No
row_41	LTN1	null	null	11172	-0.116225645	-0.25404596	No
row_42	CNGA1	CNGA1	cyclic nucleotide gated channel alpha 1	11182	-0.117405698	-0.2530036	No
row_43	TXNL4B	TXNL4B	thioredoxin-like 4B	11340	-0.132090256	-0.25961933	No
row_44	PRDX6	PRDX6	peroxiredoxin 6	11840	-0.177881435	-0.28377792	No
row_45	PHPT1	PHPT1	phosphohistidine phosphatase 1	12049	-0.196422234	-0.2922654	No
row_46	MGST2	MGST2	microsomal glutathione S-transferase 2	12218	-0.209586099	-0.29846138	No
row_47	BTF3L4	BTF3L4	basic transcription factor 3-like 4	12266	-0.215067789	-0.29817006	No
row_48	ITGAE	ITGAE	integrin, alpha E (antigen CD103, human mucosal lymphocyte antigen 1; alpha polypeptide)	12369	-0.225916848	-0.30065483	No
row_49	XKRX	XKRX	XK, Kell blood group complex subunit-related, X-linked	13020	-0.292157233	-0.33134153	No
row_50	POLR2H	POLR2H	polymerase (RNA) II (DNA directed) polypeptide H	13272	-0.318979412	-0.34052294	No
row_51	INSIG2	INSIG2	insulin induced gene 2	13368	-0.330971003	-0.3412768	No
row_52	RPS2	RPS2	ribosomal protein S2	13512	-0.347620785	-0.3443605	No
row_53	COPS4	COPS4	COP9 constitutive photomorphogenic homolog subunit 4 (Arabidopsis)	14072	-0.408545583	-0.36871526	No
row_54	CDC26	CDC26	cell division cycle 26	14324	-0.437779635	-0.37635902	No
row_55	TTC3	TTC3	tetratricopeptide repeat domain 3	14852	-0.500140667	-0.39783135	No

T-MEM biased	
Normalized Enrichment Score (NES)	-1.7465168
Nominal p-value	0
FDR q-value	5.04E-04
FWER p-Value	0.001

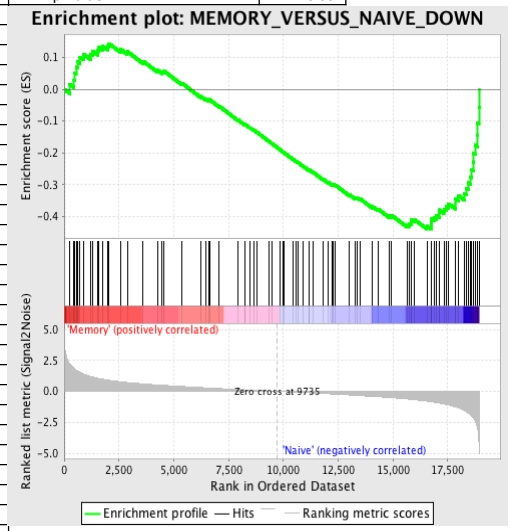

T-Naive biased

Supplemental Table 1F: Comparing transcripts DOWN in CMV-specific T_M relative to Naïve T cells from mice and humans.
List shows significantly altered mouse genes (2-fold up or down and $p<.05$). The table also includes a GSEA analysis of these mouse gene sets relative to each of the indicated human data sets, rank ordered by expression (see methods) and FWER significance to control for multiple testing.

row_56	CMSS1	null	null	14939	-0.513141811	-0.39575008	No
row_57	RPL28	RPL28	ribosomal protein L28	15661	-0.616440535	-0.42600456	No
row_58	DAPL1	DAPL1	death associated protein-like 1	15766	-0.633382142	-0.42332152	No
row_59	PRPS2	PRPS2	phosphoribosyl pyrophosphate synthetase 2	15827	-0.644233704	-0.4181648	No
row_60	EEF1E1	EEF1E1	eukaryotic translation elongation factor 1 epsilon 1	15857	-0.648591697	-0.4113078	No
row_61	INPP4B	INPP4B	inositol polyphosphate-4-phosphatase, type II, 105kDa	15986	-0.673618138	-0.40937668	No
row_62	UBE2H	UBE2H	ubiquitin-conjugating enzyme E2H (UBC8 homolog, yeast)	16554	-0.794251204	-0.4291634	Yes
row_63	RAB3IP	RAB3IP	RAB3A interacting protein (rabin3)	16744	-0.841588676	-0.4282929	Yes
row_64	RPS14	RPS14	ribosomal protein S14	16751	-0.84301734	-0.4176998	Yes
row_65	RAPGEF4	RAPGEF4	Rap guanine nucleotide exchange factor (GEF) 4	16777	-0.849250078	-0.40803358	Yes
row_66	TRIB2	TRIB2	tribbles homolog 2 (Drosophila)	16878	-0.874607146	-0.40201622	Yes
row_67	TCP11L2	TCP11L2	t-complex 11 (mouse) like 2	17003	-0.911212921	-0.39679775	Yes
row_68	CCNT1	CCNT1	cyclin T1	17122	-0.946210921	-0.39080814	Yes
row_69	KLHDC2	KLHDC2	kelch domain containing 2	17130	-0.947930574	-0.37891015	Yes
row_70	EIF3H	null	null	17334	-1.021437287	-0.37645426	Yes
row_71	RPL15	RPL15	ribosomal protein L15	17431	-1.054984808	-0.36789015	Yes
row_72	UXT	UXT	ubiquitously-expressed transcript	17544	-1.100017428	-0.35959163	Yes
row_73	EMG1	EMG1	EMG1 nucleolar protein homolog (S. cerevisiae)	17854	-1.251248837	-0.3597822	Yes
row_74	COX4I1	COX4I1	cytochrome c oxidase subunit IV isoform 1	17856	-1.251396775	-0.34363824	Yes
row_75	RANGRF	null	null	17993	-1.332128406	-0.33360818	Yes
row_76	CYB5A	CYB5A	cytochrome b5 type A (microsomal)	18277	-1.537228465	-0.32871854	Yes
row_77	SELL	SELL	selectin L (lymphocyte adhesion molecule 1)	18346	-1.622110724	-0.31132928	Yes
row_78	SATB1	SATB1	special AT-rich sequence binding protein 1 (binds to nuclear matrix/scaffold-associating DNA's)	18441	-1.738813519	-0.29380825	Yes
row_79	CCR7	CCR7	chemokine (C-C motif) receptor 7	18540	-1.883787751	-0.27462292	Yes
row_80	DPH5	DPH5	DPH5 homolog (S. cerevisiae)	18602	-1.983968496	-0.2521789	Yes
row_81	ST13	ST13	suppression of tumorigenicity 13 (colon carcinoma) (Hsp70 interacting protein)	18665	-2.091876268	-0.22839125	Yes
row_82	IFNGR2	IFNGR2	interferon gamma receptor 2 (interferon gamma transducer 1)	18693	-2.151143551	-0.20198052	Yes
row_83	ITGA6	ITGA6	integrin, alpha 6	18759	-2.333361864	-0.17522638	Yes
row_84	PDK1	PDK1	pyruvate dehydrogenase kinase, isozyme 1	18859	-2.859877586	-0.14346042	Yes
row_85	LSM7	LSM7	LSM7 homolog, U6 small nuclear RNA associated (S. cerevisiae)	18862	-2.890331745	-0.1061566	Yes
row_86	LEF1	LEF1	lymphoid enhancer-binding factor 1	18933	-4.036038399	-0.057629675	Yes
row_87	ACTN1	ACTN1	actinin, alpha 1	18942	-4.497610569	1.59E-04	Yes

Supplemental Table 1F: Comparing transcripts DOWN in CMV-specific T_M relative to Naïve T cells from mice and humans.
List shows significantly altered mouse genes (2-fold up or down and $p<.05$). The table also includes a GSEA analysis of these mouse gene sets relative to each of the indicated human data sets, rank ordered by expression (see methods) and FWER significance to control for multiple testing.